Title
Proteolysis is an evolutionarily conserved mechanism of activating NLRP1 inflammasomes.

Author
Chavarria-Smith, Joseph Edward

Publication Date
2015

Peer reviewed|Thesis/dissertation

Proteolysis is an evolutionarily conserved mechanism of activating NLRP1 inflammasomes.

by
Joseph Edward Chavarria-Smith

A dissertation submitted in partial satisfaction of the

requirements for the degree of

Doctor of Philosophy

in

Molecular and Cell Biology

in the

Graduate Division

of the

University of California, Berkeley

Committee in charge:
Professor Russell E. Vance, Chair
Professor David Raulet
Professor Laurent Coscoy
Professor Brian J. Staskawicz

Spring 2015

Proteolysis is an evolutionarily conserved mechanism of activating NLRP1 inflammasomes.

By Joseph Edward Chavarria-Smith

Abstract

Proteolysis is an evolutionarily conserved mechanism of activating NLRP1 inflammasomes.

by

Joseph Edward Chavarria-Smith

Doctor of Philosophy in Molecular and Cell Biology

University of California, Berkeley

Professor Russell E. Vance, Chair

Inflammasomes are cytosolic protein complexes that serve as platforms for the recruitment and activation of the pro-inflammatory CASPASE-1 protease (CASP1). CASP1 activation leads to processing and maturation of the cytokines interleukin-1b and -18, and a lytic form of cell death termed pyroptosis. Inflammasome assembly is initiated by cytosolic proteins in response to microbial infections, and many of these sensor proteins belong to the Nucleotide-binding domain, Leucine-rich Repeat containing protein (NLR) family. NLRP1 (NLR family, Pyrin domain containing 1) was the first NLR described to form an inflammasome, but until recently, its mechanism of activation and physiological functions in host defense have remained unclear.

In Chapter 1 we extensively review the literature on the proposed mechanisms of NLRP1 activation in humans and rodents. We discuss the activation of NLRP1 by various stimuli, including *Bacillus anthracis* Lethal Toxin, *Toxoplasma gondii*, muramyl dipeptide (MDP), and host intracellular ATP depletion. The role NLRP1 plays in pathogen recognition and resistance during infection is also discussed, as is the regulation of NLRP1 by host and viral proteins. We also discuss the unexpected differences in the mechanism of NLRP1 inflammasome activation as compared to the activation of other inflammasomes, such as the NAIP/NLRC4 inflammasomes.

In Chapter 2 we cover our discovery regarding the mechanism of mouse NLRP1B activation by Lethal Toxin (LeTx), which is composed of Lethal Factor (LF) and Protective Antigen (PA). We made the critical observation that LF cleaves NLRP1B directly near the N-terminus. We then demonstrated that LF cleavage of NLRP1B is required for NLRP1B activation and inflammasome formation. Most importantly, we were able to show that proteolysis is sufficient to activate NLRP1B when we replaced the activity of LF with a Tobacco Etch Virus (TEV) protease. We conclude by proposing that NLRP1B has evolved to respond to other proteases derived from other pathogens.

In Chapter 3 we test the hypothesis that other variants of NLRP1 expressed in mice and human are also activated by proteolysis. We first demonstrate that another allele of NLRP1B, which has no known agonist, is able to respond to cleavage and induce inflammasome

formation. We then demonstrate that this activity can also be seen with the NLRP1A paralog. Lastly, we extend this work by analyzing the human ortholog of NLRP1. Surprisingly, proteolysis is also a conserved mechanism of activating human NLRP1. Collectively, these results suggest that NLRP1 might be broadly conserved as a protease sensor in mammals, and provide an important host defense mechanism.

In Chapter 4 we report on the development of a new method of analyzing CASP1 activation. We generated a CASP1 dimerization reporter that generates the fluorescent Venus protein when an inflammasome is activated and does not induce cell death. We generated a cell line that stably expresses the reporter, NLRP1B, and ASC. This line responds to LeTx, and can be analysed by flow cytometry and live cell microscopy. This reporter also works in macrophage-like cells that endogenously express inflammasome components. As a proof of principle we demonstrate that cells with an activated inflammasome can be enriched by FACS. We believe this reporter is an ideal tool for the discovery of novel positive and negative regulators of inflammasomes. The largest advantage of the reporter is that it does not induce cell death. This feature allows for the recovery of cells from a complex mixture that would be amenable for a high thorough put screen.

Table of Contents

List of Figures and Tables

Acknowledgements

I first need to thank Russell Vance for taking me into his laboratory. While I did not join his lab in the first round, I eventually recognized my mistake and was given a second chance. I am extremely grateful for this opportunity and it was exactly what I needed. In Russell's lab I received the perfect combination of freedom, stimulation, challenge, advice, and oversight. I really enjoyed my individual meetings with Russell. As an example, I loved when we had an interesting or confusing result and we went to the drawing board to try to come up with a potential model or hypothesis. Together we came up with many models that ended up being wrong, but the process of testing this hypothesis is what taught me of how to have vision and to think like a scientist.

My progress in the lab was of course not in isolation from all other members I overlapped with from the Vance and Barton labs. I thank Greg Barton for always getting to heart of the matter and asking the difficult question. Joint lab meetings have been beneficial because of the diversity of knowledge, backgrounds and experience. I am grateful that most people in these two labs have been supportive not only professionally, but also at a personal level. I sometimes forget that not all labs have this culture where they would call their labmates true friends. In particular two labmates I developed the strongest bonds with. Kevin Barry has been my friend since graduate recruitment. It has been great to always have someone going through the exact same process, including writing this thesis and going to the gym. Bella Rauch has been a great friend and baymate. She has always had great advise in career choices, science ideas, and personal matters. I think her "oh come on" will be a good reminder to keep things in perspective when complaining about life.

I must thank Olivia Price for several contributions to this thesis and help throughout graduate school. On a practical matter, she has always helped proofread my drafts, which includes most chapters of this thesis. She is one of the few people that understands the full extent of my dyslexia and how it affects my ability to write. Olivia is one of the few people I trust in this matter because I know she will not judge me for my writing mistakes. Olivia is also the only person that would care and have the patience to help with this laborious and painful task. She has also been extremely emotionally supportive through the past nine years that I have known her. I think I will always solidly be able to count on her.

I want to thank my mom as well. I don't think I would have ever become a scientist otherwise. She inspired us to explore, love nature, and develop our own sense of wonder. While life in Costa Rica was not always easy, I am grateful for the effort she made for us to have the best education we could obtain there. She encouraged us to follow our interests and pursue our dreams. I think this might explain why I became a scientist while my sister took a much more artistic and design path.

Chapter 1: Introduction

1.1 Preview

The innate immune system in mammals includes several families of pattern recognition receptors, which initiate immune responses to microbial infection via several mechanisms. The nucleotide-binding domain and leucine-rich repeat containing protein family (NLR) is composed of approximately 20 members in the human genome (Ting et al., 2008). Because NLRs are cytosolic proteins, they are poised to respond specifically to pathogens and not to non-pathogens, as only pathogens have evolved mechanism to enter or access the host cell cytosol (Vance et al., 2009). This qualitative distinction is important in promoting appropriate inflammatory responses during infection, and indeed, inflammasomes have been shown to be critical for defense against infections with numerous pathogens (Franchi et al., 2012; Lamkanfi and Dixit, 2009; Lupfer and Kanneganti, 2012; von Moltke et al., 2013). However, the molecular mechanisms by which NLRs are activated by microbial stimuli remain poorly understood. In this review, we provide our current understanding of a particular NLR family member called NLRP1 (NLR family, Pyrin domain containing 1).

NLRP1-like genes are found in most, if not all, mammalian species for which a genome has been sequenced, including primates, rodents, ungulates, and even marsupials. NLRP1, like all NLRs, contains a central nucleotide-binding domain (NBD) and a short leucine-rich repeat domain (LRR), as depicted in Fig. 1.1. NLRP1 also contains a domain termed a "function to find" domain or FIIND (Martinon et al., 2009), which is similar to a ZU-5 and UPA domain pair found in non-NLR family proteins, such as PIDD and UNC5B (D'Osualdo et al., 2011). This domain undergoes a spontaneous self-processing (maturation) event that appears to be necessary before NLRP1 can be responsive to stimuli (Finger et al., 2012; Frew et al., 2012). In addition, in most species, NLRP1 contains two annotated effector-recruitment domains. One of these domains is an N-terminal Pyrin Domain (PYD), and the other is a C-terminal Caspase Activating and Recruitment Domain (CARD). These two effector domains are part of the death domain superfamily and are thus structurally related to each other. It is generally believed that the PYD and CARD domains mediate homotypic interactions with other downstream PYD/CARD-containing proteins, for example ASC and CASPASE-1, as is discussed below in more detail.

Even though the *NLRP1* gene is present in diverse mammalian species, NLRP1 has undergone extensive diversification within and among these species. For example, *Nlrp1* in mice has undergone at least two gene duplication events, as inferred by the presence of three paralogs (*Nlrp1a,b,c*) in the mouse genome (Table 1.1). Moreover, within the single paralog of *Nlrp1b*, five allelic variants have been identified in different inbred mouse strains, with extensive protein coding differences among them (Boyden and Dietrich, 2006). Humans and most primates appear to encode only a single NLRP1 paralog. Genomic analysis among primates indicates that NLRP1 is also among the top 150 genes exhibiting selection signatures indicative of positive (diversifying) selection (George et al., 2011; Hu et al., 2013). This signature of selection is commonly seen among immunity-related genes (Daugherty and Malik, 2012), and is consistent with evidence that NLRP1-mediated recognition of pathogens can play critical roles in host defense. Pathogen evasion of NLRP1 may thus drive the apparently rapid evolution and diversification of this gene.

NLRP1 was the first NLR shown to form a cytosolic complex, termed the inflammasome, that functions to specifically recruit and activate a downstream protease called Caspase-1 (CASP1) (Martinon et al., 2002). This initial report relied on the spontaneous activation of NLRP1 that occurs in a cellular lysate. While description of the inflammasome was a key advance, the natural physiological stimuli and mechanism of activation for this NLR have only begun to be understood. To date, several stimuli have been reported to activate various NLRP1 variants. In this review, we will discuss the various mechanisms by which NLRP1 may be activated, and compare these mechanisms to those activating other NLRs. We will also discuss how NLRP1 inflammasome activation is related to health and disease.

1.2 Main review

1.2.1 NLRP1 activation by Anthrax Lethal Toxin

Anthrax Lethal Toxin (LeTx) is an important virulence factor deployed by *Bacillus anthracis*, the causative agent of anthrax disease. LeTx is a bipartite toxin composed of protective antigen (PA) and lethal factor (LF). PA binds to a receptor on the surface of cells, and oligomerizes to form a membrane-inserted pore through which LF is delivered into the host cell cytosol. LF is a zinc metalloprotease that cleaves and inactivates all Mitogen Activated Protein Kinase Kinases (MAPKKs; also called MKKs or MEKs), with the exception of MAPKK5. LF activity appears to be critical in allowing *B. anthracis* to inactivate many cellular MAP kinase-dependent functions involved in host defense (e.g., neutrophil chemotaxis, cytokine expression, Ag presentation and adaptive immune activation), and hence, prevents efficient clearance of the bacteria (Turk, 2007). Additionally, it has been observed that in some contexts, LeTx is also able to induce a rapid and CASP1-dependent cellular lysis (Cordoba-Rodriguez et al., 2004), now termed pyroptosis (Fink et al., 2008). LeTx-dependent pyroptosis is observed only in the macrophages of specific mouse and rat strains (Boyden and Dietrich, 2006; Friedlander et al., 1993; Newman et al., 2010). Macrophage pyroptosis and mouse survival during *B. anthracis* infection are not always correlated in all mouse strains (Moayeri et al., 2004). This lack of a correlation is likely a consequence of the multiple genetic factors that are involved in resistance to infection, including the functionality of complement *C5* gene in the strains analyzed (Moayeri et al., 2010; Welkos et al., 1986). However, a critical advance in our understanding was achieved when genetic mapping in mice identified *Nlrp1b* as the locus controlling the pyroptotic response of macrophages to LeTx (Boyden and Dietrich, 2006). Years later, the homologous *Nlrp1* genes in rats were shown to mediate the pyroptotic response in this species as well (Newman et al., 2010).

The protease activity of LF is critical for activation of NLRP1B and CASP1-dependent pyroptosis, since catalytically inactive mutants of LF fail to trigger pyroptosis (Fink et al., 2008; Klimpel et al., 1994). This observation immediately suggested that LF was unlikely to activate NLRP1B by acting simply as a ligand, and instead implied that NLRP1B could sense the protease activity of LF, directly or indirectly. Boyden and Dietrich (Boyden and Dietrich, 2006) initially proposed that NLRP1B could be a direct proteolytic substrate of LF, as depicted in Fig. 1.2A ("Direct Activation Model"), but this model was difficult to experimentally support at the time. In addition, the Direct Model of NLRP1B activation was further complicated by the observation that proteasome and N-end rule inhibitors blocked NLRP1B activation. Importantly, these inhibitors did not block activation of other inflammasomes such as NAIP5/NLRC4 (Fink et al., 2008; Squires et al., 2007; Wickliffe et al., 2008a, b). In addition, these inhibitors did not affect LF entry or MAPKK cleavage. Thus it appeared the inhibitors were acting specifically on

NLRP1B. Taken together, these observations led to an "Indirect Activation Model" (Fig. 1.2B) in which LF cleaves a negative regulator of NLRP1B, leading to N-end rule and proteasome-dependent degradation of the negative regulator, and release of NLRP1B inhibition.

Ultimately, it was studies of the rat *Nlrp1* locus by the Moayeri and Leppla groups that returned the field to the "Direct Cleavage" model. While several rat alleles of the *Nlrp1* locus were discovered, they were significantly less polymorphic compared to those of mice. Two of the alleles that exhibited differential LeTx responsiveness varied by fewer than 20 residues (Newman et al., 2010). Evaluation of all the rat alleles suggested that the determinants for LF-responsiveness were dictated by the first 100 N-terminal residues of NLRP1. These same investigators later identified a potential LF-consensus cleavage site in the N-terminal portion of the CDF (LF-responsive) NLRP1 protein that was absent in the LEW (LF-unresponsive) NLRP1 variant (Levinsohn et al., 2012). The ability of LF to cleave the CDF responsive-allele of NLRP1 was then experimentally confirmed in cells and with purified proteins, indicating that LF cleavage could be direct. Mutagenesis of the proposed LF target site in the CDF-allele to residues found in the LEW allele abrogated cleavage, and importantly, also abrogated the ability of the protein to activate CASP1. These data provided evidence for a correlation between LF-dependent cleavage and activation of NLRP1, but they did not establish cleavage is sufficient for NLRP1 activation. Indeed it remained possible that mutation of the cleavage site altered the structure and function of NLRP1 in unintended ways. Furthermore, it was expected that mouse NLRP1B, which also responds to LeTx, should be activated via the same mechanism as rat NLRP1, but primary sequence comparisons did not indicate clear conservation of the LF-cleavage site in mouse NLRP1B (Chavarria-Smith and Vance, 2013; Hellmich et al., 2012), raising the question of whether the mouse NLRP1B was also activated by cleavage.

Hellmich and colleagues eventually determined that mouse NLRP1B was also cleaved directly by LF (Hellmich et al., 2012). However, both an LF-responsive NLRP1B variant (from BALB mice) and a non-responsive NLRP1B variant (from NOD mice) were cleaved by LF, implying that LF cleavage could not be the only polymorphic determinant controlling NLRP1 inflammasome formation in mice. Indeed, the NOD allele is likely inactive because it does not auto-process its FIIND domain (Frew et al., 2012), a necessary maturation step required prior to inflammasome activation (see above). The authors noted that each NLRP1B protein is preferentially cleaved at slightly different positions: between K38-L39 for the BALB allele, and K44-L45 for the NOD allele. Since the primary sequence surrounding both of these sites between the two strains is identical, other portions of the two proteins must dictate site specificity. Importantly, it also remained unclear if cleavage by LF was required or sufficient for mouse NLRP1B activation.

Following on from the above observations, we also found that LF was also able to cleave the N-terminus of the LF-responsive NLRP1B variant from BALB mice (Chavarria-Smith and Vance, 2013). Mutation of putative cleavage sites, including both sites found by the Moayeri group, revealed that K44-L45 is the most likely LF cleavage site. Importantly, a strict correlation between cleavage sensitivity and inflammasome activation was observed, again suggesting that cleavage of NLRP1B is required for its activation by LF. To address the further question of whether N-terminal cleavage was sufficient to induce activation of NLRP1B, we replaced the LF-cleavage site in NLRP1B with a Tobacco Etch Virus (TEV) protease cleavage site. The resulting NLRP1B-TEV variant could be activated by cleavage by TEV protease in the absence of LF. Importantly, the TEV protease is highly specific; thus, our results indicated that while LF may cleave other substrates in cells, cleavage of these other substrates does not appear to be

required for NLRP1B activation. Since the TEV system can be used to activate NLRP1B in the complete absence of LF, our data also imply that NLRP1B need not bind LF in order to be activated. Instead, the data are most consistent with a model in which direct cleavage of NLRP1B is sufficient for its activation (Fig. 1.2A). This model is also consistent with our data indicating that expression of a 'pre-cleaved' NLRP1B protein, lacking the first 44 residues, is constitutively active and able to induce IL-1B processing in the absence of LF.

As mentioned above, a major piece of evidence in favor of the Indirect Model of NLRP1 activation was the observation that proteasome inhibitors are able to potently and specifically block NLRP1B activation by LF. How can this observation be reconciled with the now favored Direct Model of NLRP1 activation? One possibility is that the N-terminal 44 amino acid fragment of NLRP1B that is liberated by LF-dependent cleavage must be degraded before NLRP1B activation can proceed. However, overexpression of this N-terminal fragment did not reduce inflammasome formation, as might be predicted if it performed an inhibitory function. In addition, the proteasome inhibitor MG-132 also failed to block cleavage of NLRP1B (Chavarria-Smith and Vance, 2013). Therefore it remains unknown how this inhibitor blocks NLRP1B activation.

The precise biochemical mechanism by which NLRP1B is activated upon cleavage remains unclear. A simple model is that the N-terminus is necessary to maintain auto-inhibition, perhaps via an interaction with the LRR domain, which is also known to be required for maintaining NLRP1B in an inactive state prior to LF cleavage. Whether there is a direct interaction between the N-terminus and the LRR remains unknown. Auto-inhibition of NLRP1B (and inducible activation by LF cleavage) can surprisingly be maintained even when the N-terminus of NLRP1B is truncated up to residue 40 (Neiman-Zenevich et al., 2014). Confusingly, however, TEV-induced cleavage in the context of a full-length NLRP1B at this same position (between amino acids 38 and 39) gave a different result, and produced an active NLRP1B (Chavarria-Smith and Vance, 2013). Nevertheless, it does not appear that the N-terminus must be cleaved at a very precise location in order to activate NLRP1B, raising the attractive possibility that other proteases from different microbial or host sources might also be able to activate NLRP1B. If there is selective pressure for NLRP1 to evolve to be cleaved by other pathogen-derived proteases, it could explain why the N-terminal portions of NLRP1B in mice and rats tend to be highly variable (Boyden and Dietrich, 2006; Newman et al., 2010). Indeed, it may be unlikely that infection with *B. anthracis* is itself a major natural selective pressure driving the evolution of murine NLRP1B, since in the wild, *B. anthracis* appears primarily to infect grazing herbivores. It is currently unknown if the N-terminus of NLRP1 of other species, such as humans, also performs a role in auto-inhibition, and thus, it is unknown whether human or primate NLRP1 proteins are also activated by proteolysis. Human NLRP1 does not appear to contain an obvious LF cleavage site and has not been shown to be cleaved or activated by LF (Moayeri et al., 2012). As mentioned above, NLRP1 in most species, with the exceptions of rodents, has an N-terminal Pyrin domain (PYD) followed by a linker region to the NBD (Fig. 1.1). So far, it has not been functionally shown that this PYD is important for recruiting ASC or any other protein. Instead, over-expression studies indicate that the PYD is dispensable for CASP1 activation and/or ASC binding, because the C-terminal CARD of NLRP1 is able to perform these functions (Finger et al., 2012). This suggests that it is at least possible that a protease could cleave the linker region between the PYD and the NBD, and activate other forms of NLRP1.

Prediction of what additional proteases, if any, might cleave NLRP1 is not straightforward. Indeed, it was not even immediately obvious that NLRP1 in rodents could be a substrate of LF. For one, LF does not have a stringently defined cleavage consensus sequence. The LF target sequence appears to be defined by a few positively charged residues and hydrophobic residues (+++ x h+h) (Turk, 2007), which can be found in many protein sequences by chance. In addition, the site cleaved by LF in NLRP1 in mice and rats does not perfectly satisfy the ideal consensus LF-site (Chavarria-Smith and Vance, 2013; Hellmich et al., 2012; Levinsohn et al., 2012). Furthermore, it appears that the specificity of LF for substrates might not be dictated entirely by the amino acid sequence within the cleavage site. The MAPKKs have been reported to bind LF even when the cleavage site is entirely missing, and thus interaction of LF with other regions of its substrates could influence substrate specificity (Turk, 2007). Non-cleavage site interactions could explain why the two mouse variants (BALB and NOD) of NLRP1 were reported to be cleaved at different sites despite the cleavage site itself being identical (Hellmich et al., 2012). Another difficulty in predicting the protease sensitivity of NLRP1 proteins is that even incomplete or inefficient cleavage appears sufficient for activation. For example, mouse NLRP1B does not seem to be an ideal substrate for LF. The MAPKKs can be almost completely cleaved within 1-2 hours in cells treated with LeTx, but in this same timeframe, only a small fraction of NLRP1B is cleaved (Chavarria-Smith and Vance, 2013; Hellmich et al., 2012; Levinsohn et al., 2012). Cleavage *in vitro* with purified protease is similarly inefficient. It is unknown how much of the relative pool of NLRP1B inside the cells must be cleaved in order to form an inflammasome. However, given that mouse macrophages show robust signs of pyroptosis, CASP1 and IL-1B processing within 90 minutes (Fink et al., 2008; Nour et al., 2009; Wickliffe et al., 2008a), and that at this time point only a small fraction of NLRP1B is cleaved (Chavarria-Smith and Vance, 2013; Levinsohn et al., 2012), one can infer that the threshold for inflammasome formation is low, and that cleavage of a small fraction of NLRP1B is sufficient for functional NLRP1B activation. Mechanistically it is unclear if only the N-terminally cleaved NLRP1B molecules assemble to form an inflammasome, or if bystander (uncleaved) NLRP1 molecules cooperate in formation of the scaffolding and CASP1 recruitment platform. This may be especially relevant if NLRP1 protomers are already in a preformed complex that does not induce CASP1 dimerization and activation until an N-terminal cleavage event produces a conformational shift of one of the molecules that transmits a "signal" to activate partner NLRP1s. Addressing these mechanistic questions will require biochemical and structural dissection of NLRP1 activation.

1.2.2 NLRP1 activation by bacterial muramyl dipetide (MDP)

While murine and rat NLRP1 can be directly activated by LF cleavage, the mechanism of human NLRP1 activation has been unclear. An early study of the mechanism by which human NLRP1 is activated used a cell-free system with recombinant purified NLRP1 (Faustin et al., 2007). In this study, it was observed that a fragment of bacterial petidoglycan, muramyl dipeptide (MDP), was able to induce ATP binding and oligomerization of NLRP1, and these processes correlated with CASP1 activation. The specificity of this stimulus was confirmed with the use of synthetic MDP, and the fact that the LD, but not the DD, enantiomer of MDP was capable of inducing CASP1 activation. Furthermore, MDP was able to induce a mobility shift of monomeric NLRP1 when analyzed by native PAGE. This shift was greatly enhanced in the presence of Mg^{2+}/ATP, suggesting an oligomer or inflammasome complex had been assembled. The most straightforward interpretation of these results was that MDP bound to NLRP1, resulting in exchange of ADP for ATP, and hence NLRP1 oligomerization. However, a

limitation of this study was that it did not demonstrate whether MDP binds NLRP1 directly, nor what domain within NLRP1 is involved in ligand-sensing. A further confusing aspect of this study is that the purified NLRP1 did not show any signs of FIIND auto-processing, which is now known to be critical for NLRP1 to induce CASP1 activation in cells (Finger et al., 2012; Frew et al., 2012). The lack of FIIND processing may be explained by the fact that the version of human NLRP1 used in the study was reported to lack exon 14, and the region of the protein encoded by this exon seems necessary for FIIND processing and NLRP1 activation (Finger et al., 2012). It is possible that when analyzing purified protein *in vitro*, the necessity for FIIND processing for CASP1 activation can be overcome, but that this is not the case when studying activation of NLRP1 in mammalian cells. Nevertheless, the relevance of the observations using purified NLRP1 in an *in vitro* cell-free system remains unclear, and there is no consensus as to whether MDP is a true NLRP1 ligand.

Later studies evaluated the ability of MDP to activate NLRP1 in cells. This has been a controversial area, due to the fact that other cytosolic sensors of MDP have also been proposed, namely NOD2 and NLRP3 (Girardin et al., 2003; Inohara et al., 2003; Martinon et al., 2004). One study used the macrophage-like human cell line THP-1. Upon stimulation of these cells with MDP and ATP (2.5mM), IL-1B processing and co-immunoprecipitation of NLRP1 with ASC was observed. This result is difficult to interpret given that extracellular ATP at this concentration is sufficient to activate the NLRP3 inflammasome via P2X7R, when cells are primed to express NLRP3 (Mariathasan et al., 2006; Solle et al., 2001). In this case, MDP stimulation, probably acting via NOD2, appears sufficient to prime NLRP3 expression. The dependency of the response of THP-1 cells to MDP on NLRP1 was confirmed via the use of a single siRNA oligo in THP-1 cells. Given that siRNAs are now appreciated to frequently produce off-target effects, it would be interesting to test the role of NLRP1 in the response of THP-1 cells to MDP by generating NLRP1 knockout cells using CRISPR-Cas9 systems.

The ability of MDP to activate NLRP1 was also tested in murine macrophages of a B6 background (Bruey et al., 2007; Hsu et al., 2008), which express *Nlrp1a/b (Sastalla et al., 2013)*, but are not responsive to LeTx (Boyden and Dietrich, 2006). Bruey et al observed MDP-dependent IL-1B and CASP1 processing, but the NLRP1 dependency of this response was not directly tested. Hsu et al stimulated macrophages with MDP and TiO_2, and observed CASP1 and IL-1B processing (Hsu et al., 2008). The use of TiO2 is claimed to enhance intracellular delivery of MDP. Unfortunately, TiO_2 nanoparticles are also known to activate NLRP3 in cells that have been primed with LPS (Yazdi et al., 2010). Nonetheless, this group excluded a role for NLRP3, as they observe the same effect of MDP within macrophages of an *Nlrp3*-deficient mouse. The Hsu et al study also established that NOD2 is required for the response to MDP, consistent with the established role for NOD2 in sensing MDP (Girardin et al., 2003). However, their surprising conclusion was that NOD2 does not activate a transcriptional response to MDP, but instead, co-associates with NLRP1 to form a complex that activates CASP1. The authors observe CASP1 directly binding to the CARDs of NOD2, but it is unclear what role NLRP1 would provide in CASP1 activation if NOD2 both responds to MDP and directly recruits CASP1. The dependency on NLRP1 for this response was shown again with the use of a single shRNA targeting NLRP1 in human THP-1 cells, and this is only able to partially reduce the IL-1B responses upon stimulation. A different study evaluated pyroptosis of human macrophage cell lines, including THP-1 cells, when electroporated in the presence MDP, and observed no substantial change in cell viability (Shi et al., 2014). This would suggest that NLRP1 is not being activated by MDP under these conditions.

Another recent study used newly generated *Nlrp1b* knock-out mice on the 129S genetic background (Kovarova et al., 2012). The 129S allele of *Nlrp1b* is normally responsive to LeTx. This study established that the MDP+TiO_2 response is completely *Nlrp1b*-independent, while the LeTx response is strictly *Nlrp1b*-dependent. Instead, macrophages primed with LPS were found to secrete IL-1B in response MDP+TiO_2 and TiO_2 alone, in an *Nlrp3*-dependent manner. No single model can reconcile all of these observations, but one model we favor is that MDP acts primarily to potentiate NLRP3 priming via activation of NOD2-RIP2 transcriptional signaling. The second signal for NLRP3 activation is then provided by ATP or TiO_2. In this model, MDP would not function as a direct ligand for NLRP1. Consistent with this model, another group failed to detect an interaction between MDP the NLRP1 LRR domain (Reubold et al., 2014). Alternatively, it also possible that the B6 alleles of *Nlrp1* and/or the human ortholog do respond to MDP, but this needs to be carefully evaluated with gene knockout models.

1.2.3 Rodent NLRP1 activation in response to *Toxoplasma gondii*

Another stimulus proposed to activate NLRP1 is infection with the parasite *Toxoplasma gondii*. Interestingly, rat strains of different genetic backgrounds exhibit large differences in resistance to *T. gondii* (Cavailles et al., 2006). This motivated the genetic mapping of loci that could explain such differences in resistance. A 1.7cM *Toxo1* locus was identified on Ch10, spanning >7.6Mb and encoding over 86 putative genes, including *Nlrp1* (Cavailles et al., 2006). This locus was recently narrowed down by two groups to a region less than 1Mb in length (Cavailles et al., 2014; Cirelli et al., 2014). Further analysis by both groups strongly implicated *Nlrp1* as the primary candidate gene that dominantly provides resistance to *T. gondii* infections. The resistance observed during infections with *T. gondii* correlated with signs of inflammasome activation *in vitro*, but interestingly, responses to *T. gondii* did not correlate with responses to LeTx. For example, macrophages from *T. gondii*-resistant LEW rats, which encode a LeTx non-responsive allele of *Nlrp1* (Newman et al., 2010), undergo lytic cell death and IL-1B processing and secretion in response to *T. gondii* infection (Cavailles et al., 2014; Cirelli et al., 2014; Ewald et al., 2014). Conversely, macrophages from *T. gondii*-susceptible CDF or BN rats, which encode a LeTx responsive allele of *Nlrp1*, remain mostly viable over the same time period and do not secrete IL-1B readily. Furthermore, knockdown of *Nlrp1* in LEW rat macrophages increased host cells' viability, presumably because they no longer underwent CASP1-dependent pyroptosis (Cirelli et al., 2014). Conversely, over-expression of the LEW *Nlrp1* allele in CDF rat macrophages resulted in a loss in host cell's viability, or pyroptosis, upon *in vitro* infection with *T. gondii* (Cirelli et al., 2014). With the development of new genetic tools such as CRISPR-Cas9 systems to modify genomes, it will be interesting to confirm these results *in vivo*.

Furthermore, the mechanism by which *T. gondii* activates NLRP1 is unknown. The two rat alleles that differ in their responses to *T. gondii* exhibit fewer than 20 amino acid polymorphisms and most of these differences are clustered near the N-terminus (Newman et al., 2010). These same residues determine responsiveness of NLRP1 to LF, but as mentioned above, LF-responsive alleles are non-responsive to *T. gondii*, and *vice-versa*. This raises the obvious question of whether *T. gondii* secretes a protease with a cleavage site specificity distinct from LF into the cytosol of infected macrophages, where it could cleave and activate NLRP1. Moayeri and colleagues also noticed that rat NLRP1 was only able to induce pyroptosis when it was introduced into non-responsive rat macrophage cell line, but not when it was introduced into a mouse macrophage cell line, or human cell lines that also expressed *Casp1* and *Il1b* (Cirelli et al., 2014). This observation implies a role for species-specific factors in NLRP1 activation, and thus appears to conflict with a simple direct cleavage model. Instead, the authors speculate that a

rat or macrophage specific positive or negative regulator might respond to *T. gondii* and regulates NLRP1 activation in a manner dependent on amino acid polymorphisms found at the NLRP1 N-terminus.

Inflammasome activation by *T. gondii* in mice was also recently evaluated by two research groups (Ewald et al., 2014; Gorfu et al., 2014). In both studies, bone marrow macrophages were found to induce significant amounts of IL-1B upon *T. gondii* infection. The dependency of this response on NLRP1 is not as clear as is seen with rats, and significant differences *in vitro* and *in vivo* were observed, especially with respect to the contributions of other NLRs. Both groups observed *Nlrp3*-dependent inflammasome activation in response to *T. gondii*, but only one group saw enough residual IL-1B in *Nlrp3*$^{-/-}$ cells to propose that NLRP1 could be playing a role in macrophage inflammasome activation (Ewald et al., 2014). Gorfu and colleagues observed no reduction of IL-1B release in macrophages lacking the *Nlrp1a,b,c* cluster, suggesting that *T. gondii* does not significantly activate NLRP1 *in vitro* (Gorfu et al., 2014). Somewhat surprisingly, however, this same study observed a resistance defect during acute *T. gondii* challenges in *Nlrp1* cluster KO mice. Since the *Nlrp1*-deficient mouse was made in a B6 background, it could be that these alleles of *Nlrp1a* and *Nlrp1b* are not very responsive to *T. gondii,* and are incompletely responsive to LeTx. This possibility was explored by Ewald et al as they first noticed that macrophages from a 129 mouse can induce nearly five times more IL-1B as compared to B6 macrophages during *T. gondii* infections. To test whether the NLRP1B allele of 129 mice is responsive to *T. gondii* infection, a copy of the 129 allele of *NLRP1B* was introduced into a B6 macrophage cell line (Ewald et al., 2014). This genetic complementation enhanced the IL-1B and pyroptotic response. This suggests that murine NLRP1B is able to sense *T. gondii*, but is less robustly responsive than the rat alleles. This may also explain why pyroptosis of mouse macrophages is not readily detectable during *T. gondii* infections (Ewald et al., 2014; Gorfu et al., 2014).

As in rats, the mechanism of NLRP1 activation by *T. gondii* in mice is still unclear. No cleavage of the mouse 129 NLRP1B variant was observed in cell lysates or supernatants of infected cells (Ewald et al., 2014). While this might suggest that the response is cleavage-independent, proteolytic activation of NLRP1B in *T. gondii* infection cannot be entirely ruled out, as it is often difficult to detect the N-terminal cleavage product (Ewald et al., 2014).

Human susceptibility to congenital toxoplasmosis has been linked to *NLRP1* polymorphisms (Witola et al., 2011). This study assessed the effect of knocking down *NLRP1* transcript levels in a human macrophage-like cell line, and knockdown of *NLRP1* was found to decrease macrophage viability in culture over the time of the infection. This is surprising if indeed human NLRP1 senses *T. gondii*, since one might expect that a decrease in NLRP1 should hinder pyroptosis and increase macrophage viability. However, parasite replication did increase in cells lacking NLRP1, and the authors speculate that unregulated parasite growth and egress could explain the increase in host cell death. The levels of processed IL-1B were also reduced with NLRP1 knockdown, but so were the transcripts of *IL1B*, *IL18* and *CASP1*, raising doubts about the specificity of the knockdown shRNA. The SNPs associated with congenital toxoplasmosis were also not mechanistically investigated (Witola et al., 2011).

1.2.4 NLRP1 activation by reduction in cellular ATP levels

In addition to sensing microbial stimuli, NLRP1 has also been proposed to detect metabolic disturbances (Liao and Mogridge, 2013). Mogridge and colleagues found that reduction of cellular ATP production by chemical inhibition of glycolysis and oxidative phosphorylation led to NLRP1B and CASP1-dependent IL-1B processing and secretion in

fibroblasts reconstituted with the NLRP1B inflammasome. The amount of cellular ATP inversely correlated with NLRP1B-dependent inflammasome formation. Detectable responses were observed when ATP levels were reduced to 70%, and when hypoxic conditions were combined with low glucose availability, suggesting that ATP-depletion could be a physiological trigger of NLRP1. Interestingly, this response differed from the response to LeTx in that it was partially dependent on ROS production and AMPK phosphorylation, which is activated when high AMP/ATP ratios are achieved in the cell. LeTx was not observed to cause ATP level to decrease, and ATP deprivation did not induce measurable N-terminal cleavage of NLRP1, suggesting the two responses are mechanistically distinct. This was confirmed in a later study, in which an LF-cleavage resistant full-length NLRP1B, and several N-terminal truncations of NLRP1B that are LF-unresponsive, were found to be responsive to metabolic disruption (Neiman-Zenevich et al., 2014). Comparison of the 129 and CAST alleles indicates that the 129 allele induces more IL-1B secretion in response to ATP depletion, even though both respond comparably to LeTx. The 129 allele of NLRP1B contains a repeat within the FIIND that is not found in the CAST allele, and deletion of either one of these repeats in the 129 NLRP1 protein blunts the metabolic inhibition response, but does not affect the LeTx response. Consequently, the authors hypothesize that these repeated segments are involved in the sensing of ATP levels by an unknown mechanism. Interestingly, mutation of the ATP-binding Walker A motif of NLRP1B caused NLRP1B to exhibit spontaneous inflammasome activity. This was a surprising finding, given that ATP binding is required for the activation of other NLR family members, including NLRP3, NOD2, NOD1 and human NLRP1 (Faustin et al., 2007; Neiman-Zenevich et al., 2014; Tanabe et al., 2004). However, it appears that ATP binding may negatively regulate NLRP1 and this may explain how NLRP1 responds to decreased cellular levels of ATP. Further testing in primary bone marrow macrophages from *NLRP1* knock-out mice would be ideal to confirm a role for NLRP1 in sensing of altered ATP levels. It would also be interesting to test if this is a conserved response in rat and human variants of NLRP1 and whether it plays any role *in vivo*.

1.2.5 Role of NLRP1 in pathogen resistance

The ability of LeTx to induce pyroptosis of murine macrophages and dendritic cells was initially thought to be part of the virulence mechanism of the toxin that reduced bacterial clearance by these phagocytes (Terra et al., 2010). Two studies later carefully tested the role of NLRP1B during *B. anthracis* infections and arrived at the conclusion that the inflammasome response induced by LeTx is actually host-protective. One group used congenic mice expressing two different alleles of *Nlrp1b*, one LeTx-responsive and the other not, in a B6 background (Moayeri et al., 2010). The other group used a transgenic mouse line that expresses the LeTx-responsive *NLRP1B* allele 1 in the B6 genetic background (Terra et al., 2010). Both groups observed that NLRP1 activation provided increased resistance to lethal challenge with *B. anthracis*. The protective role of NLRP1B in inflammasome activation was independent of the route of infection and whether the bacteria were in spore or vegetative form. The enhanced resistance was further shown to require *Casp1*, *Il1r*, and neutrophil-dependent clearance (Moayeri et al., 2010). Taken together, the results suggest that NLRP1 activation protects against *B. anthracis* infection by induction of IL-1B secretion, downstream chemokine production, neutrophil recruitment to the site of infection, and phagocytosis and killing of the bacteria.

Systemic administration of purified LeTx in mice is sufficient to induce animal death, but this is independent of NLRP1B, and can take more than 48h, much slower than typical inflammasome responses (Moayeri et al., 2004; Moayeri et al., 2012; Terra et al., 2010). Instead, the LF-induced lethality observed in mice requires LF entry into cardiomyocytes and vascular

smooth muscle cells (Liu et al., 2013). Surprisingly, and in contrast to mice, LeTx intoxication of rats does appear to be dependent on NLRP1 and can occur in less than an hour (Newman et al., 2010). In rats, the lethal effects of LF are consistent with a vascular collapse similar to what has been observed with systemic activation of the NAIP5/NLRC4 inflammasome in mice (von Moltke et al., 2012b). Mice also exhibit a rapid systemic response to LF (Terra et al., 2010; Terra et al., 2011) but for reasons likely related to the expression levels of key effector proteins, this response is not lethal as it is in rats.

As mentioned above, the role of NLRP1 during *Toxoplasma gondii* infections is most evident in rats. Rats that express LeTx-non-responsive but *T. gondii*-responsive Nlrp1 alleles, such as LEW rats, are able to clear parasites early during the acute phase of infection, which reduces the establishment of cysts in tissues such as the brain or muscle (Cirelli et al., 2014). Rats with alleles of *Nlrp1* that do not show signs of inflammasome activation with *T. gondii* develop chronic infections and form transmissible cysts. In mice, NLRP1 also seems to have an important protective role during *T. gondii* infections (Gorfu et al., 2014), but the role of allelic differences in *Nlrp1* has not been directly tested *in vivo*. Furthermore, inflammasome-dependent resistance to *T. gondii* in mice is likely to result from a combination of the activation of both NLRP3 and NLRP1 *in vivo*. Two groups observed that Casp1/11 knockout mice exhibit higher parasite burdens, but the studies differed in whether there are effects during the acute or chronic phase of infection (Ewald et al., 2014; Gorfu et al., 2014). Gorfu et al observed NLRP1-dependent survival of mice and a reduction in parasite burden during acute *T. gondii* infection. The combined protection provided by of NLRP1 and NLRP3 activation is dependent on IL-18 and IL-1 receptor signaling. The authors proposed that pyroptosis itself could limit growth and dissemination of parasites early in infection, and that IL-18 could provide additional protection via the induction of IFN-g. Ewald et al observed a role for CASP1 in preventing cyst formation during the chronic phase, but little effect on the health of the animals during the acute phase, as monitored by body weight (Ewald et al., 2014). It will be interesting to test *Nlrp1b*-deficiency in the 129 genetic background, as *in vitro* experiments suggest that the 129 *Nlrp1b* allele is more responsive to *T. gondii* (Ewald et al., 2014).

1.2.6 NLRP1 polymorphisms and disease

Single nucleotide polymorphisms (SNPs) in the vicinity of the *NLRP1* gene have been associated with autoimmune, autoinflammatory and other diseases including vitiligo, rheumatoid arthritis, systemic sclerosis, Crohn's disease, and melanoma (Finger et al., 2012). Many of these are in non-coding regions and may thus affect transcription of *NLRP1*, but this needs further evaluation (Jin et al., 2007). Of those SNPs that affect the protein primary sequence, few have been tested for their functional affects in isolation (Levandowski et al., 2013), with the exception of M1184V. NLRP1 M1184V exhibits increased FIIND processing and an increased ability to induce IL-1B processing, when over-expressed in fibroblasts, as compared to wild-type NLRP1 (Finger et al., 2012). This hyperactive phenotype might explain its association with disease risk.

An interesting example of the effects of spontaneous NLRP1 activity was uncovered during a forward genetic screen in mice (Masters et al., 2012). A mutant mouse with a neutrophilic phenotype was identified, and the causative mutation was mapped to *Nlrp1a*. This mutation causes an amino acid substitution at glutamine 593 to proline (Q953P) in a region between the NBD and the LRR. This mutation likely produces a constitutively active version of NLRP1A, as no secondary stimulus was required for IL-1B production of LPS primed macrophages. This report provided the first indication that NLRP1A is also able to form an inflammasome, as only NLRP1B had previously been known to do. Mice that were homozygous

for the Q953P mutation succumbed to death between 3-5 months of age. These mice have neutrophil numbers that are 15 higher than wild type mice, and exhibit significant lymphopenia and splenomegaly. The disease could be rescued by crossing the mice to *Casp1/11*$^{-/-}$, or *Il1r*$^{-/-}$ backgrounds, confirming a role for the inflammasome in the phenotype of the mice.

1.2.7 Host and Viral Regulators of NLRP1

As described above, inappropriate or excessive inflammasome activation can lead to significant pathology. Thus, negative regulation of inflammasome activation is likely critical to prevent this pathology. Direct negative regulation of NLRP1 has been demonstrated by Bcl-2 and Bcl-XL proteins, which are also important in regulation of apoptosis (Bruey et al., 2007). These two proteins were found to bind NLRP1, but not other NLRs, in an LRR-dependent manner. The binding of Bcl-2/XL is postulated to prevent NLRP1 from efficiently forming an inflammasome. The region of Bcl-2/XL that is sufficient to negatively regulate NLRP1 was narrowed to a small flexible loop that is not required for regulation of apoptosis. A synthetic peptide that mimics this loop of Bcl-XL is sufficient to recapitulate this activity of the full-length protein in a cell-free system. Binding of this loop prevents ATP binding of NLRP1 and hence blocks its oligomerization into an inflammasome. This proposed mechanism of inhibition is interesting, given that ATP binding appears to negatively regulate the murine NLRP1 ortholog, as discussed above. This may reflect a fundamental difference in how human and mouse NLRP1 are regulated. It is also unclear how Bcl-2 regulation is bypassed in the presence of cognate NLRP1 stimuli. The authors note that the loop is known to undergo post-translational modifications that could be induced by other cellular signaling pathways, and this could license NLRP1 for activation, but so far this has not been demonstrated. Bcl-2 is also claimed to negatively regulate the murine ortholog of NLRP1, but in these experiments, MDP was used to activate NLRP1. As discussed above, it is not clear this is a bona fide agonist for mouse NLRP1. It would thus be interesting to test the role of Bcl-2 in response to LeTx-dependent activation of NLRP1B.

Viruses frequently evolve mechanisms to evade host immunity. Vaccinia virus (VV), a poxvirus, encodes several anti-apoptotic Bcl-2 homologues, and one of these, F1L, has also been shown to bind and negatively regulate NLRP1 (Gerlic et al., 2013). F1L, like Bcl-2/XL, shares the ability to block ATP binding of NLRP1 when tested *in vitro*. Vaccinia virus mutants that lack F1L induce more IL-1B production in human THP-1 cells, consistent with NLRP1 negative regulation. F1L is also able to bind mouse NLRP1, but an inhibitory effect was not directly tested. Infection of mice with Vaccinia Virus lacking F1L or with F1L mutants that do not bind NLRP1 had reduced lethality and virulence. An important caveat with this study is that these effects were not shown to be NLRP1B or CASP1-dependent. Furthermore, viral titers were not consistently lower, raising questions about the precise mechanism of resistance. How VV activates NLRP1 in the absence of F1L has not been directly examined. As expected for a DNA virus, the main inflammasome activated by VV appears to be the AIM2 inflammasome, not NLRP1 (Hornung et al., 2009; Rathinam et al., 2010). Kaposi's Sarcoma-associated Herpes Virus (KSHV or HHV8) has also been proposed to encode a negative regulator of NLRP1 (Gregory et al., 2011). The Orf63 gene of KSHV encodes a protein that is predicted to have sequence similarity to NLRP1's NBD and LRR domain. Orf63 was shown to bind NLRP1, NOD2 and NLRP3, and ectopic expression of Orf63 was able to reduce IL-1B secretion in THP-1 cells that were stimulated with MDP. Unfortunately, the NLRP1 dependence of the response was not tested. Orf63 was further suggested to prevent CASP1 recruitment of NLRP1 and

reduce NLRP1 self-association. KSHV infection of primary human monocytes induces low levels IL-1B secretion, and this is modestly enhanced by *Orf63* knockdown. The mechanism by which HSHV, another DNA virus, would activate NLRP1 in the absence of Orf63 has also not been explored.

1.2.8 Models of activation and comparison to other inflammasomes

As should be evident from the above discussion, the biochemical mechanism of NLR activation is in general poorly understood, and it is unclear how much mechanistic conservation exists among various NLRs. The NAIP/NLRC4 inflammasomes provide an interesting contrast with the NLRP1 inflammasome. Each NAIP/NLRC4 inflammasome contains two different NLRs: a NAIP (NLR family, apoptosis inhibitory protein) family member, and NLRC4 (NLR family, CARD domain containing 4). Distinct from the mechanisms discussed above for NLRP1, the NAIP/NLRC4 inflammasomes appear to be activated in a prototypical receptor-ligand manner (Kofoed and Vance, 2011; Zhao et al., 2011). Different NAIP proteins have been shown to directly bind specific cognate bacterial protein ligands, such as flagellin. This binding promotes the co-oligomerization of ligand-bound NAIPs with NLRC4 and subsequent recruitment of ASC and CASP1 (Kofoed and Vance, 2011). The NAIP/NLRC4 proteins are believed to reside in the cytosol in a monomeric state prior to stimulation, and the LRR domains in NAIP and NLRC4 are required to maintain them in this state. Originally it was believed that ligand recognition occurs via the LRR, resulting in relief of LRR-mediated autoinhibition. However, more recent data have suggested that ligand recognition appears instead to be determined by a helical domain proximal to the NBD (Tenthorey et al., 2014). Specifically how ligand binding promotes NBD-mediated oligomerization has not been experimentally determined. As discussed above, and in contrast to activation of NAIP/NLRC4, mouse NLRP1B does not follow a ligand-receptor mode of activation when activated by LF. Instead, LF proteolytically cleaves the N-terminus of NLRP1B, resulting in NLRP1B activation. Since the activating cleavage event can be carried out by an ectopic protease, it appears that NLRP1 does not need to directly recognize LF as a ligand in order to be activated (Chavarria-Smith and Vance, 2013). Thus, the ligand-dependent mechanism of NAIP/NLRC4 activation does not appear to apply to NLRP1B.

NLRP1B also differs from NLRC4 in that NLRP1B does not seem to be monomeric prior to inflammasome activation. Size exclusion chromatography reveals that NLRP1B is already in a large complex around 800kDa in lysates of unstimulated macrophages. LeTx stimulation results in CASP1 recruitment to this pre-formed NLRP1B complex (Nour et al., 2009). One model is that the pre-assembled NLRP1B complex is in a conformation that is not able to induce CASP1 dimerization and activation, and N-terminal cleavage induces conformational changes within the oligomer that promotes CASP1 binding and dimerization. In the NAIP5/NLRC4 inflammasome, the NBD domains are necessary to mediate oligomerization (Kofoed and Vance, 2011). The domains required for NLRP1 to form a complex that can activate CASP1 seems to be different from other NLRs. This is evident when analyzing mutants of NLRP1B that completely lack the NBD-LRR, as they still self-associate, and are spontaneously active (Frew et al., 2012; Liao and Mogridge, 2009). Assembly of the NLRP1 inflammasomes instead appears to be mediated by a small portion of the FIIND and CARD, at least in overexpression scenarios. This suggests that the rest of NLRP1B is not required for oligomerization, but may instead play a role in maintaining the protein in the inactive state. Upon N-terminal cleavage, these domains transduce a signal to the C-terminal effector domain to promote CASP1 dimerization. The composition of the inactive versus active complex is unknown. For example, while FIIND processing is a

requirement for inflammasome activation, it is unknown if all of the subunits in the active complex have a processed FIIND. Indeed, in unstimulated cells, there appears to be a rough 1:1 ratio of FIIND processed to unprocessed NLRP1 (Frew et al., 2012). Similarly, it is unknown if all of the subunits in the active complex have cleaved N-termini, or if a single cleaved NLRP1 can cause the entire complex to become active.

One feature NLRP1 has in common with most NLRs is that the LRR of NLRP1B plays an essential function in preventing spontaneous activation (Liao and Mogridge, 2009). However, distinct from other NLRs, the N-terminus of NLRP1 also plays a role in auto-inhibition, and whether this involves interactions with the LRR, is unknown. NLRC4 is the only NLR for which a crystal structure has been solved, and this structure suggests that NLRC4 is maintained in an autoinhibited state by *cis* interactions between the LRR and the NBD that fold the protein into a tertiary compact (inactivated) state (Hu et al., 2013). If NLRP1 is pre-oligomerized in the inactive state, then it appears that the mechanism by which the LRRs inhibit NLRP1 would have to be distinct from their role in NLRC4.

It less clear whether human NLRP1 is pre-associated in a complex prior to stimulation. The original description of this inflammasome suggests that human NLRP1 is also in a preformed complex in cellular lysates, and through activation by an unknown signal, the complex promotes co-association of ASC and CASP1 (Martinon et al., 2002). In contrast, a very different model is proposed by the cell-free study of NLRP1 activation by MDP (Faustin et al., 2007). In this model, NLRP1 is monomeric prior to stimulation, and MDP licenses ATP binding and subsequent oligomerization via the NBD. In this model, ATP binding, and most likely hydrolysis, is required for NLRP1 oligomerization. As discussed above, this latter model is complicated by the lack of observable FIIND processing, which is required for human NLRP1 activation (Finger et al., 2012). Structural studies using electron microscopy also indicate that NLRP1 complexes can be found prior to MDP/ATP stimulation, but that the frequency of these complexes increases upon stimulation (Faustin et al., 2007). Thus, mechanistic insights into NLRP1 activation will require further structural studies comparing the unstimulated and stimulated states of NLRP1.

NLRP1 of all species contains a CARD domain (Fig. 1.1). In addition, the NLRP1 proteins of most species, except rodents, also contain a Pyrin Domain (PYD). The presence of two effector domains has caused confusion regarding the role of each domain. The initial description of the NLRP1 inflammasome proposed that the PYD was important for binding of a PYD-CARD adaptor protein, ASC, and that ASC then recruited and activated CASP1 (Martinon et al., 2002). The NLRP1 CARD was proposed to mediate a direct interaction with CASP5. Most studies now indicate that CASP1 can bind directly to the C-terminal CARD domain in the case of mouse and human NLRP1 (Faustin et al., 2007; Frew et al., 2012; Nour et al., 2009). The PYD of human NLRP1 is dispensable for CASP1 activation and binding of ASC, but the NLRP1 CARD is completely required for ASC binding, which presumably occurs via a CARD-CARD interaction (Finger et al., 2012). Thus, the role of the NLRP1 PYD is currently uncertain. Furthermore, upon NLRP1B activation in mice, CASP1 and IL-1B processing are highly dependent on ASC, while pyroptosis is not (Broz et al., 2010). It can therefore be inferred that ASC must also bind NLRP1 via its CARD, and form a focus that efficiently induces processing of CASP1 and its substrates (Broz et al., 2010). CASP11, which is a functional mouse ortholog of CASP5 in humans, has also been shown to bind NLRP1B (Nour et al., 2009). However, CASP11 does not seem to have an essential role in mediating NLRP1-dependent pyroptosis or cytokine processing, as both of these events occur efficiently in macrophages from 129 mice,

which are naturally deficient in CASP11 (Kayagaki et al., 2011). It also appears that the function of human NLRP1 does not require an interaction with CASP5, as the NLRP1 inflammasome and subsequent activities can be reconstituted in 293T cells, which do not express CASP5 (or its paralog, CASP4) (Finger et al., 2012; Franchi et al., 2012). In fact, CASP4/5 and CASP11 have now been identified to have a very different cellular function, namely, to be direct sensors of intracellular LPS. In fact, the function of the CASP4/5/11 CARD appears to be to bind directly to LPS (Shi et al., 2014). Thus it is uncertain whether CASP5 and CASP11 play any physiological role in the function of NLRP1.

1.3 Conclusion

Our understanding of NLRP1 activation has come a long way since the first description of the inflammasome (Martinon et al., 2002). We now know that multiple pathogens and stimuli can activate NLRP1. Moreover, we now understand that direct cleavage is a mechanism of activation of mouse and rat NLRP1, at least in the case of lethal factor protease. Whether NLRP1 can be activated by other pathogen-derived or cellular proteases is an important question to be investigated in future studies.

NLRP1 is just one member of the large and complex NLR protein family. Although the stimuli and molecular mechanisms underlying the activation of most NLRs remain poorly understood, it is already clear that these stimuli and mechanisms differ considerably across NLR family members. Striking differences are apparent even in the comparison of just two NLRs, the NLRP1B and NAIP/NLRC4 inflammasomes. NLRP3 is one of the most studied NLRs, and is known to be stimulated by a wide variety of agonists, but no single unifying molecular model appears to account for NLRP3 activation, and likely its mode of activation will differ from both NLRP1 and NAIP/NLRC4. Thus, further studies of the NLR family is required to gain insight into their breadth of pathogen responses and how their dysregulation is associated with disease.

1.4 Acknowledgement

This section was originally written as a NLRP1 literature review for *Immunological Reviews* volume 65 (Chavarría-Smith and Vance, 2015).

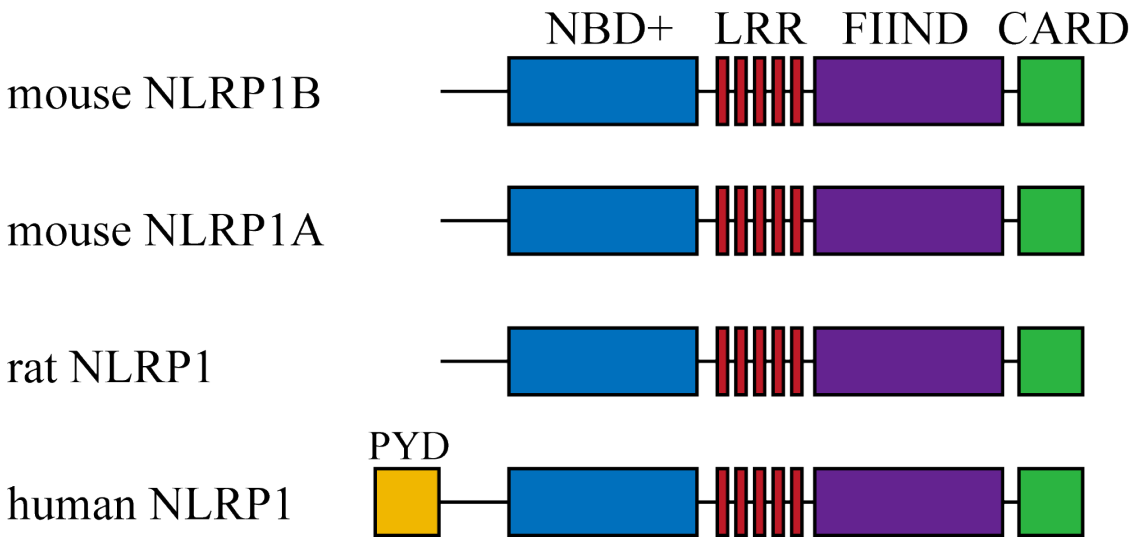

Figure 1.1 Domain structure of NLRP1 proteins.
All members of the NLRP1 family have a nucleotide binding domain (NBD) accompanied by a helical domain 1, winged helix domain, and a helical domain 2, which are denoted by the + sign here for simplicity (NBD+). The leucine-rich repeat (LRR) domain, the function to find domain (FIIND), and the caspase activating and recruitment domain (CARD) are found in all members of the NLRP1 family. The N-terminal pyrin domain (PYD) is found in human NLRP1 and other non-rodent species. A third mouse paralog, Nlrp1c, is a predicted pseudogene and is not expected to form a functional inflammasome.

NLRP1 variant	**Reported Stimuli**	**FIIND processing**
mouse *Nlrp1a* (B6)	none	yes (unpublished)
mouse *Nlrp1b* Allele-1 (BALB, 129)	LF, *T. gondii*, ATP depletion	yes
mouse *Nlrp1b* Allele-2 (B6)	*T. gondii*	yes (unpublished)
mouse *Nlrp1b* Allele-3 (NOD)	none	no
mouse *Nlrp1b* Allele-5 (CAST)	LF	yes
rat *Nlrp1* Allele-2 (CDF)	LF	yes
rat *Nlrp1* Allele-5 (LEW)	*T. gondii*	yes
human *NLRP1*	MDP?	yes

Table 1. 1 NLRP1 homologs and reported stimuli.

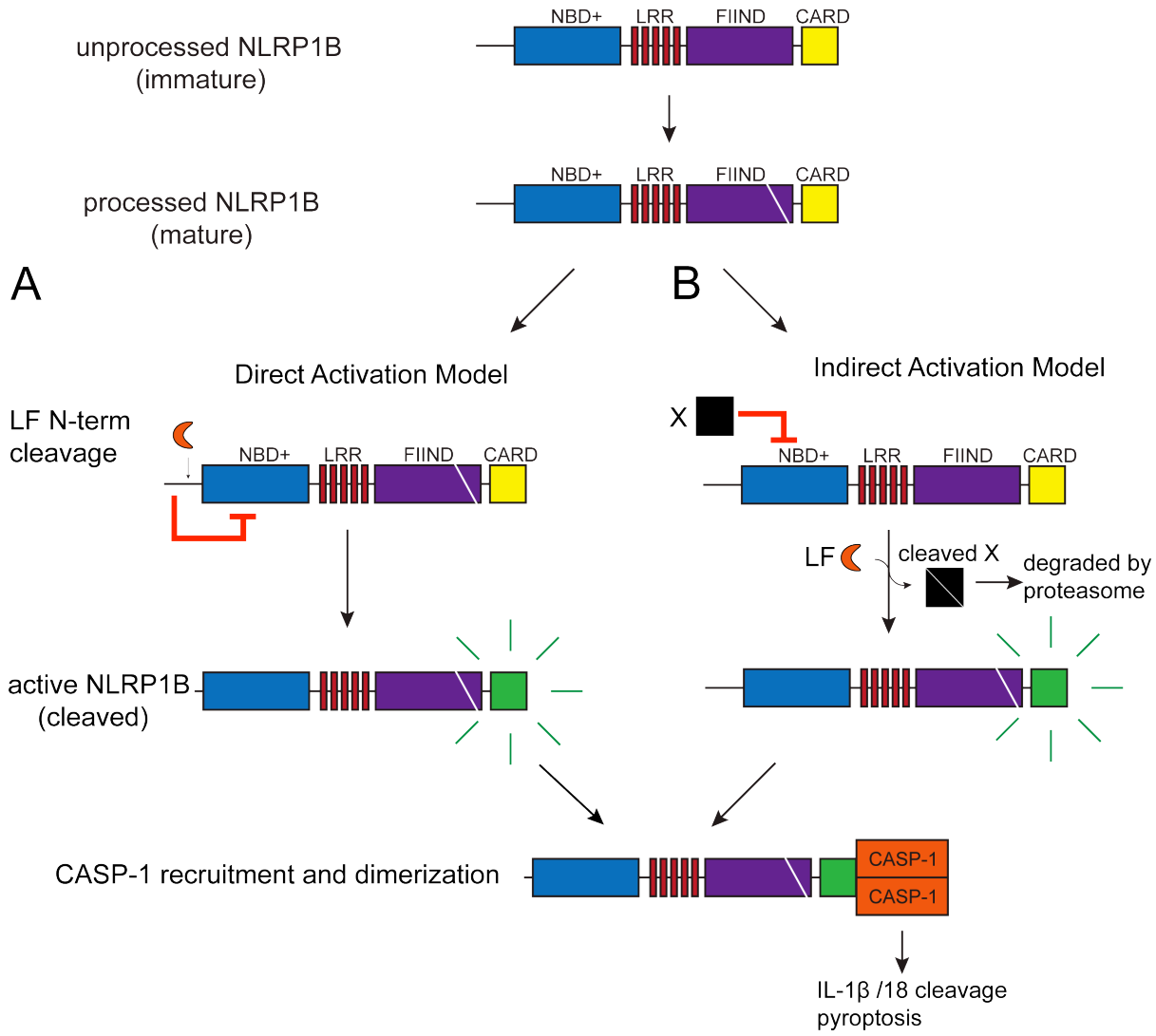

Fig. 1.2. Models of mouse NLRP1B activation by anthrax lethal factor.
NLRP1B must first undergo FIIND self-processing as a maturation event to become responsive to LF-induced activation.
(**A**) In the "Direct Activation Model" the N-terminal portion of NLRP1B maintains NLRP1B in an "off" state. Lethal factor directly cleaves this N-terminal region of NLRP1B, and removal of the N-terminus activates NLRP1B. Activated NLRP1B recruits and dimerizes CASP1 through the CARD domain. Dimerized or activated CASP1 subsequently cleaves IL-1B, IL-18 and induces pyroptosis.
(**B**) In the "indirect activation model", NLRP1B is negatively regulated by an unknown host-factor X. LF cleaves X, resulting in its destabilization and degradation by the proteasome. Degradation of X relieves inhibition of NLRP1B, allowing NLRP1B to become active and recruit and activate CASP1.

Chapter 2: Direct proteolytic cleavage of NLRP1B is necessary and sufficient for inflammasome activation by anthrax lethal factor

2.1 Abstract

Inflammasomes are multimeric protein complexes that respond to infection by recruitment and activation of the Caspase-1 (CASP1) protease. Activated CASP1 initiates immune defense by processing inflammatory cytokines and by causing a rapid and lytic cell death called pyroptosis. Inflammasome formation is orchestrated by members of the nucleotide-binding domain and leucine-rich repeat (NLR) or AIM2-like receptor (ALR) protein families. Certain NLRs and ALRs have been shown to function as direct receptors for specific microbial ligands, such as flagellin or DNA, but the molecular mechanism responsible for activation of most NLRs is still poorly understood. Here we determine the mechanism of activation of the NLRP1B inflammasome in mice. NLRP1B, and its ortholog in rats, is activated by the lethal factor (LF) protease that is a key virulence factor secreted by *Bacillus anthracis*, the causative agent of anthrax. LF was recently shown to cleave mouse and rat NLRP1 directly. However, it is unclear if cleavage is sufficient for NLRP1 activation. Indeed, other LF-induced cellular events have been suggested to play a role in NLRP1B activation. Surprisingly, we show that direct cleavage of NLRP1B is sufficient to induce inflammasome activation in the absence of LF. Our results therefore rule out the need for other LF-dependent cellular effects in activation of NLRP1B. We therefore propose that NLRP1 functions primarily as a sensor of protease activity and thus could conceivably detect a broader spectrum of pathogens than just *B. anthracis*. By adding proteolytic cleavage to the previously established ligand-receptor mechanism of NLR activation, our results illustrate the remarkable flexibility with which the NLR architecture can be deployed for the purpose of pathogen-detection and host defense.

2.2 Non-technical Summary

Recognition of pathogens by the innate immune system is necessary for initiating an appropriate immune response. The innate immune system must distinguish pathogens from abundant harmless microbes present within the host and the environment, and scale the response appropriately. It has been proposed that the host can respond specifically to pathogens by monitoring common virulence-associated activities, previously termed "patterns of pathogenesis," that are used by pathogens to survive and replicate within their hosts. For example, pathogens can manipulate host functions by delivering toxins into host cells. In response, the host encodes dedicated cytosolic sensors to detect these toxins, but the molecular basis for how the sensors recognize the toxins is poorly understood. Here we define the molecular mechanism by which a mouse sensor, NLRP1B, directly recognizes the activity of a bacterial toxin, lethal factor. Lethal factor is a protease secreted by *Bacillus anthracis*, the causative agent of anthrax. We show that anthrax lethal factor cleaves NLRP1B and this cleavage event is both necessary and sufficient for the activation of this sensor. Our findings raise the possibility that NLRP1B could sense the activity of other proteases encoded by diverse pathogens.

2.3 Introduction

Recognition of pathogens is an essential first step in the initiation of protective host immune responses. Recognition of pathogens has been shown to be mediated by several families of germ-line encoded receptors that include the Toll-like receptors (TLRs), Nucleotide-binding domain and Leucine-rich Repeat containing proteins (NLRs), and RIG-I-like receptors (RLRs) (Takeuchi and Akira, 2010). Most TLRs, NLRs, and RLRs for which activation mechanisms have been defined appear to function as "pattern recognition receptors" (Janeway, 1989) that directly bind to molecular structures called pathogen-associated molecular patterns (PAMPs) that are broadly conserved among many microbes. In addition to detection of PAMPs, it has been previously proposed that the innate immune system might also respond to 'Patterns of Pathogenesis', the virulence-associated activities that pathogens utilize to invade or manipulate their hosts (Vance et al., 2009). Detection of pathogen-associated activities might be a beneficial innate immune strategy, complementary to PAMP recognition, as it could allow the innate immune system to discriminate pathogenic from non-pathogenic microbes, and scale responses appropriately, despite the fact that pathogenic and non-pathogenic microbes often share the same PAMPs. However, few instances of a molecular mechanism by which a pathogen-encoded activity could be detected have been described in mammals. For example, a previous study showed how pathogen-induced inhibition of protein synthesis by *Legionella pneumophila* could be detected, leading to a specific cytokine response (Fontana et al., 2011; Shin et al., 2008). Disruption of the actin cytoskeletal signaling network by an *E. coli* toxin was also found to lead to a protective innate immune response (Boyer et al., 2011). Overall, however, there is still considerable uncertainty as to whether or how 'patterns of pathogenesis' are sensed by the innate immune system.

Anthrax lethal toxin (LeTx) is a critical virulence factor secreted by *Bacillus anthracis*. LeTx is composed of two proteins: protective antigen (PA) and lethal factor (LF). PA binds to anthrax toxin receptors on host cells, and subsequently translocates the zinc-metalloprotease, LF, into the cytosol. The canonical proteolytic substrates of LF are mitogen-activated protein kinase kinases (MAPKKs) 1-4 and 6-7 (Duesbery et al., 1998; Vitale et al., 1998). Cleavage by LF inactivates MAPKKs and results in the disruption of signaling pathways involved in host defense (Bardwell et al., 2004; Chopra et al., 2003). Macrophages from certain strains of mice and rats respond to LeTx by undergoing a rapid and lytic form of Caspase-1 (CASP1)-dependent cell death called pyroptosis (Bergsbaken et al., 2009; Boyden and Dietrich, 2006; Friedlander, 1986; Friedlander et al., 1993; Newman et al., 2010). The ability to undergo pyroptosis in response to LeTx was genetically mapped to the *Nlrp1b* gene in mice (Boyden and Dietrich, 2006), and subsequently to the orthologous *Nlrp1* gene in rats (Newman et al., 2010). Importantly, mice harboring an allele of *Nlrp1b* that is responsive to LeTx are protected from challenge with *B. anthracis* spores (Moayeri et al., 2010; Terra et al., 2010). This protection correlates with enhanced production of IL-1β, recruitment of neutrophils to the site infection, and decreased bacterial counts, and these processes were dependent on expression of the interleukin-1 receptor (Moayeri et al., 2010; Terra et al., 2010). Despite the importance of NLRP1B in host defense against *B. anthracis*, the mechanism of NLRP1B activation by LF remains unclear.

NLRP1B belongs to the NLR family of innate immune sensors (Ting et al., 2008; Tschopp et al., 2003; von Moltke et al., 2012a). Several NLRs, including NLRP1, have been found to assemble into oligomeric complexes, called 'inflammasomes' (Martinon et al., 2002), in response to a variety of infectious or noxious stimuli (von Moltke et al., 2012a). The primary function of inflammasomes appears to be to form a platform for activation of inflammatory

caspase proteases, most notably CASP1, but the molecular mechanism by which NLRs are activated is poorly understood (von Moltke et al., 2012a). Although NLRP1 proteins contain NBD and LRR domains, as do all other NLRs, the domain organization of NLRP1 differs from other NLRs in two respects. First, NLRP1 proteins contain a C-terminal Caspase Activation and Recruitment Domain (CARD), whereas the CARDs in other NLRs are usually N-terminal. The second unique feature of NLRP1 proteins is that they contain an unusual domain called the 'function-to-find' (FIIND) domain (Tschopp et al., 2003). The FIIND is located between the LRRs and the C-terminal CARD (Fig. 1.1), and was recently shown to undergo an auto-proteolytic processing event that results in the C-terminal CARD being cleaved from the rest of the NLRP1 protein (D'Osualdo et al., 2011). It is believed that the N- and C-terminal auto-processed fragments of mature NLRP1B remain associated with each other despite cleavage of the polypeptide chain (Frew et al., 2012). The FIIND auto-processing event occurs constitutively, prior to NLRP1B activation by LF, but for reasons that remain unclear, is required for the ability of NLRP1 to activate CASP1 (Finger et al., 2012; Frew et al., 2012).

Several inflammasomes have been suggested to be activated upon direct binding to specific bacterial ligands. For example, another NLR-family member, NAIP5, assembles into an inflammasome upon binding to flagellin, whereas the related NAIP2 inflammasome assembles upon binding to the inner rod proteins from a variety of bacterial type III secretion systems (Kofoed and Vance, 2011; Zhao et al., 2011). A direct receptor-ligand model also applies to the ALR-family AIM2 inflammasome, which is activated upon direct binding to microbial DNA (Burckstummer et al., 2009; Fernandes-Alnemri et al., 2009; Hornung et al., 2009; Roberts et al., 2009). In contrast, certain inflammasomes, notably the NLRP3 inflammasome, are believed not to bind directly to bacterial ligands, but have instead been proposed to respond to virally encoded ion channels (Ichinohe et al., 2010), bacterial toxins, or other cellular stresses, via indirect mechanisms (von Moltke et al., 2012a). However, the molecular basis for how these stresses are sensed by NLRP3 remains unclear. By contrast, the molecular basis for indirect pathogen recognition by plant NLRs has been well-established (Chisholm et al., 2006; Jones and Dangl, 2006). For example, the plant NLR RPS2 has been shown to be maintained in an inactive state by its association with RIN4, a host protein that is targeted for degradation by a bacterial protease (Axtell and Staskawicz, 2003; Mackey et al., 2003). RPS2 thus detects the activity of a bacterial protease indirectly by monitoring or 'guarding' the integrity of the protease substrate. Direct proteolytic cleavage of a plant NLR by a pathogen-encoded protease has not been described.

NLRP1B responds to the protease activity of LF, as catalytically inactive forms of LF do not activate NLRP1 (Fink et al., 2008; Klimpel et al., 1994). This suggests that NLRP1 does not recognize LF via simple receptor-ligand binding, such as that occurs with the NAIP or AIM2 inflammasomes. Boyden and Dietrich initially hypothesized that LF could cleave and activate NLRP1B (Boyden and Dietrich, 2006), but evidence for this simple model of NLRP1B activation was not provided. In fact, several groups have demonstrated that the activity of the proteasome is specifically required for this inflammasome and not for other inflammasomes such as the NAIP5/NLRC4 inflammasome (Fink et al., 2008; Wickliffe et al., 2008a). In addition, inhibitors of the N-end rule degradation pathway block NLRP1B activation but do not affect the ability of LF to cleave MAPKKs (Wickliffe et al., 2008b). In contrast to a model in which NLRP1B is activated upon cleavage by LF, these observations suggest that LF might activate NLRP1B by cleaving and destabilizing a negative regulator of NLRP1B. This 'indirect' model resembles the activation of the certain NLRs, e.g., RPS2, in plants. Recently, however, it was

shown that the NLRP1 proteins from Fischer rats and BALB/c mice can be directly cleaved near their N-termini by LF (Hellmich et al., 2012; Levinsohn et al., 2012). Mutation of the cleavage site in rat NLRP1 rendered NLRP1 resistant to cleavage by LF and also prevented NLRP1 activation in response to LF. These results suggest that cleavage of rat NLRP1 by LF is essential for NLRP1 activation, but it is difficult to rule out the possibility that mutation of the cleavage site disrupted the fold of NLRP1, or rendered NLRP1 non-functional for other reasons. In addition, the site at which LF cleaves rat NLRP1 is not conserved in the mouse (Hellmich et al., 2012), and moreover, the functional effects of mutating the mouse cleavage site have not been assessed. Lastly, and most importantly, existing studies have not ruled out the involvement of other LF-dependent cellular events in NLRP1B activation, as cleavage of NLRP1 was not shown to be sufficient for its activation.

Here, we present data that suggest that murine NLRP1B requires LF-dependent cleavage for its activation. We further demonstrate that cleavage is sufficient for NLRP1B inflammasome activation in the absence of LF, which rules out a requirement for cleavage of other LF substrates in activation of NLRP1B. Our results provide evidence for a simple direct mechanism by which an innate immune sensor detects a pathogen-encoded activity. In addition, our results open the possibility that NLRP1 could function as a direct cytosolic sensor of other pathogen-derived proteases. More broadly, by adding direct proteolytic cleavage to the existing ligand-receptor models for NLR activation, our results also illustrate the remarkable adaptability of the NLR architecture to function as pathogen-detectors in host defense.

2.4 Results

2.4.1 Mouse NLRP1B is cleaved by LF

The N-termini of mouse NLRP1B and rat NLRP1 were recently reported to be cleaved by LF (Hellmich et al., 2012; Levinsohn et al., 2012). Interestingly, these proteins do not exhibit much similarity in the region surrounding the cleavage site (Fig. 2.1A), whereas the rest of the protein is highly conserved between mice and rats (37% amino acid identity from position 1-54 vs. 70% identity from residue 55 to the C-terminus). The N-terminal fragment produced by LF is under 10kDa and appears to be unstable, making it difficult to detect by conventional western blotting techniques in cell lysates. Thus, to confirm that mouse NLRP1B is cleaved by LF, we augmented the mass of the putative N-terminal fragment by 29 kDa by fusing full-length NLRP1B to enhanced green fluorescent protein (EGFP) and a hemagglutinin (HA) affinity-tag. We transfected this construct into HEK 293T cells and then treated the cells with LeTx. As reported previously, NLRP1B constitutively but only partially auto-processes its FIIND domain in untreated cells, resulting in a loss of 29kDa from the C-terminus, and producing a doublet of 140 kDa and 169 kDa that we will refer to as the ‘processed’ and ‘unprocessed’ forms of NLRP1B, respectively (Fig. 2.1B and D) (Frew et al., 2012). After LeTx addition, an N-terminal fragment smaller than 37 kDa, but larger than EGFP-HA alone (29 kDa), begins to accumulate inside cells. To distinguish LF-dependent cleavage from auto-processing of the FIIND domain, we will refer to the LF-dependent fragments as ‘cleaved’ (as opposed to ‘processed’) NLRP1B (Fig. 2.1D). With kinetics correspondi.ng to the appearance of the cleaved N-terminal fragment, the amount of the detectable uncleaved NLRP1B decreased over time, consistent with removal of the N-terminal tag. The LF-dependent cleavage of NLRP1B is not complete even after 6 hours, and thus occurs much more slowly than the LF-dependent cleavage of the MAP kinase kinase MEK2, a canonical LF substrate, which appears complete within 2 hours (Fig. 2.1B).

To test if LF cleaves NLRP1B directly, without the GFP fusion, we expressed an HA-tagged NLRP1B in 293T cells, immunoprecipitated NLRP1B, and then treated the purified protein with recombinant LF *in vitro*. In the sample treated with LF, a fragment smaller than 10kDa is produced (Fig. 2.1C), suggesting that LF can cleave mouse NLRP1B directly near the N-terminus, confirming recent findings (Hellmich et al., 2012).

2.4.2 Cleavage is required for LF activation of NLRP1B

Even though the cleavage site in rat NLRP1 is not well-conserved in mouse NLRP1B (Fig. 2.1A), two sequences can be found in the N-terminus of mouse NLRP1B that partially fit the previously established consensus specificity of LF (Hellmich et al., 2012) (Fig. 2.3A). For clarity, we refer to the putative site nearest to the N-terminus (cleavage after K38) as site-1, and the C-terminal site (cleavage after K44) as site-2 (Fig. 2.1D and 2.3A). These two sites were also identified as putative LF cleavage sites in a recent study (Hellmich et al., 2012), but their functional importance was not addressed. We attempted to generate cleavage resistant (CR) forms of NLRP1B by mutating each site. We made a variety of amino acids substitutions at site-1 (CR1A-D) and site-2 (CR2A-C) (Fig. 2.3A), utilizing residues that have previously been used to render MKK3 and MKK6 cleavage resistant (Park et al., 2002), or residues not found in LF consensus sites (Turk et al., 2004; Zakharova et al., 2009). These mutants were transfected into 293T cells, and cells were then treated with LeTx and assayed for cleavage. Mutation of cleavage site-2 produced a cleavage-resistant form, despite the fact that site-1 is intact in this mutant (Fig. 2.2A and 2.3A-C). By contrast, mutation of cleavage site-1 had little or no effect on NLRP1B cleavage (Fig. 2.3A-C). When *Casp1* and *Il1b* cDNA expression vectors were cotransfected into this same 293T system, only CR2A and CR2B were defective for induction of IL-1β processing into p17 above the basal processing induced by CASP1 and NLRP1B prior to stimulation (Fig. 2.3B-C). Thus, while confirming the previous finding that both site-1 and site-2 of mouse NLRP1B can be cleaved by LF (Hellmich et al., 2012), these results suggest that site-2 is the predominant LF target within NLRP1B in cells.

We tested the ability of the CR2A NLRP1B mutant to form an inflammasome capable of promoting pyroptosis. In these experiments, we used immortalized macrophages from a C57BL/6 (B6) mouse, because the endogenous B6 allele of NLRP1B is not responsive to LeTx. As expected, immortalized B6 macrophages transduced with a retroviral construct expressing the wild-type 129S1 allele of NLRP1B became sensitive to LeTx and underwent pyroptosis, as assessed by release of cytosolic lactate dehydrogenase (LDH) into the supernatant (Fig. 2.2B). By contrast, transduction of B6 macrophages with the CR2A NLRP1B mutant did not confer any measurable sensitivity to LeTx over the same time period. This difference in responsiveness is not due to differences in expression of the NLRP1B alleles (Fig. 2.6A). B6 cells harbor a functional NAIP5 inflammasome; thus, as a further control, the NLRP1B-transduced cells can be tested for inflammasome responses to the cytosolic presence of flagellin. We therefore delivered flagellin to the cytosol, via the protective antigen translocation channel used by lethal factor, as a fusion to the translocation signal in LF (dubbed 'FlaTox') (von Moltke et al., 2012b) (Fig. 2.2B). Cells transduced with wild-type and CR2A NLRP1B were equally susceptible to FlaTox, indicating that they expressed functionally equivalent levels of anthrax toxin receptor, CASP1, and downstream effectors required for pyroptosis. These data demonstrate that the ability of mouse NLRP1B to respond to LF correlates with the ability of LF to cleave NLRP1B at its N-terminus.

2.4.3 LF, expressed in the cytosol in the absence of PA, is sufficient to activate NLRP1B

The ability of LF to cleave and activate NLRP1B has only been tested in the presence of PA, since PA is typically required in order to deliver LF to the cytosol. It is therefore unclear if PA is only necessary for the translocation of LF in to the cytosol, or if it is also required for NLRP1B activation. We decided to test the ability of LF expression to induce pyroptosis and cytokine secretion in B6 and 129 immortalized macrophage-like cell lines with a Tet-On inducible vector. We transduced these cell lines with a lentiviral Tet-On GFP or LF expression vector and then treated the transduced cells with doxycycline to induce GFP or LF expression. LF expression was able to consistently induce pyroptosis in 129 (NLRP1B LeTx-responsive) cells but not B6 (NLRP1B LeTx-nonresponsive) cells (Fig. 2.4A). Further addition of PA had no additional effect on pyroptosis induction. Similar results were obtained when IL-1β production was used to monitor NLRP1B activation (Fig. 2.4B). These results show that the cytosolic presence of LF is sufficient to activate NLRP1B and that additional putative signals provided by PA pore formation are not required.

2.4.4 Cleavage of NLRP1B is sufficient for inflammasome activation

Together the above results suggest that mouse NLRP1B requires direct cleavage in order to be activated by LF, but it is difficult to rule out the formal possibility that the CR2A mutant is misfolded or is otherwise non-functional for reasons unrelated to its resistance to cleavage by LF. Moreover, the above experiments did not address whether cleavage alone is sufficient for activation of NLRP1B. For example, LF may have other substrates that must be cleaved in addition to NLRP1B, or LF itself could provide a ligand-like signal for the cleaved NLRP1B receptor. To address these possibilities, we replaced the predicted LF cleavage sites-1 and -2 in NLRP1B with a Tobacco Etch Virus (TEV) NIa protease cleavage-site (Fig. 2.3A). TEV protease was selected because it has no known endogenous substrates in mouse or human cells. We transfected 293T cells with plasmids expressing the wild-type and TEV-site forms of NLRP1B, along with plasmids encoding CASP1, pro-IL-1β, and either LF or TEV protease. As expected, wild-type NLRP1B was cleaved only in the presence of LF, and this coincided with the generation of mature IL-1β (Fig. 2.5A). Importantly, NLRP1B harboring a target sequence for TEV protease in place of the LF target sequence at site-2 (TEV-site2 NLRP1B) was cleaved efficiently by TEV protease, and this cleavage was sufficient to promote IL-1β processing. Consistent with the relatively low sequence specificity of LF, the TEV-site2 NLRP1B protein was also cleaved by LF, but this cleavage was inefficient as most of the NLRP1B remained uncleaved, and IL-1β was not efficiently processed. Cleavage of TEV-site1 also was sufficient to induce IL-1β processing, but this occurred upon expression of either LF or TEV proteases. Furthermore, the TEV-induced cleavage at site-1 produced a fragment of NLRP1B that was smaller than the fragment produced by LF expression (Fig. 2.5A and 2.3D). Consistent with the mutagenesis experiments shown in Fig. 2.2A-B, this observation may indicate that LF prefers to cleave at site-2, which is still present in the TEV-site1 NLRP1B protein. Taken together, these results suggests that cleavage of NLRP1B at either site-1 or site-2 is sufficient to induce inflammasome activation independently of other LF-dependent cellular effects.

We also confirmed that cleavage of NLRP1B is sufficient to induce pyroptosis in macrophages cell lines. We transduced immortalized B6 macrophages with two different retroviral vectors, one expressing GFP-NLRP1B and the other expressing TEV protease with an IRES-Thy1.1 expression marker. If cleavage is sufficient to activate NLRP1B, it is expected that only cells expressing both components would undergo pyroptosis and therefore be

underrepresented in the live population of cells. We analyzed the percentage of cells that contained both retroviruses by measuring THY1.1 surface-expression and GFP fluorescence by flow cytometry. As expected, an underrepresentation of the THY1.1 and GFP double-positive population was specifically seen in cells transduced with TEV and TEVsite2-NLRP1B, while the frequency of THY1.1+ cells was similar in cells that where negative for both forms of NLRP1B (Fig. 2.5B).

To further confirm that cleavage of NLRP1B is sufficient for inflammasome activation, we transduced RAW 264.7 cells with retroviral vectors encoding various NLRP1B alleles, as well as a lentiviral Tet-On vector that inducibly expresses GFP, TEV-protease or LF after exposure of cells to doxycycline. In this system, TEV expression induced high levels of LDH release only for cells expressing TEVsite2-NLRP1B. As expected, since RAW cells express an endogenous functional allele of NLRP1B, LF induced pyroptotic lysis of cells expressing either wild-type or TEVsite2-NLRP1B (Fig. 2.5C). The percent LDH release was generally consistent with the percentage of cells that expressed both constructs (Fig. 2.6B). These data demonstrate that cleavage of NLRP1B is sufficient to activate this inflammasome in macrophages and cause pyroptosis.

2.4.5 No apparent role for the N-terminal NLRP1B cleavage fragment

We next tested whether the N-terminal fragment generated by cleavage of NLRP1B by LF at site-2 must be present along with the corresponding C-terminal fragment. We generated a construct to express a 'pre-cleaved' C-terminal fragment by deleting residues 1-44 of full-length NLRP1B and replacing amino acid 45 (leucine) with an initiator methionine. The resulting C-terminal fragment contains all known functional domains of NLRP1B (Fig. 2.1D). In the 293T cell system, high levels of spontaneous IL-1β cleavage was observed upon expression of the precleaved NLRP1B. The activity of pre-cleaved NLRP1B was comparable to that of a ΔLRR mutant, a form of NLRP1B that is known to be constitutively active (Fig. 2.5D and 2.7C) (Liao and Mogridge, 2009). When the N-terminal fragment (amino acids 1-44) was coexpressed with the precleaved C-terminal fragment, no change in the amount of IL-1β processing was observed (Fig. 2.7B), suggesting it is neither necessary nor inhibitory when expressed in trans. For all of these experiments, the differences in the amount of IL-1β cleavage were not explained by differences in expression of NLRP1B (Fig. 2.7A-C)

2.4.6 Proteasome inhibitors and FIIND processing do not affect LF-dependent cleavage

NLRP1B inflammasome activation can be blocked by proteasome inhibitors, an effect that is observed with multiple inhibitors and is specific to the NLRP1B inflammasome and not the NAIP/NLRC4 inflammasome (Fink et al., 2008; Wickliffe et al., 2008a). The mechanism by which proteasome inhibitors affect NLRP1B inflammasome activation is not currently known. Therefore, we tested whether the proteasome inhibitor MG132 blocked NLRP1B cleavage. In the 293T system, an equivalent amount of cleaved of NLRP1B occurred in the presence of MG132 and its vehicle (Fig. 2.8A), suggesting NLRP1B cleavage is not the step at which MG132 interferes with NLRP1B activation (Fig. 2.9A).

The FIIND of NLRP1B contains a ZU-5/UPA-like domain that can auto-process, and this auto-processing is required for NLRP1B activation (D'Osualdo et al., 2011; Frew et al., 2012). We tested if auto-processing at the FIIND region is prerequisite for N-terminal cleavage by LF. We tested the FIIND mutant S984A, which cannot auto-process, and found it to be indistinguishably sensitive to LeTx cleavage as wild-type NLRP1B (Fig. 2.8B). Thus FIIND

auto-processing appears to be required for a downstream step in NLRP1B activation (Fig. 2.9B), and is not required for NLRP1B to be sensitive to LeTx cleavage.

2.5 Discussion

Activation of the NLRP1B inflammasome by LeTx is an important resistance mechanism during *Bacillus anthracis* infections in mice (Moayeri et al., 2010; Terra et al., 2010). However the question of how NLRP1B senses the protease activity of LF remains unresolved. Here we investigated the molecular mechanism by which the protease activity of *B. anthracis* lethal toxin could be detected by NLRP1B. Our studies provide a clear molecular mechanism for how a pathogen-encoded activity (or 'pattern of pathogenesis'(Vance et al., 2009)) can be sensed by the innate immune system.

Two recent studies by Moayeri and colleagues provided a considerable advance in our understanding of NLRP1B activation by LeTx (Hellmich et al., 2012; Levinsohn et al., 2012). These two studies showed that both rat and mouse NLRP1 can be cleaved near the N-terminus by LF, and that mutation of the cleavage site abolished responsiveness of rat NLRP1 to LF. While these findings strongly suggest that direct cleavage of rat NLRP1 could be its mechanism of activation, the functional role of cleavage of mouse NLRP1B was not addressed, and it is also possible that mutation of the cleavage site blocked activation of rat NLRP1 by affecting the folding or assembly of NLRP1. Most significantly, the question of whether cleavage of NLRP1B was sufficient for its activation has not been addressed. This question is especially important to address because LT has been shown to have complex effects on cells, including disruption of MAP kinase signaling (Ali et al., 2011; Park et al., 2002; Turk, 2007), that could conceivably play a role in NLRP1B activation. Moreover, several other cellular functions, such as proteasome activity and N-end rule degradation pathways, have been implicated in NLRP1B activation (Fink et al., 2008; Wickliffe et al., 2008a, b). Therefore, to demonstrate that cleavage of NLRP1B is sufficient to induce inflammasome activation, we engineered an allele of NLRP1B that could be activated by the heterologous TEV protease. This protease is not known to have endogenous substrates in mouse or human cells, so is likely to exert its effects solely via direct cleavage of the engineered NLRP1B protein. Indeed, the TEV protease did not activate NLRP1B unless NLRP1B contained a site that could be cleaved by TEV (Fig. 2.5A). Recent data have suggested that mouse NLRP1B can be cleaved at two distinct sites by LF (Hellmich et al., 2012), but our cleavage site mutants and TEV-site forms of the receptor are most consistent with site-2 (cleavage between residues 44-45) being the predominant cleavage site. Interestingly, this site coincides with the same amino acid position as the LF cleavage site in rat NLRP1, even though the sequences of the two sites are not conserved (Fig. 2.1A). The low degree of target sequence specificity exhibited by LF may have allowed the sequence of the cleavage site in NLRP1 to diverge without losing responsiveness to LF. The position within NLRP1 at which LF cleaves may be determined in part by interactions between LF and regions of NLRP1 outside of the cleavage site. Indeed, similar non-cleavage-site interactions appear to control the specificity of LF for its other known substrates, the MAPKKs (Chopra et al., 2003; Vitale et al., 1998). The divergence of the amino acid sequence of the N-terminus of NLRP1B is interesting given the high degree of conservation in the rest of the protein. This divergence may be due to random drift of a structurally unconstrained domain, or alternatively, the divergence may reflect evolutionary pressure for NLRP1 to be recognized by other pathogen-encoded proteases. Notably, our data suggest that cleavage outside of the primary LF target site (e.g., at site-1) can also activate NLRP1B (Fig. 2.5A), although it is unclear if LF can cleave and activate NLRP1B

at this position. In addition, our data suggest that cleavage of NLRP1B does not necessarily have to be complete to be sufficient to permit inflammasome assembly and CASP1 activation. Taken together, these observations suggest that NLRP1B could be responsive to proteases from other pathogens even if these proteases cleave NLRP1B at different sites with low efficiency. Indeed, countless pathogens, including bacteria, viruses and parasites, depend on cytosolically-localized proteases for virulence (Anderson et al., 2009; Li et al., 2012; Potempa and Pike, 2009; Toh et al., 2010). Therefore the presence of cytosolic proteases could be considered a 'pattern of pathogenesis' (Vance et al., 2009), that could be detected by NLRP1 proteins to allow the innate immune system to discriminate pathogenic and harmless microbes. The divergence of rat and mouse NLRP1 may thus reflect evolution under the selective pressure imposed by distinct sets of pathogens in the two different rodents species. It will be interesting to determine if other proteases can activate rodent NLRP1s.

The detection of protease activity by NLRP1B represents a fundamentally distinct mode of pathogen recognition in vertebrates as compared to the classic mode of direct recognition of PAMPs observed with most innate immune receptors of the TLR, NLR and RLR families. The N-terminus of NLRP1B appears to function to detect LF activity in a manner analogous to the 'decoy' model (van der Hoorn and Kamoun, 2008), which has been previously proposed to explain detection of certain pathogen effectors by plant NLRs. The proteolytic mechanism by which NLRP1B is activated represents one of the few examples in mammals in which a molecular mechanism has been established for how an innate immune sensor can respond to a pathogen-encoded activity.

It is currently unknown how cleavage of the N-terminus results in structural changes that lead to NLRP1B activation. A simple model is that the N-terminus of NLRP1B mediates an auto-inhibitory intramolecular interaction, perhaps via an interaction with the LRR domain, which is known also to be required for auto-inhibition of NLRP1B (Fig. 2.5D) (Liao and Mogridge, 2009). An alternative model that is not excluded by our data is that the removal of the original N-terminus allows the neo-N-terminus to provide a positive signal to activate NLRP1B. More complicated models involving interactions with other proteins can also be envisaged. We did not observe an inhibitory role of the N-terminal fragment when expressed in trans (Fig. 2.7). This suggests that the N-terminus is necessary to maintain NLRP1B in a conformation that is inactive, but can only do so when the N-terminus is covalently attached to the rest of NLRP1B.

In addition to proteolytic cleavage by LF, additional layers of NLRP1B regulation appear to exist. For example, FIIND auto-processing is required for NLRP1B activity, for reasons that remain poorly understood (Frew et al., 2012). Since we found that FIIND auto-processing mutants are still cleaved by LF, the role of FIIND auto-processing appears not to be to render NLRP1B susceptible to cleavage by LF. Further complexities in NLRP1B activation are also suggested by the observation that proteasome and N-end rule pathway inhibitors appear to specifically prevent NLRP1B-dependent CASP1 activation (Fink et al., 2008; Wickliffe et al., 2008a, b). Even though previous studies have shown that proteasome inhibitors do not block cleavage of MAPKK by LF (Fink et al., 2008; Wickliffe et al., 2008a), we tested if proteasome inhibition might affect cleavage of NLRP1B, which appears to be a less optimal substrate than the MAPKKs. However, we observed no effect of the proteasome inhibitor MG132 on the ability of LF to cleave NLRP1B. Thus it remains unclear how this inhibitor specifically blocks the NLRP1B inflammasome and not other inflammasomes. Models that attempt to explain the mechanism of NLRP1B are further complicated by other unique features of NLRP1B. For example, ATP binding to the NBD of NLRP1B is not necessary for inflammasome activation,

and mutants of NLRP1B that are unable to bind ATP are actually constitutively active (Liao and Mogridge, 2012). This is contrary to what is known for other mammalian NLRs, where ATP binding appears to be required for oligomerization and downstream signaling (von Moltke et al., 2012a). Furthermore, gross truncations of NLRP1B can also lead to constitutively active forms of NLRP1B that contain only the very C-terminal CARD and a portion of the FIIND (Liao and Mogridge, 2009). Thus, other disturbances, by proteolysis or by other means, to the overall structure of NLRP1B could lead to loss of the conformation that mediates auto-inhibition.

In general, the molecular conformational changes that occur in NLRs as they transition from an inactive to an active state are poorly understood. Thus, our studies of NLRP1B provide an important point of comparison that helps us to develop a broader understanding of the NLR class of innate immune sensors and the mechanisms of their activation.

2.6 Materials and Methods

2.6.1 Plasmids and constructs

HA-NLRP1B was amplified from a *Nlrp1b* (DQ117584.1) cDNA (gift of E. Boyden and B. Dietrich, Harvard Medical School) with primers 1-2 and cloned into pCMSCV-IRES-hCD4 using the XhoI and NotI restriction sites (Table 2.1). A construct for expression a GFP-HA-NLRP1B fusion was created by amplifying HA-NLRP1B with primers 3-4 and cloning the resulting PCR product into MSCV downstream of and in-frame with GFP using NotI and SalI sites. TEV expression constructs were created by amplifying a His6-TEV ORF with the primers 7-9 and 8-9 into pCMSCV-IRES-Thy1.1 and pFG12-rtTA-IRES-Thy1.1, respectively. LF was similarly cloned into the same vectors as TEV, but with the primers 10-11 and 12-13 using a template provided by Bryan Krantz (UC Berkeley). Mutagenesis of *Nlrp1b* was performed using Quickchange (Stratagene/Agilent), but modified by substituting the *Pfu* polymerase for PrimeSTAR HS (TAKARA/Clonetech). The primers used are listed in Table 2.1.

2.6.2 Cell culture

HEK293T (ATCC) cells were grown in complete media (DMEM, 10%FBS, 100 U/ml Penicillin, 100 µg/ml Streptomycin, and supplemented with 2mM L-glutamine). RAW 264.7 and immortalized B6 macrophages were grown in complete media (RPMI 1640, 10%FBS, 100 U/ml Penicillin, 100 µg/ml Streptomycin).

2.6.3 DNA transient transfections

HEK 293T cells were seeded the day prior to transfection at a density of $1.5x10^5$ cells/well in a 24-well plate with complete media. DNA complexes were made with Lipofectamine 2000 (Invitrogen) according to manufactures instructions and overlaid on cells for 24-36 hours.

2.6.4 Western Blots

Cells were lysed in RIPA buffer supplemented with 1mM PMSF and 1×X Complete Protease Inhibitor Cocktail (Roche). Lysates were spun down at max speed at 4C for 20min and supernatants were mixed with 6× Laemmli sample buffer. To detect full length NLRP1B, lysates were incubated at room temperature prior to SDS-PAGE. To analyze all other proteins, including the N-terminally cleaved form of NLRP1B, samples were boiled for 10min prior to separation. SDS-PAGE was performed with Novex BisTris gel system according to manufacturer instructions (Invitrogen). Separated proteins were transferred on to Immobilon-FL PVDF membranes. Membranes were blocked with Odyssey® blocking buffer (Licor). The following

antibodies were used for the following antigens: HA mAB 3F10 (Roche), MEK-2 SC-13115 (Santa Cruz), Beta Actin SC-4778 (Santa Cruz), IL-1B AF-401-NA (R&D systems). Secondary antibodies anti-rat, mouse and goat were all conjugated to Alexa Flour-680 (Invitrogen).

2.6.5 Immunoprecipitation and LF *in vitro* cleavage assay

Transfected cells were lysed in a non-denaturing buffer (1% NP-40, 137mM NaCl, 2mM EDTA, 20mM Tris pH 8 supplemented with protease inhibitors). Cleared lysates were bound to EZview Red Anti-HA Affinity Gel (Sigma) washed four times with lysis buffer, once in LF cleavage buffer (10mM NaCl, 5uM ZnSO4, 10mM HEPES pH 7.4), and resuspended back into cleavage buffer. One microgram of recombinant LF was added to immunoprecipitated NLRP1B and incubated at 37°C for 2 hours, and analyzed by western blotting as described above

2.6.6 Cytotoxicity/Pyroptosis assay and IL-1β secretion

Macrophages were seeded one day prior to treatment in a 96well plate at $5x10^4$ cell/well in RPMI media without phenol red. The next day cells were treated with LeTx 1μg/ml, FlaTox 1μg/ml (von Moltke et al., 2012b), or doxycycline at 5μg/ml in ethanol for the indicated time, and spun down at 400 ×*g*. For IL-1β release cells were pretreated/cotreated with 1μg/ml of Pam3CSK4. Supernatants were removed and assayed for LDH and IL-1β release as described previously (Lightfield et al., 2008).

2.7 Acknowledgements

This chapter was originally written as a peer-reviewed article, which was submitted and accepted in PLOS Pathogens (Chavarria-Smith and Vance, 2013)

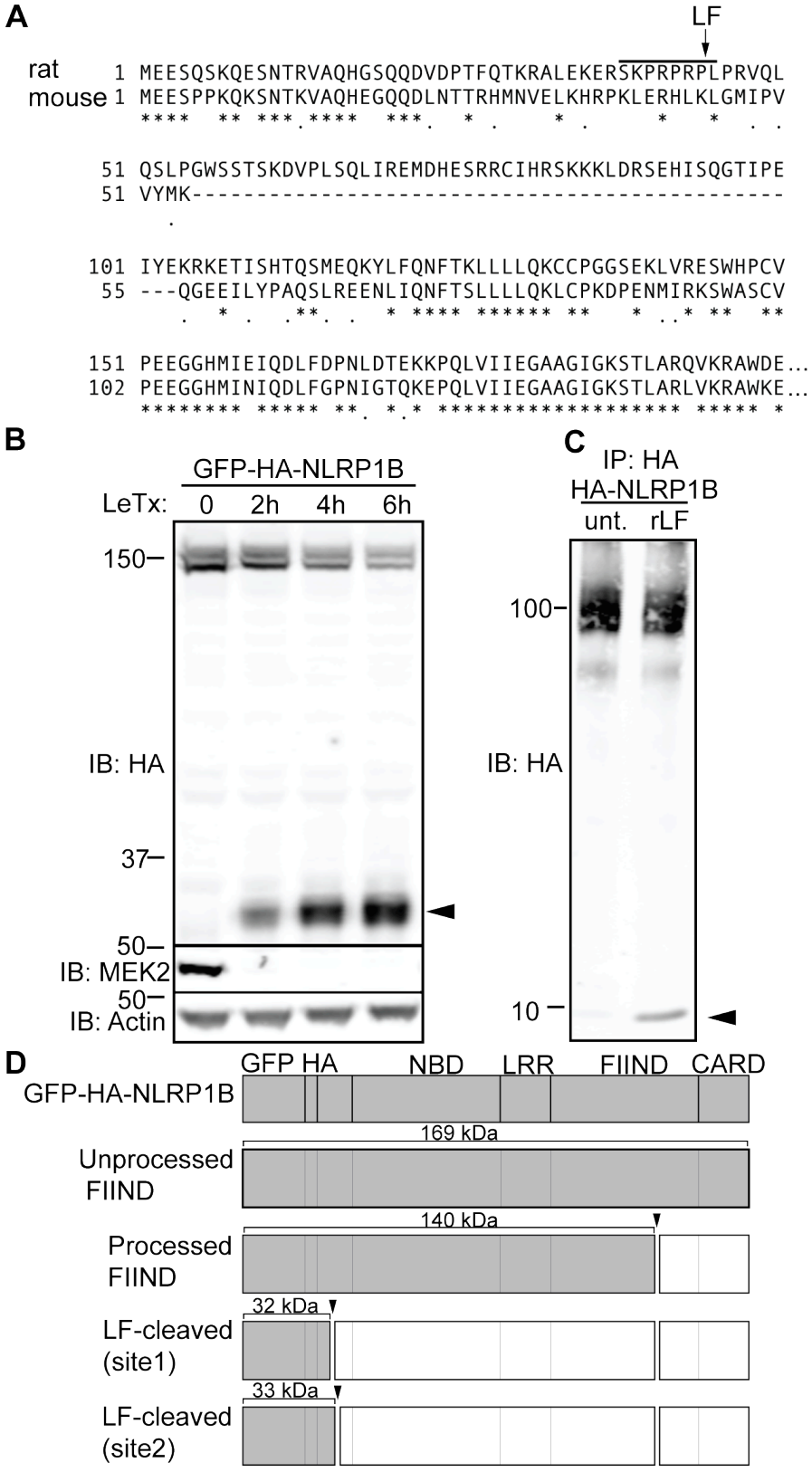

Figure 2.1 Murine NLRP1B from 129S1 mice is cleaved directly by LeTx.

A) Protein sequence alignment of the N-terminal region of murine NLRP1B (129S1 allele) and rat NLRP1 (Fischer/CDF allele) was determined by ClutalW with a BLOSUM series matrix. The LF cleavage motif and cleavage site are identified in the rat allele by the bar and arrow above the rat sequence. B) GFP-HA-NLRP1B was transfected into HEK 293T cells and then treated with 1μg/ml LeTx over the indicate time points followed by immunoblotting (IB) for HA on non-boiled lysates, and boiled lysates when probed with MEK2 and beta-actin antibodies. The arrow-head refers to the LeTx-dependent N-terminal cleavage fragment. C) HA-NLRP1B expressed in 293T cells, immunoprecipitated (IP) with anti-HA beads, and treated with recombinant LF (rLF) for 2h, followed by immunoblotting for HA. D) Graphic representation of the GFP-HA-NLRP1B construct and annotated functional domains. The different forms of NLRP1B observed are shaded in gray along with their predicted molecular weights, when immunoblotted with an anti-HA antibody.

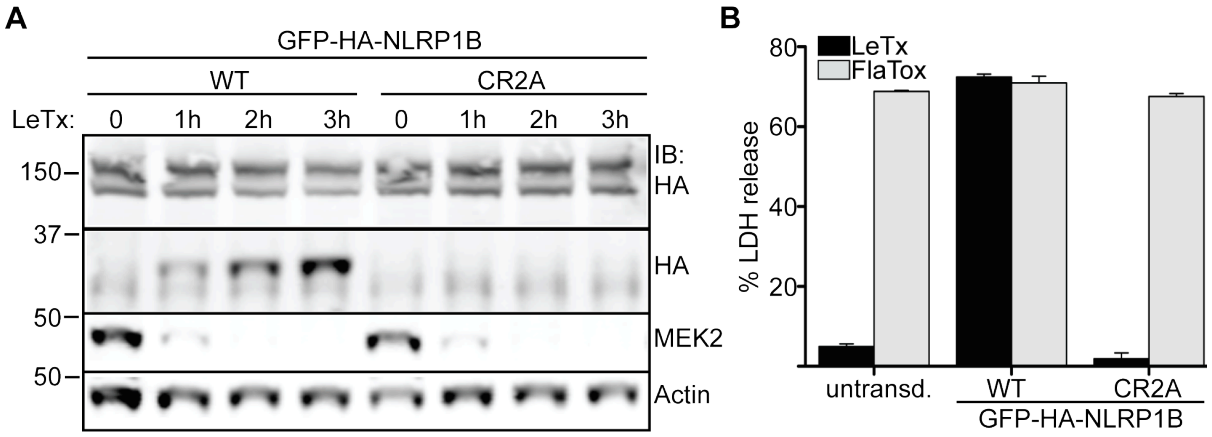

Figure 2.2 Mouse NLRP1B cleavage by LF is required for inflammasome activation. A) Both WT and CR2A GFP-HA-NLRP1B were transfected into 293T cells and then treated with LeTx for the indicated times, and cleavage was monitored by immunoblotting with indicated antibodies. B) Immortalized macrophages from a C57BL6 mouse were transduced with both forms of GFP-HA-NLRP1B and then treated with LeTx or LFn-Fla+PA (FlaTox). Pyroptosis was assayed by LDH release and normalized to complete detergent lysis. Error bars represent plus and minus one standard deviation from the mean.

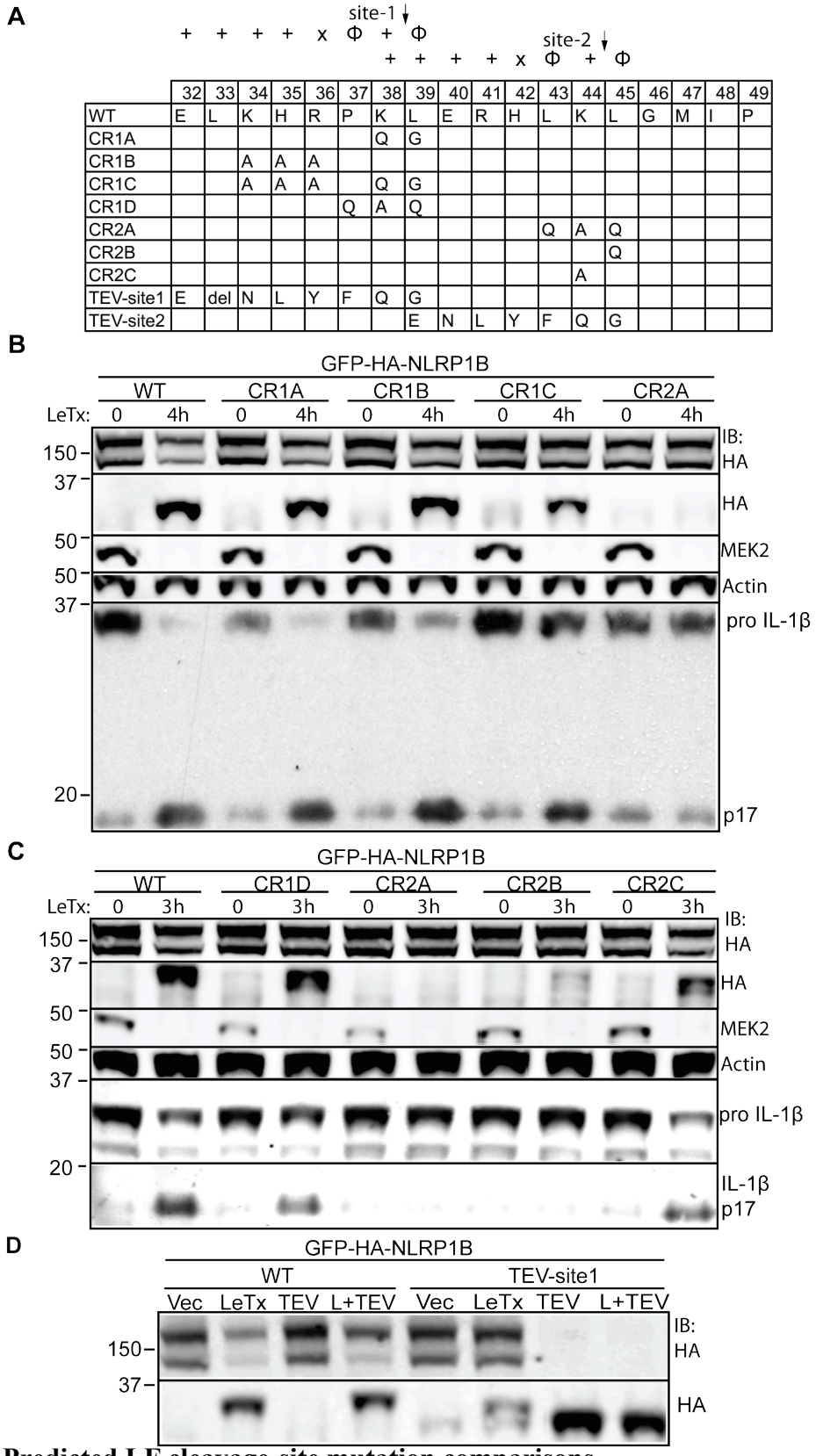

	32	33	34	35	36	37	38	39	40	41	42	43	44	45	46	47	48	49
WT	E	L	K	H	R	P	K	L	E	R	H	L	K	L	G	M	I	P
CR1A							Q	G										
CR1B			A	A	A													
CR1C			A	A	A		Q	G										
CR1D						Q	A	Q										
CR2A												Q	A	Q				
CR2B														Q				
CR2C													A					
TEV-site1	E	del	N	L	Y	F	Q	G										
TEV-site2								E	N	L	Y	F	Q	G				

Figure 2.3 Predicted LF cleavage-site mutation comparisons.

A) LF cleavage-site1 predicts cleavage between K38-39 and the motif surrounding this site was progressively mutated away from the consensus motif. Cleavage-site 2 predicts cleavage between K44 and L45, and this site was muted only at residues immediately surrounding the site. TEV cleavage sites were introduced to produce cleavage after residue 38 for site-1, and residue 44 for site-2. B) Cleavage site-1 mutant series (CR1A-D) and CR2A were transfected into 293T cells and treated with 1μg/ml LeTx for 4h, analyzed by western blotting with the indicated antibodies. The bottom blot was done in the presence of *Casp1* to determine the extent of IL-1β processing. C) WT, CR1D, CR2A-C GFP-HA-NLRP1B were transfected into 293T cells and treated with 1μg/ml LeTx for the indicated time points and cleavage and IL-1β processing was assayed by western blotting. D) WT and TEV-site1 GFP-HANLRP1B were cotransfected with TEV or empty expression vector into 293T cells. Thirty-six hours post transfection cells were treated with LeTx for 4h, then lysed and analyzed by immunoblotting with an anti-HA antibody.

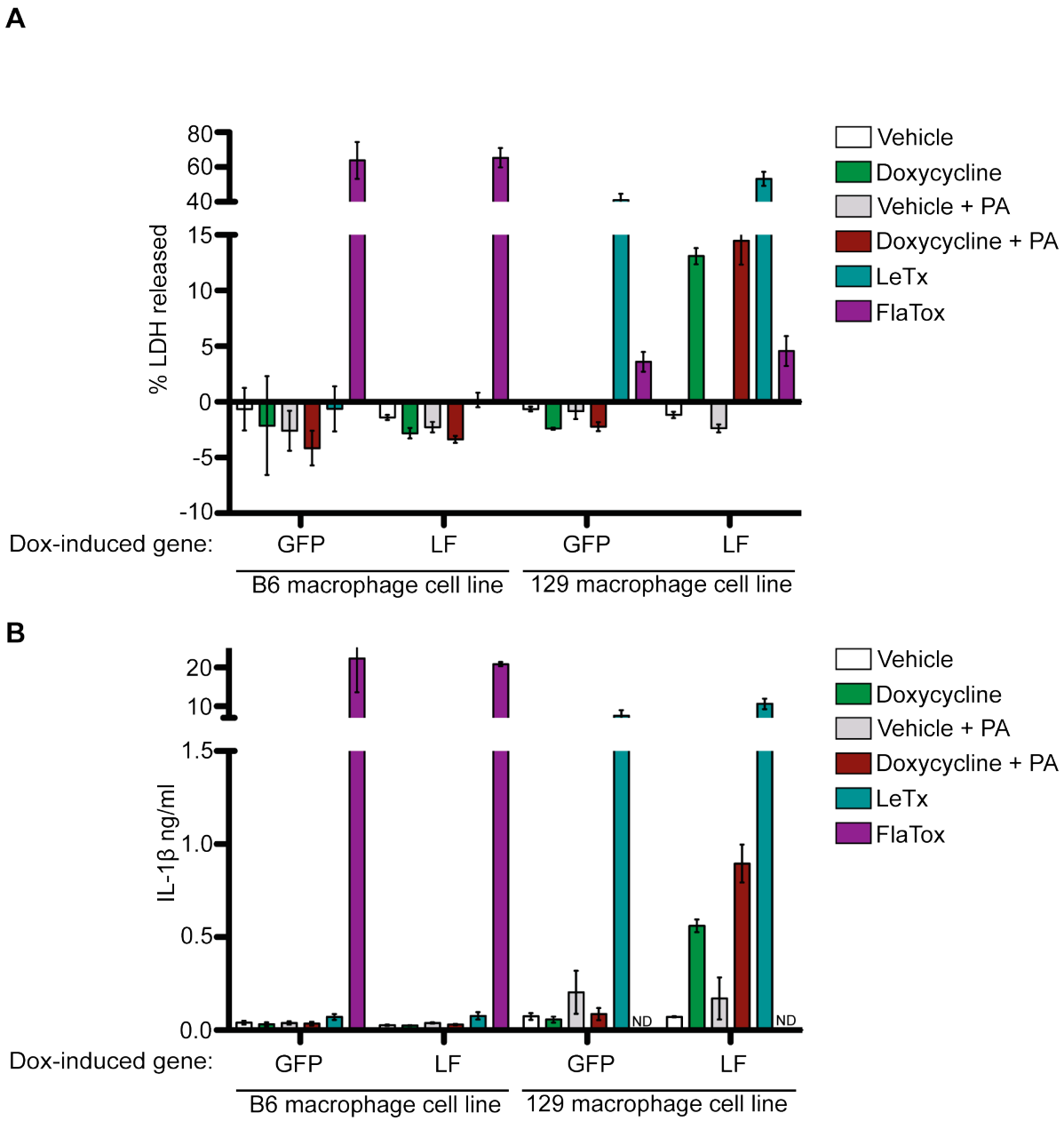

Figure 2.4 LF expression is sufficient to induce pyroptosis and IL-1b in 129 macrophages. Immortalized C57BL/6 (B6) and 129 macrophages were transduced with a Tet-On construct expressing the GFP or LF. Cells were treated with 1µg/ml Pam3CSK4, 5µg/ml doxycycline and 1µg/ml PA for 20h and supernatants were assayed for LDH release and IL-1b release into the supernatant. Cells were also treated with 1µg/ml LeTx and 5µg/ml FlaTox for 4h prior supernatant collection. Error bars represent plus and minus one standard deviation from the mean. ND stands for not determined.

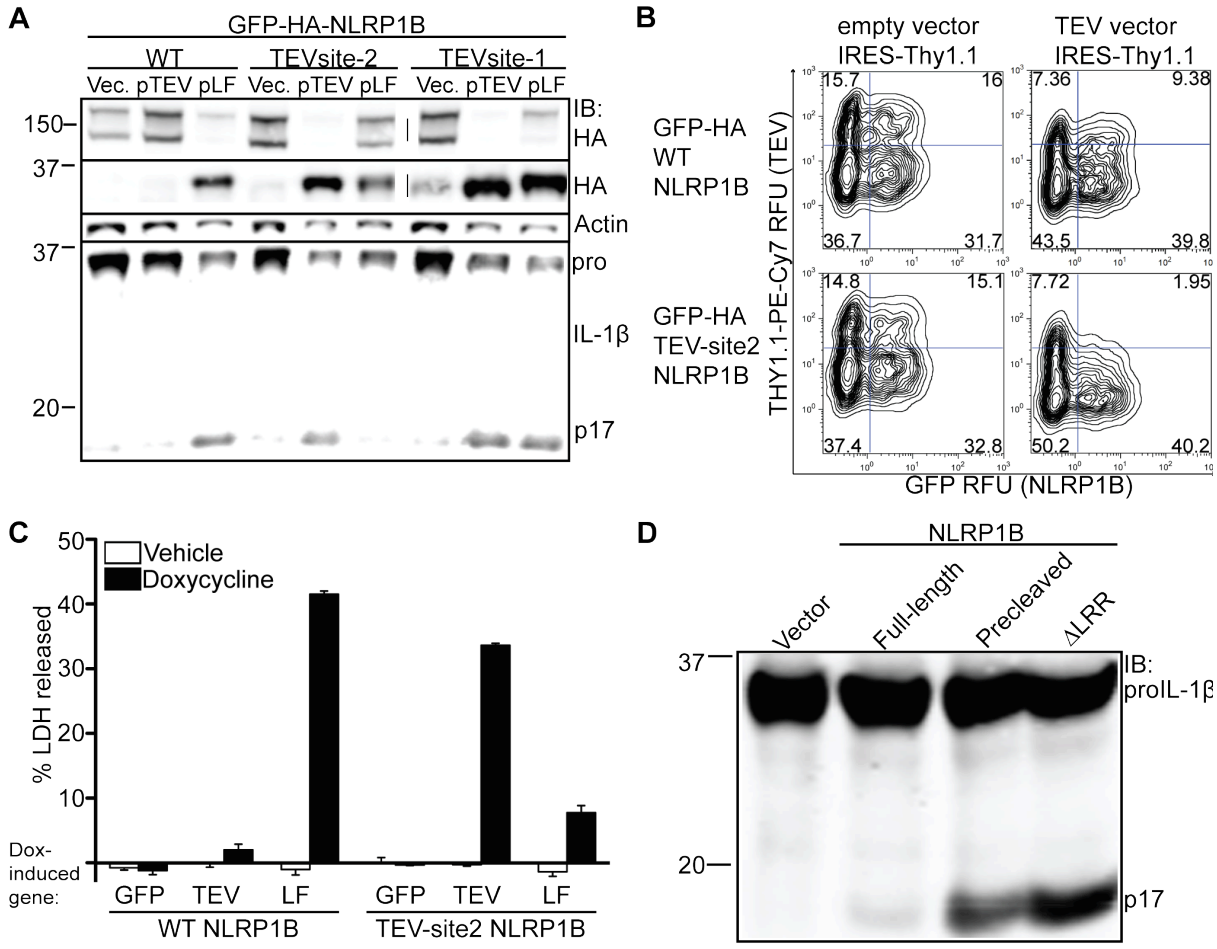

Figure 2.5 Cleavage of NLRP1B is sufficient to promote inflammasome activation. A) 293T cells were transfected with WT, TEV-site2 or TEV-site1 GFP-HA-NLRP1B along with empty vector, TEV expression vector, or a LF expression plasmids. In all conditions cells were also co-transfected with *Casp1* and *Il1b* expression vectors. Cleavage of GFP-HA-NLRP1B and IL-1β was determined 24h post transfection. B) Immortalized B6 macrophages were transduced with a retrovirus encoding the indicated GFP-HA-NLRP1B form followed by a sequential transduction with a TEV-expression retrovirus co-expressing THY1.1. Percent transduction was determined by measuring expression of the respective retroviral integration markers (GFP and anti-THY1.1-PE-Cy7) by flow cytometry, and are expressed in relative fluorescent units (RFU). The numbers within each quadrant represent the percentage of live cells within the respective quadrant. C) RAW264.7 macrophages were transduced with GFP-HA-NLRP1B and a Tet-On construct expressing the indicated gene. Cells were treated with 5μg/ml doxycycline for 20h and supernatants were assayed for LDH release. D) 293T cells were transfected with empty vector, FL-NLRP1B-HA, the truncated NLRP1B-HA, or ΔLRR HA-NLRP1B, along with *Casp1* and *Il1b* and assayed by immunoblotting.

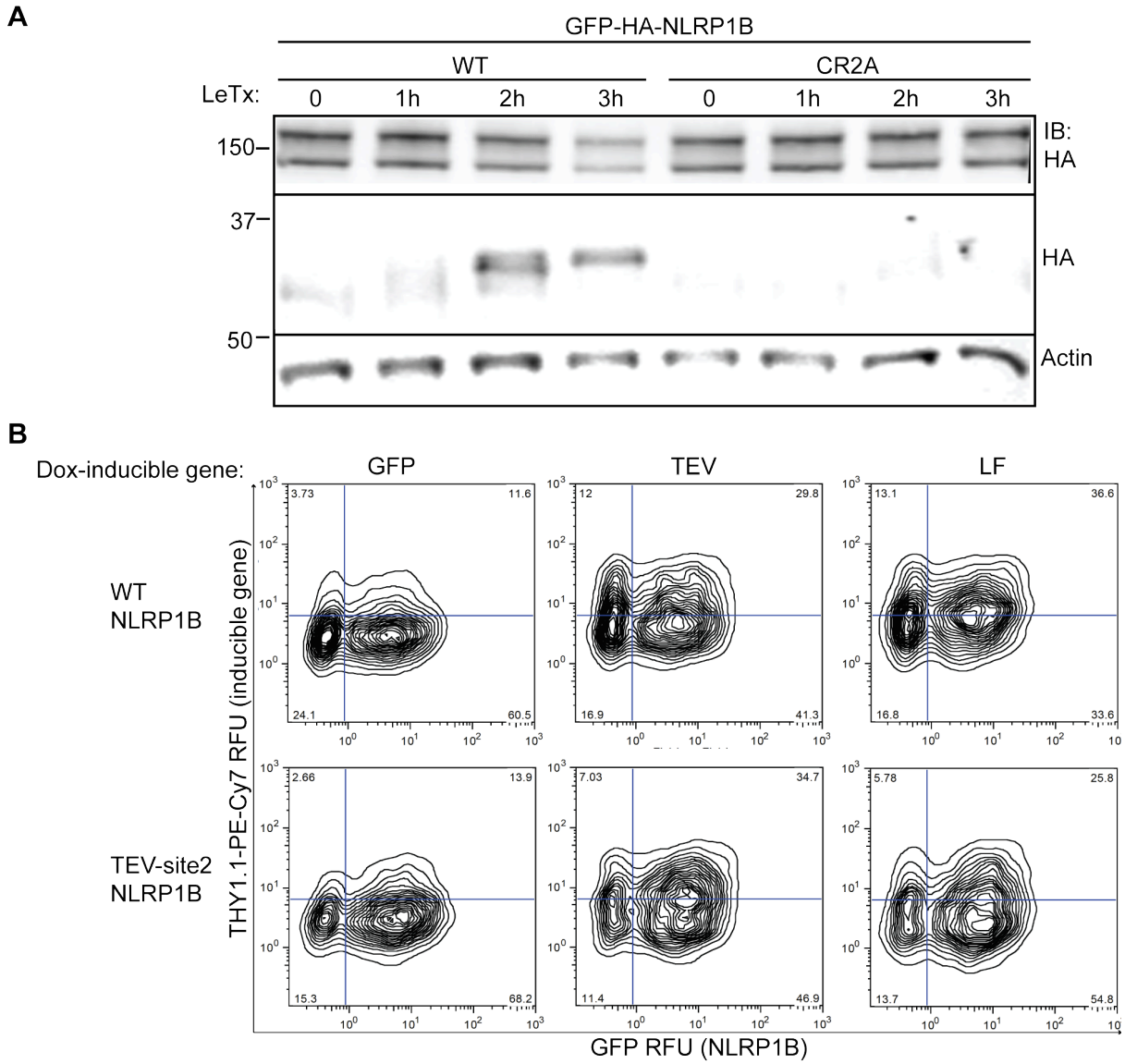

Figure 2.6 Transduction efficiency is the same in macrophage cell lines.
A) Immortalized B6 macrophages were transduced with WT and CR2A GFP-HA-NLRP1B. Expression and cleavage of each NLRP1B was determined by western blotting. Glycine (5mM) was added 1 hour post the addition of LeTx to block lysis of cells in the 2h and 3h time points. B) Percent transduction of RAW 264.7 macrophages was determined by measuring THY1.1 surface expression for the Tet-On vector, and GFP expression for the NLRP1B vector under non-inducing conditions by flow cytometry. GFP and anti-THY1.1-PE-Cy7 fluorescence are expressed in relative fluorescence units (RFU). The numbers within each quadrant represent the percentage of live cells within the respective quadrant.

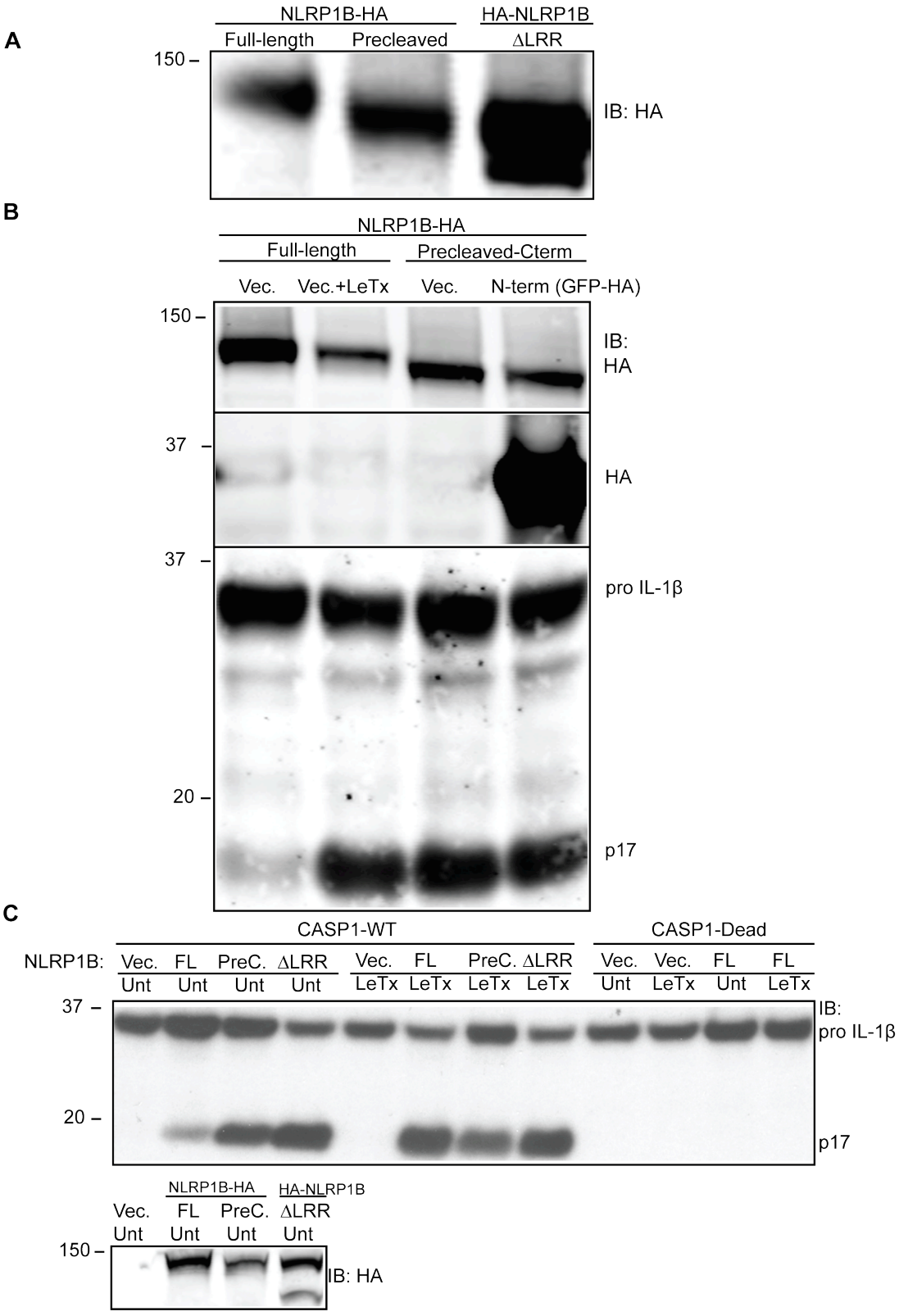

Figure 2.7 NLRP1B's N-terminal fragment has no role in inflammasome activation when expressed in trans.

A) Expression of FL, precleaved and ΔLRR mutants of NLRP1B were determined by anti-HA immunoblotting. B) 293T cells were cotransfected with C-terminally HA tagged WT or precleaved NLRP1B along with *Casp1* and *Il1b* expression constructs. The N-terminal fragment (residues 1-44) fused to GFP-HA was co-transfected with the C-terminal fragments and assayed for IL-1β 24h post-transfection. C) Processing of IL-1β in 293T cells was determined to be dependent on NLRP1B expression and the catalytic activity of CASP1.

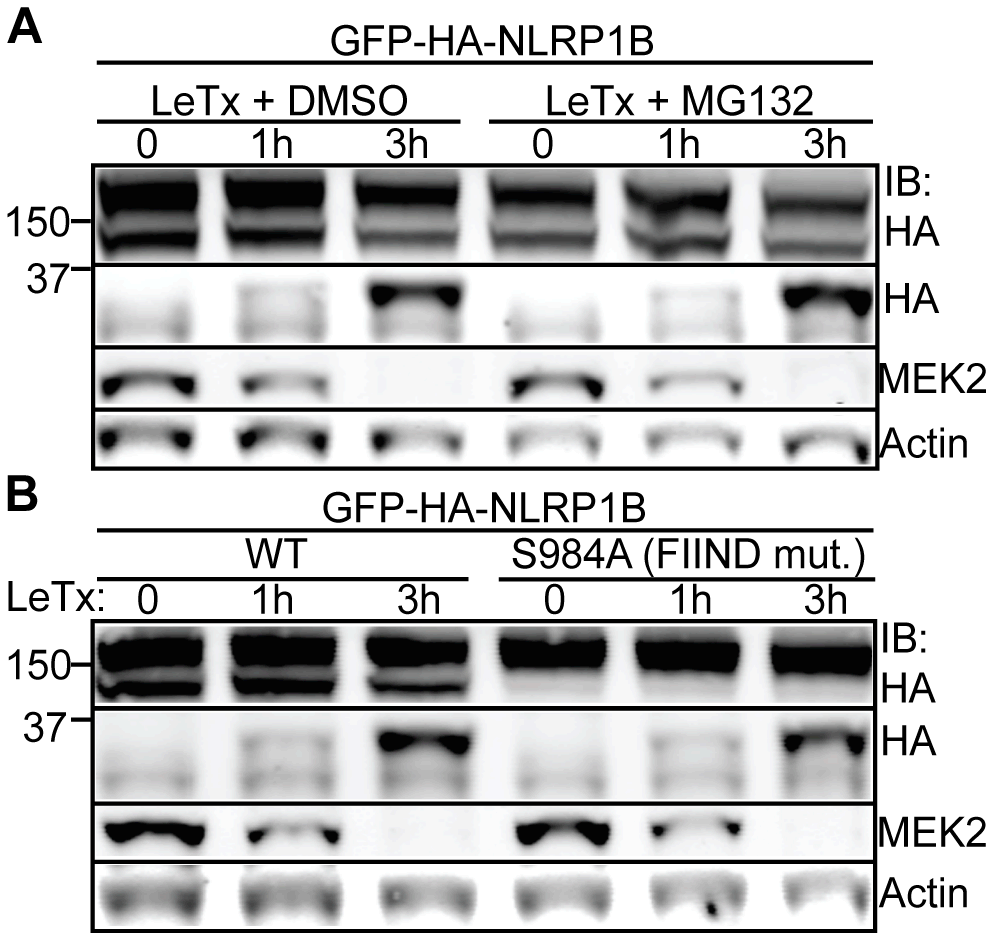

Figure 2.8 Proteasome inhibition and FIIND-processing do not affect NLRP1B cleavage by LF.
A) 293T cells expressing GFP-HA-NLRP1B were co-treated with 1μg/ml LeTx and 10μM MG132 (proteasome inhibitor) or the DMSO vehicle and assayed for cleavage. B) Cleavage susceptibility of WT and S984A (FIIND mutant) GFP-HA-NLRP1B was determined in 293T cells at the indicated time points.

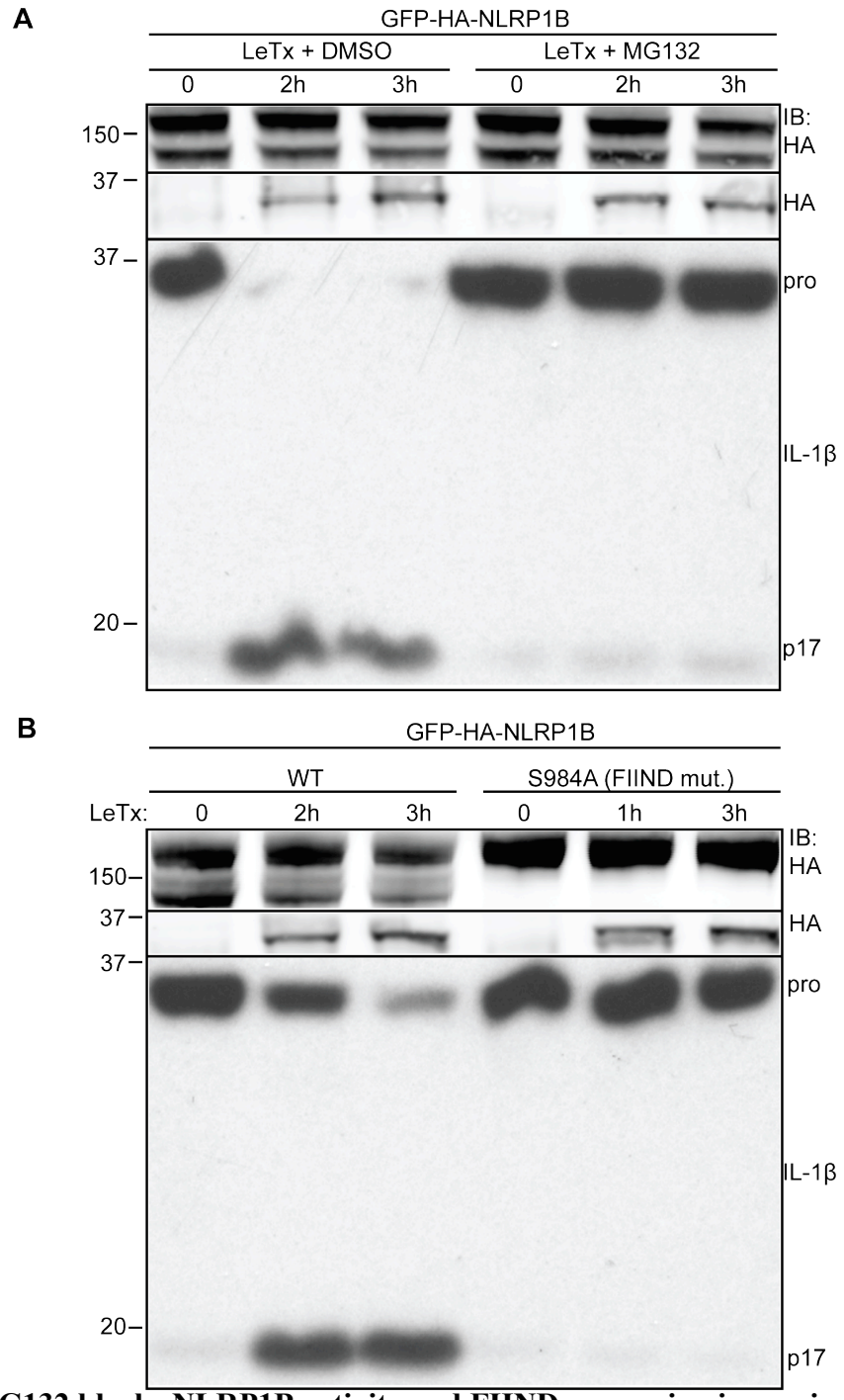

Figure 2.9 MG132 blocks NLRP1B activity and FIIND processing is required in 293T cells.

A) IL-1β processing was analyzed in 293T cells expressing GFP-HA-NLRP1B, *Casp1*, *Il1b* and treated with MG132 (proteasome inhibitor) and LeTx for the indicated time points. B) The necessity of FIIND domain processing for NLRP1B activation in 293T cells was determined by measuring IL-1β processing in cells expressing GFP-HA-NLRP1B, *Casp1*, *Il1b,* after treatment with LeTx for the indicated time points.

	Cloning primer names	primer sequence
1	HA-N1b-XhoI-F	atCTCGAGgccaccATG TACCCATACGACGTCCCAGACTACGCT GAAGAATCCCCACCCAAG
2	N1b-NotI-R	atatGCGGCCGCTCAGGATCCCAAAGAGACCC
3	GFP-HA-N1b-F-NotI	atatGCGGCCGCt ATGTACCCATACGACGTCC
4	GFP-HA-N1b-R-SalI	atatatGTCGACTCAGGATCCCAAAGAGACCC
5	Precleaved-F (L45 start)	atatCTCGAGgccaccATG GGAATGATTCCAGTAGTATATATGAAGC
6	N-terminal fragment (K44 stop) R	atatCTCGAGTTA CTTCAAGTGTCTCTCTAGCTTGGGTCTG
7	TEV-ORF-NotI-F	atatGCGGCCGC ATGCATCACCATCACCATCACGG
8	TEV-ORF-BamHI-F	atatGGATCCgccaccATGCATCACCATCACCATCACGGAG
9	TEV-ORF-BamHI-R	tatatGGATCC TCA TTGCGAGTACACCAATTC
10	LF-ORF-BamHI-F	atatGGATCCgccaccATGGCGGGCGGTCATGGTGATGTAGG
11	LF-ORF-XbaI-R	atatTCTAGATTATGAGTTAATAATGAACTTAATCTG
12	LF-ORF-NotI-F	atatGCGGCCGCgccaccATGGCGGGCGGTCATGGTGATGTAGG
13	LF-ORF-SalI-R	atatGTCGACTTATGAGTTAATAATGAACTTAATCTG

	Mutagenesis primer names	primer sequence
14	CR1A-F	GCTGAAGCACAGACCC caGggA GAGAGACACTTGAAGCTAGG
15	CR1A-R	GCTTCAAGTGTCTCTCTccCtgGGGTCTGTGCTTCAGCTCTAC
16	CR1B-F	GACATATGAATGTAGAGCTG gct gcc gca CCCAAGCTAGAGAGACACTTGAAGC
17	CR1B-R	CAAGTGTCTCTCTAGCTTGGGtgcggcagcCAGCTCTACATTCATATGTCTCG
18	CR1C-F	GACATATGAATGTAGAGCTG gct gcc gca CCC caGggA GAGAGACACTTGAAGC
19	CR1C-R	GCTTCAAGTGTCTCTCTccCtgGGGtgcggcagcCAGCTCTACATTCATATGTC
20	CR1D-F	GCTGAAGCACAGA Caa gcG CaA GAGAGACACTTGAAGCTAGG
21	CR1D-R	GCTTCAAGTGTCTCTCTtGCgcttGTCTGTGCTTCAGCTCTAC
22	CR2A-F	GACCCAAGCTAGAGAGACAC caa gcg caa GGAATGATTCCAGTAGTATATATGAAGCAGG
23	CR2A-R	ATATATACTACTGGAATCATTCCttgcgcttgGTGTCTCTCTAGCTTGGGTCTGTGCTTC
24	CR2B-F	GACCCAAGCTAGAGAGACACTTGAAGcaaGGAATGATTCCAGTAGTATATATGAAGCAGG
25	CR2B-R	ATATATACTACTGGAATCATTCCttgCTTCAAGTGTCTCTCTAGCTTGGGTCTGTGCTTC
26	CR2C-F	GACCCAAGCTAGAGAGACAC TTG gcg CTA GGAATGATTCCAGTAGTATATATGAAGCAGG
27	CR2C-R	ATATATACTACTGGAATCATTCCTAGcgcCAAGTGTCTCTCTAGCTTGGGTCTGTGCTTC
28	TEVsite1-F	GACATATGAATGTAGAG aac ctg tat ttt cag ggc GAGAGACACTTGAAGCTAGGAATG
29	TEVsite1-R	CAAGTGTCTCTCgccctgaaaatacaggttCTCTACATTCATATGTCTCGTTGTGTTC
30	TEVsite2-F	GACCCAAG gag aac ctg tat ttt cag ggc GGAATGATTCCAGTAGTATATATGAAGCAGG
31	TEVsite2-R	CTACTGGAATCATTCCgccctgaaaatacaggttctcCTTGGGTCTGTGCTTCAGCTC
32	Delta-LRR-F	CTTCTACAATCTTAAATTCACC CTGTCCTCTCTCAGTGCCCAGG
33	Delta-LRR-R	CCTGGGCACTGAGAGAGGACAGGGTGAATTTAAGATTGTAGAAG
34	S984A-F	TGAAAAACCCAAGCTTC gct CCAATGGGAGTTGTACTGAG
35	S984A-R	GTACAACTCCCATTGGagcGAAGCTTGGGTTTTTCAGTAC

Table 2.1 Primer sequences used for cloning.

Chapter 3: Proteolysis is a conserved mechanism of activating mammalian NLRP1

3.1 Introduction:

Mammals have evolved multiple mechanisms of detecting microbes in order to mount immune responses during infection. While immune responses occur in response to both commensal and pathogenic microbes, a qualitative distinction is made between the two. The type and magnitude of the response is scaled appropriately to promote clearance of pathogens and avoid immunopathology, which could otherwise occur in response to ubiquitous and commensal microbes. One family of pattern recognition receptors that can discriminate between pathogens and commensals is the nucleotide-binding domain (NBD) and leucine-rich repeat containing protein family (NLR) (von Moltke et al., 2013). NLRs are cytosolic proteins that can be activated upon pathogen access to the host cell cytosol. Pathogens use different virulence mechanisms, such as toxins and bacterial secretion systems, to access the cytosol, resulting in NLR activation. Upon activation, several NLRs have been shown to form a scaffold which recruits and activates the protease CASP-1, and this scaffold is termed an inflammasome. Active CASP-1 is best known for cleaving, maturing, and secreting the cytokines IL-1B and IL-18, as well as leading to the lytic cell death known as pyroptosis.

The molecular mechanisms by which different NLRs are activated in response to pathogen stimulation are not completely understood. In fact, few examples of the basic mechanism of NLR activation are known, and for some NLRs this mechanism is controversial. For example, in the murine system it has been shown that NAIP1 binds the needle protein of bacterial Type III secretion systems (TIII SS), NAIP2 binds the inner rod protein of TIII SS, and NAIP5 binds bacterial flagellin. Interestingly, humans only have a single NAIP gene, but have a conserved mechanism of activation in response to needle proteins of the TIII SS, similarl to murine NAIP1 (Rayamajhi et al., 2013; Zhao et al., 2011). Upon ligand binding, NAIPs co-associate with a different NLR member, NLRC4, and together form the active inflammasome that recruits and activates CASP-1 and ASC (Kofoed and Vance, 2011). Thus, the NAIP/NLRC4 inflammasome seems to be activated by a straightforward ligand-receptor-type mechanism.

The study of NLRP1B, another murine NLR, has indicated that its mechanism of activation is quite distinct from the NAIPs, as it is not simply a ligand-receptor mode of activation. Instead, NLRP1B is activated by the protease activity of anthrax lethal factor (LF) (Boyden and Dietrich, 2006), which is produced by *Bacillus anthracis*, the causative agent of anthrax. LF and protective antigen (PA) together form Lethal Toxin (LeTx), and PA transports LF into the host cell's cytotosol to cleave and inactivate most MAPKKK. Lethal factor also cleaves NLRP1B proximal to its N-terminus, and this is both necessary and sufficient for NLRP1B inflammasome formation and CASP-1 activation. Lethal factor is one of the few *bona fide* stimuli reported for NLRP1B. NLRP1B is highly polymorphic in mice (Boyden and Dietrich, 2006), and only two of five identified alleles have been shown to respond to LF. Furthermore, it is unknown if allele 2, the allele found in B6 mice, fails to respond to LF because it is not cleaved by LF, or if it has lost all function as an inflammasome. Similarly, it is not clear whether NLRP1A, the other murine paralog, is able to form an inflammasome, since no natural stimuli capable of activating NLRP1A have been identified. Only one previous study provides evidence to support the fact that NLRP1A can also form an inflammasome. This study identified a mouse carrying a mutation in NLRP1A (Q593P) that has a phenotype consistent with a

spontaneously active inflammasome (Masters et al., 2012), but the role of the wild-type NLRP1A is less clear. Recently, several groups have provided evidence that NLRP1B in mice and NLRP1 in rats are both important for resistance to *Toxoplasma gondii* infections (Cavailles et al., 2014; Cirelli et al., 2014; Ewald et al., 2014), suggesting that NLRP1 is being activated by this pathogen. While the mechanism by which *T. gondii* activates NLRP1 is unknown, it is tempting to speculate the mechanism is also via direct proteolysis. An attempt to detect cleavage of the 129 allele of NLRP1B during *T. gondii* infection did not support this hypothesis (Ewald et al., 2014), but it is technically challenging to detect cleavage of NLRP1B when the response to *T. gondii* is slower and lower in magnitude when compared to LF.

The mechanism of activation of the human ortholog of NLRP1 is controversial and suggested to be distinct from the murine NLRP1B. Human NLRP1 was actually the first NLR shown to assemble into a multiprotein 'inflammasome' complex (Martinon et al., 2002), but in this study, NLRP1 was activated spontaneously in cellular lysates. Thus, the mechanism by which NLRP1 is activated in response to a specific stimulus was not addressed. A different study of the human NLRP1 inflammasome observed that muramyl dipeptide (MDP), a fragment of peptidoglycan found in bacterial cell walls, stimulated the oligomerization of NLRP1 in a cell-free system. However, subsequent analyses of this response in human and mouse cells have raised doubts that MDP is a specific agonist for NLRP1, rather than activating other NLRs (Girardin et al., 2003; Inohara et al., 2003; Martinon et al., 2004). In particular, it has been difficult to disentangle the ability of MDP to prime inflammasome expression via the NOD2 sensor from potential direct agonist effects of MDP on NLRP1. Importantly, genetic data demonstrating a requirement for NLRP1 in the inflammasome response to MDP is currently lacking.

One important structural difference between human NLRP1 and rodent NLRP1 is the presence of an N-terminal Pyrin domain (PYD) in the human isoform. It remains controversial whether the NLRP1 PYD is essential for CASP-1 activation. However, if the PYD domain is necessary for inflammasome formation, then this might preclude proteolytic cleavage as a mechanism of activation, at least if proteolysis were to occur in a position conserved in mouse NLRP1B.

In this study, we demonstrate that proteolysis is a mechanism of activation conserved across all mammalian NLRP1 homologs and paralogs we tested. We took advantage of our ability to reconstitute NLRP1 inflammasomes individually in heterologous cells to show that N-terminal cleavage is sufficient for NLRP1 activation. This method avoids the problem with other inflammasomes being inadvertently activated when using cells such as macrophages, which can form multiple inflammasomes. In short, we observed that induced proteolysis of two distinct murine alleles of NLRP1B and the NLRP1A paralog are sufficient to cause inflammasome activation. Surprisingly, the human NLRP1 ortholog could also be activated via direct proteolysis. We observed that the PYD is dispensable for inflammasome formation, which is consistent with proteolysis being a mechanism of activation. Taken altogether, we believe that NLRP1 in most mammalian species is likely to have conserved its mechanism of activation via proteolysis. While the basic mechanism is conserved, we believe the proteases and their sources, which trigger NLRP1 activation, are different for these different homologues of NLRP1.

3.2 Results:

3.2.1 Cleavage and activation of the B6 NLRP1B isoform

NLRP1B is highly polymorphic in mice, and five different alleles have been identified (Boyden and Dietrich, 2006). Of these five alleles, two respond to LF to form an inflammasome to promote pyroptosis. Macrophages of B6 mice, which encode allele-2, express an NLRP1B transcript, but it is unknown why these cells do not respond to LF. It is unclear if the B6 NLRP1B isoform can form an inflammasome, as no clear agonist has yet been reported for it. A predicted protein sequence alignment of the LF-responsive allele-1, expressed in 129 mice, and the B6 allele of NLRP1B, reveals that 190 of 1233 amino acids are not conserved. Due to these numerous differences, it is unclear which differences determine the lack LF responsiveness in the B6 isoform. Most of these differences are present in the N-terminal half of the protein (Fig. 3.1A), while the C-terminal portion which contains the CARD is identical (Boyden and Dietrich, 2006). The presence of an intact CARD suggests that the B6 isoform is still capable of recruiting CASP-1 as an inflammasome when activated. Comparison of the N-terminal LF-cleavage site in the 129 allele and the B6 allele identifies few amino acid differences immediately surrounding the site (Fig. 3.1A and Fig. 3.2A), but it is not clear whether these differences account for non-responsiveness to LF.

We therefore first investigated if LF cleaves the B6 isoform of NLRP1B. To efficiently monitor N-terminal cleavage of NLRP1B of 129 mice, we had previously fused GFP-HA at the N-terminus of NLRP1B (Chavarria-Smith and Vance, 2013). This construct enhances N-terminal fragment detection by augmenting its size and stability in the cytosol. Therefore we also fused the B6 allele to GFP-HA. We transfected both alleles of NLRP1B into HEK 293T cells along with expression plasmids encoding Casp1 and Il1b to reconstitute a functional inflammasome. Surprisingly, the B6 isoform of NLRP1B promoted significant amounts of IL-1B processing even in the absence of LF. This suggests that B6 NLRP1B, despite all of the polymorphisms, is capable and sufficient to form an inflammasome when over-expressed (Fig 3.1B). However, the high amount of cleaved IL-1β induced by B6 NLRP1B without stimulation was unexpected, and was much greater than the basal activity of the 129 allele, despite comparable processing of the FIIND in both isoforms. LeTx treatment did not further increase the amount of cleaved IL-1B (p17) in cells expressing the B6 allele. In addition, we did not observe LF-dependent cleavage of the B6 isoform, but did observe the expected cleavage of the 129 isoform. In order to reduce the levels of spontaneous activation seen with the B6 NLRP1B isoform, we serially diluted the amount of NLRP1B encoding plasmid. We observed a dose-dependent decrease in the amount of spontaneous IL-1B processing under these conditions (Fig 3.1C). A 64-fold reduction in the amount of plasmid encoding the B6 allele was required to achieve a similar level of cleaved p17 as seen with the starting amount of 129 allele encoding plasmid. We interpret that the B6 allele is capable of forming an inflammasome, but the mechanisms of auto-inhibition are weaker and can be overcome when exogenously over-expressed.

While the B6 allele is not cleaved or responsive to LF stimulation, we hypothesized that the B6 isoform might still be activated by proteolysis, but by proteases with specificities different than the LF protease. Following a strategy we used previously with the 129 NLRP1B allele (Chavarria-Smith and Vance, 2013), we tested this hypothesis by engineering a tobacco etch virus (TEV) protease cleavage-site in the B6 isoform. The TEV site was inserted in B6 NLRP1B at a position homologous to the site at which 129 NLRP1B is cleaved by LF. We then expressed the B6-TEV allele along with TEV protease or LF-protease and assessed

inflammasome formation via IL-1B processing. Interestingly, the B6-TEV isoform induced significant amounts of IL-1B processing in the presence of TEV protease, and not LF protease (Fig. 3.1D). This activation was comparable to the wild-type 129-allele NLRP1 activation by LF, or TEV activation of the 129 allele with a TEV site. Consistent with the lack of cleavage observed upon LeTx treatment (Fig. 3.1B), the WT B6 isoform was neither cleaved nor responsive to LF over-expression (Fig. 3.1D).

We further investigated the determinants for the differences in LF cleavage sensitivity between the two NLRP1B isoforms. As seen in Fig. 3.1A and 3.2A, three different residues in the vicinity of the LF-cleavage site of the 129 allele are polymorphic in the B6 allele, and we hypothesized that this might explain differential LF proteolysis. We sequentially mutated these three residues in the 129 allele to match the ones found in the B6 allele, and then tested the sensitivity of the resulting proteins to LF cleavage. 129/B6-A (L39P/R41G) and 129/B6-B (M47T) exhibited a minimal reduction in LF-dependent cleavage and inflammasome responsiveness (Fig. 3.2B-C). Combining the two sets of mutations to generate 129/B6-C resulted in a protein with only a partially reduced level of LF-cleavage. This result implies that amino acid polymorphisms outside the immediate vicinity of the cleavage site might also contribute to differential proteolysis of the two isoforms. A previous paper examining cleavage of a polypeptide encoding the first 118 amino acids of 129 NLRP1B indicated that K38 and K44 were necessary for susceptibility to cleavage by LF (Hellmich et al., 2012), but mutating both residues simultaneously in the context of the full-length protein did not affect sensitivity of 129 NLRP1B to cleavage (Fig. 3.2C). This indicates that these residues are incomplete determinants of LF sensitivity and implies that residues outside the cleavage site are important in determining LF sensitivity.

It remains unclear how the presence of the N-terminus maintains NLRP1B in an "off" state, and how proteolysis activates NLRP1B. We had previously expressed a "pre-cleaved" mimic of the 129 allele, termed G46 here, and observed spontaneous IL-1β processing in the absence of LF. We made other pre-cleaved NLRP1B of differing lengths of the 129 allele to further understand the minimal amount of N-terminus that promotes auto-inhibition. A version of NLRP1 generated by starting translation at codon 38 (termed L39) has low spontaneous activation, but can still be activated upon LF cleavage, consistent with Liao et al 2014 (Fig. 3.2E). Expression of a pre-cleaved starting translation at codon 44 or 45 (termed L45 and G46) had spontaneous activity and was not further stimulated by LT. This suggests that residues 38-44 are important in maintaining the protein inactive prior to stimulation.

3.2.2 Cleavage and activation of mouse NLRP1A

B6 macrophages also express a transcript for NLRP1A, but since B6 macrophages do not respond to LF it is presumed that NLRP1A is not activated by LF. Comparison of the primary amino acid sequences of B6-NLRP1A versus NLRP1B again reveals numerous polymorphisms within the N-termini (Fig. 3.3A). In addition, no known stimulus has been shown to activate NLRP1A. Thus, it remains unclear whether NLRP1A is cleaved by LF and whether NLRP1A could form a functional inflammasome (in response to LF or other stimuli).

We generated an expression construct to express the reference sequence for NLRP1A found in NCBI (NM_001004142.2). We first tested if expression of NLRP1A is sufficient to produce a functional inflammasome in the previously described 293T reconstituted system. Overexpression of NLRP1A in this system indeed led to substantial IL-1B processing, comparable to the amount induced by overexpression of the 129 allele of NLRP1B prior to stimulation (Fig. 3.3B). Consistent with the lack of responsiveness of B6 macrophages to LeTx,

LeTx did not enhance the amount of IL-1β processing in cells expressing NLRP1A, whereas 129-NLRP1B did respond to LeTx. To directly test whether LF can cleave NLRP1A, we fused GFP-HA to the N-terminus of NLRP1A as previously described. Co-expression of NLRP1A and LF did not result in detectable N-terminal cleavage, which is robustly seen with the 129-NLRP1B paralog (Fig. 3.3C).

In order to test whether proteolysis could act as a sufficient stimulus to activate B6-NLRP1A, we engineered a TEV-protease site into NLRP1A at a site homologous to the site of LF cleavage in 129-NLRP1B. Interestingly, specific proteolysis of the NLRP1A-TEV isoform by TEV protease did induce a large increase in the amount of IL-1B, comparable to what is observed with 129-TEV-NLRP1B or 129-WT-NLRP1B with TEV protease and LF protease, respectively (Fig. 3.3C). Importantly, this TEV-induced activation correlated with N-terminal cleavage of NLRP1A, and was not observed with NLRP1 forms that lack the TEV-protease site.

3.2.3 Cleavage and activation of human NLRP1:

The human ortholog of NLRP1 has an N-terminal Pyrin domain (PYD), which is not found in rodent NLRP1. Initial reports of the NLRP1 inflammasome suggested that the PYD was necessary for ASC and CASP1 co-recruitment, but other recent reports suggest this is not the case (Finger et al., 2012). The previously suggested necessity of the PYD for NLRP1 function was a major reason for doubting that N-terminal proteolysis is a conserved mechanism for human NLRP1 activation. We therefore decided to test human NLRP1 in our reconstituted system. We cloned a human NLRP1 cDNA encoding the reference sequence isoform 1 (NM_033004.3), and reconstituted the inflammasome in 293Ts with mCasp1, hASC, and mIl1b expression vectors. As a positive control, we also generated an expression construct encoding a variant deleted of LRR domain, as ΔLRR mutants of NLR proteins are typically constitutively activated. In addition, we generated a construct lacking the N-terminal PYD to test its necessity for inflammasome formation. When high levels of NLRP1 are expressed, we observed significant signs inflammasome activation processing with all NLRP1 constructs (Fig. 3.4A). To assess differences in inflammasome activity among the constructs we titrated the amount of NLRP1 expression plasmid added to the system. Surprisingly, at the lowest levels tested, we still observed significant NLRP1-dependent IL-1β processing. The ΔPYD isoform exhibited a slightly higher level of spontaneous activity when compared to the full-length protein. This not only indicates that the PYD is dispensable for inflammasome formation, but also suggested that proteolysis of the N-terminal PYD domain might produce an activated NLRP1 protein.

Human NLRP1 has an interdomain linker longer than 100 residues, connecting the PYD and the NBD, which has no predicted secondary structure (Fig. 3.4B). We hypothesized that this unstructured region might be sensitive to proteases and that proteolysis would lead to NLRP1 activation. We engineered two different TEV-protease sites into this unstructured interdomain linker. One TEV-protease site was inserted immediately after the PYD, and the other was placed prior to the beginning of the predicted NBD (Fig. 3.4B). We tested the ability of TEV protease to activate both of these NLRP1 constructs. Both versions of NLRP1 containing a TEV-protease site induced higher levels of IL-1B cleavage when coexpressed with TEV protease. This activity was dependent on the TEV-protease site, as it did not occur with the WT version of NLRP1. TEV cleavage resulted in activation comparable to the level observed with the ΔLRR-NLRP1 positive control. The LF cleavage sites identified in rodent NLRP1 does not appear to be conserved in human NLRP1, and LeTx stimulation of human macrophages also does not seem to lead to inflammasome activation (Moayeri et al., 2012). Despite this, it has not been directly

tested if LF can cleave or activate human NLRP1. In our system, ectopic expression of LF did not induce detectable cleavage of NLRP1, nor did it lead to NLRP1 activation.

The PYD appears to be present in most orthologs of NLRP1, with mice and rats representing the main exceptions among mammals. Our observation that the PYD is not essential for human NLRP1 activation raises the important question of why the PYD has been conserved in most mammalian NLRP1 isoforms. We hypothesized that perhaps the PYD is necessary for maintaining auto-inhibition of NLRP1, and proteolysis would remove this inhibition. We tested if the PYD is specifically required to maintain NLRP1 auto-inhibited or if an unrelated protein sequence could mimic the role of the PYD. We generated a series of constructs that fused GFP to the N-terminus of NLRP1 and tested the necessity of the PYD to achieve proteolysis dependent activation (Fig. 3.4C). Surprisingly, replacement of the PYD with a GFP domain was able to maintain the protein in an auto-inhibited state. Additionally, even when the PYD was deleted, TEV-dependent proteolysis again activated NLRP1 at the same two sites tested in the full-length context.

While it was previously reported that primate NLRP1 exhibits a strong overall signature of positive selection (George et al., 2011), previous analyses did not pinpoint the regions of the protein that were diversifying most rapidly. Careful analysis of signatures of positive selection in transcripts of 10 different primates identified 14 codons with a high probability of being repeatedly under positive selection (Fig 3.5A). Four of these codons correspond to the interdomain linker region where we expect protease sensitivity to be an agonistic signal. This observation is consistent with the region being under selective pressure to diversify and respond to different proteases in different primate species.

ATP binding to human NLRP1 has also been reported to be required for inflammasome oligomerization and CASP1 activation (Faustin et al., 2007). A requirement for ATP binding does not seem to be exhibited by murine NLRP1B. Instead, preventing ATP binding by mutation of the Walker A motif appears to lead to a constitutively active version of the protein (Liao and Mogridge, 2013) (Fig. 3.5C). We decided to test the effect of mutating the Walker A motif in K340A and K340R in human NLRP1. Surprisingly, but consistent with observations with mouse NLRP1B, Walker A mutations did not abrogate the ability of human NLRP1 to promote IL-1B processing when NLRP1 is expressed ectopically (Fig. 3.5B).

Human and murine NLRP1 have also been reported to be negatively regulated by Bcl-2 and Bcl-xL proteins (Bruey et al., 2007). This regulation is reported to be mediated by direct binging to the LRR, a mechanism that is also reported to prevent ATP binding to the NBD (Bruey, 2007 and Faustin, 2009). Given that we do not observe a necessary role for ATP binding and inflammasome activation, we decided to test the role of Bcl-xL in this model. We compared the ability of both mouse 129-NLRP1B and human NLRP1 to be suppressed by Bcl-xL over-expression in our 293T reconstituted system. In contrast to previous reports, we could not detect any effects of Bcl-xL on the activity of full-length NLRP1 of either origin (Fig. 3.5D).

A previous report indicated that a splice variant of human NLRP1, lacking exon 14, is inactive in cells due to a defect in FIIND autoprocessing (Finger et al., 2012). Surprisingly, this inactive variant is the version used in multiple reports, including the MDP dependent activation and Bcl-xL regulation (Fauting, Bruey and Faustin). We obtained this variant from the authors and tested its activity in our system. Indeed, we did not observe significant IL-1β processing with NLRP1Δexon14 (Fig. 3.5E), consistent with the previous report from Finger (Finger et al., 2012). This lack of activity also correlated with a lack of FIIND processing phenotype, as most of the protein was in the unprocessed state of ~160kDa as reported in (Finger et al., 2012).

3.3 Discussion

Understanding the mechanism by which LF cleaves and directly activates NLRP1B in 129 mice led to the obvious question of the generality of proteolysis as a mechanism of NLRP1 activation in other mice strains and other species. As previously mentioned, there are multiple alleles and paralogs of NLRP1 in mice. For most of these variants, no clear agonist has been discovered. Since many of these homologs exhibit strong conservation of their CARD, we speculated that they are not pseudogenes, and are likely to retain inflammasome function.

When we evaluated LF sensitivity of NLRP1A and NLRP1B of B6 mice, we did not observe any N-terminal cleavage. This directly explains why B6 macrophages do not form an inflammasome when they are treated with LeTx (Boyden and Dietrich, 2006). The reasons for why neither of these paralogs are cleaved by LF are harder to discern. Differences in the protein sequence of B6 and 129 NLRP1B suggest that M47 (129) vs T47 (B6) partially affects LF susceptibility. This is in contrast to other differences immediately surrounding the LF-cleavage site (L39P and R41G) that seem to have no effect. Moayeri's group observed that allele-3 in AKR mice is cleaved preferentially at position 44-45, and allele-1 in 129 is preferentially cleaved at position 38-39 (Hellmich et al., 2012). This difference in cleavage pattern is confusing given that both alleles have identical primary sequences surrounding either of the sites. One caveat to the Moayeri study is that they analysed a truncated polypeptide (the first 118 N-terminal residues), and not full-length proteins. In our hands, when evaluating NLRP1B allele-1 (129) cleavage we observed LF preference for residues 44-45, as only mutations in residues 43-45 affected LF susceptibility (Chavarria-Smith and Vance, 2013). Interestingly, K38A/K39A mutation to full-length 129 NLRP1B did not affect LF cleavage, which is cleavage-resistant in the report by Hellmich et al. Taken together, we hypothesize that other regions of NLRP1, present in the full-length NLRP1B context, help determine LF-substrate affinity and the site of cleavage. This hypothesis is consistent with the way in which LF recognizes it cognate substrates, the MAPKKs or MKKs (Turk, 2007). LF substrate specificity is reported to be determined by the cleavage-site itself and a C-terminal region termed LFIR (Chopra et al., 2003). This other C-terminal region might explain why a Map2k2 cDNA, which did not encode any of the N-terminal cleavage site, was originally discovered as an LF interaction protein in a yeast two hybrid assay (Vitale et al., 1998). Analogously, we expect that another domain of NLRP1B might interact with LF and determine its substrate affinity.

Until now it was not known if B6 mice expressed a functional NLRP1B that could form an inflammasome. Because NLRP1B is highly polymorphic in mice, and the B6 NLRP1B isoform exhibits the highest degree of divergence compared to isoforms known to forms inflammasomes, it is hard to predict a conservation of function. Two of the alleles of NLRP1B in mice, for example those that can be found in AKR or DBA, cannot form functional inflammasomes, suggesting the B6 allele of NLRP1B could be have the same problem. This is the first report that determines that the B6 allele of NLRP1B matures its FIIND, and is sufficient to activate CASP-1 as an inflammasome. We expect that the spontaneous activity observed upon over-expression is unlikely to be physiological, and that endogenous NLRP1B in macrophages is expressed at levels significantly below the threshold that produces spontaneous activation. The differences in basal activity between the 129 allele and the B6 allele does suggest that the 129 allele has a stronger propensity to maintain auto-inhibition. Despite these differences, we found that cleavage of the B6 isoform with TEV-protease site results in cleavage-dependent B6 NLRP1B activation. This suggests that the B6 isoform of NLRP1 is activated by a conserved cleavage-dependent mechanism, but that it might have evolved to respond to other proteases. If

LF responsiveness by NLRP1 in rodents is an ancestral trait, there might not be a large fitness cost to lose responsiveness to this protease. This might be the case if *B. anthracis* is not a prevalent pathogen to different populations of rodents in the wild, and therefore might not be a strong force driving natural selection.

NLRP1A, a paralog of NLRP1B that likely arose by gene duplication, also does not respond to any reported stimuli. The only indication that NLRP1A can form an inflammasome is from genetic evidence from a mouse carrying a mutation in NLRP1 that suggests it is a spontaneously active inflammasome. While this suggests that NLRP1A-Q593P can form an inflammasome, the function and natural mechanism of activation of wild-type NLRP1A is far less clear. Our results provide evidence that NLRP1A also has conserved the mechanism of activation via proteolysis like the NLRP1B paralog. Like NLRP1B of B6 mice, NLRP1A also has a M47T substitution when compared to 129 NLRP1B, and might partially explain the lack of LF dependent cleavage.

The mechanism of human NLRP1 has been controversial as its reported stimulus and mechanism of activation has been proposed to be very different from the murine NLRP1B. As mentioned above, human NLRP1 was the first inflammasome described, and in the initial study, it was claimed that the PYD mediated ASC and CASP1 co-recruitment (Martinon et al., 2002). However, a recent study disputed this conclusion as they observed that the PYD was dispensable for CASP1 activation or ASC binding when the components were over-expressed in mammalian cells (Finger et al., 2012). Here, we report that the PYD is necessary for maintaining NLRP1 in an auto-inhibited state, but not for CASP-1 activation. Unexpectedly, we were able to replace this PYD-dependent auto-inhibition function with an unrelated protein fold (GFP). This may suggest that the PYD fold might sterically hinder NLRP1from assembling into an active inflammasome. This also might explain why rodents have lost the PYD altogether, and have evolved a different N-terminal sequence to replace the PYD and maintain auto-inhibition. We do interpret our findings with caution, however, as there might be other subtle positive or negative regulatory roles for this domain that might be important in NLRP1's endogenous setting and with other partner proteins.

Despite previous publications to the contrary, our results suggest that the mechanism of human NLRP1 activation closely resembles that of the mouse. The transcriptional variant used here does efficiently autoprocess its FIIND domain and FIIND processing correlated with inflammasome activity. Similar to the findings of Finger et al, we assessed the inflammasome potential of the transcript of NLRP1 provided by Faustin et al., which lacks exon 14. In agreement with Finger, we do not observe efficient FIIND processing or inflammasome activity of the Δexon 14 variant. Faustin et al. previously suggested that human NLRP1 and mouse NLRP1B also differ with respect to nucleotide binding (Faustin et al., 2007). In their cell free system, Faustin et al. observed a requirement of ATP for NLRP1 oligomerization and CASP-1 activation. Furthermore, they observed that a mutation to the Walker A motif (K340M), necessary for ATP binging in many ATPases, disrupted the ability of the NBD to oligomerize. Interestingly, previous studies of mouse NLRP1B walker A mutants showed the opposite effect, and they were found to be spontaneously active (Liao and Mogridge, 2013), a result we confirm here. We evaluated the effect of the Walker A mutation (K340R, K340A) in the context of the FL human NLRP1 in cells. We observed that an intact Walker A motif is dispensable for inflammasome formation. Taken together, our findings suggest that human NLRP1 has even more structural and functional similarities with murine NLRP1 than previously appreciated.

The claim that MDP is a specific stimulus of NLRP1 is also controversial for many reasons. On one hand, this is the reported ligand of another NLR, NOD2, which might indirectly and partially explain the responses observed with MDP in human cell lines. A major criticism of the experiments using MDP as a stimulant of NLRP1 activation in cells is that in many of these reports, MDP was delivered in combination with other compounds such as ATP and TiO2, which are known to activate another inflammasome, NLRP3 (Kovarova et al., 2012; Mariathasan et al., 2006; Yazdi et al., 2010). In fact, a recent study evaluated the necessity of Nlrp1b, Nlrp3, and Nod2 in murine macrophages stimulated with MDP and/or Nlrp3 agonists (Kovarova et al., 2012). This study observed robust signs of inflammasome activation that were completely dependent on Nod2 and Nlrp3 but were independent of Nlrp1b. We believe that many of the results suggesting human NLRP1 is responsive to MDP might similarly be explained by signaling via other receptors.

While human NLRP1 response to MDP has not been disproven, we investigated an alternative hypothesis: namely, that human NLRP1, like mouse NLRP1 isoforms, is activated by proteolysis. Consistent with our expectations, we observed proteolysis-dependent activation of human NLRP1. Even though human cells do not seem to pyroptose in response to LeTx(Moayeri et al., 2012), it is unclear if this is because LF does not cleave NLRP1. We did not observe NLRP1 cleavage or activation when LF was ectopically co-expressed. We hypothesize that NLRP1 might indeed be activated via a similar proteolytic mechanism in diverse species, but the different proteases that activate NLRP1 may differ in different species and populations. We noted that in primates, NLRP1 exhibits a strong signature of positive selection (George et al., 2011). Positive selection is commonly observed in immune-related defense genes, driven by their participation in an 'evolutionary arms race' with pathogens. In theory, pathogens evolve mechanisms for evading recognition by the action of the immune system, which counter-selects for variation in the host defense genes. Many examples of this form of co-evolution have been observed with viruses and host defense pathways. One expectation might be that most immune sensors should have as strong a signature of positive selection. In fact, this does not seem to be the case in general, and genes such as NOD2, NOD1, and TLRs that recognize non-protein PAMPS, including MDP, do not seem to have a large signature of positive selection (George et al., 2011). This might reflect the relative difficulty pathogens might have in modulating the structure of these non-protein ligands to evade recognition. If MDP were the main agonist for NLRP1, it would be surprising for recognition of MDP to be a varying selective force that resulted in this signature of positive selection. Interestingly, four of the codon positions we identified that appear to be under positive selection map to the inter-domain region between the PYD and the NBD. This linker is in the region where we found that proteolysis can activate human NLRP1. Secondary structure predictions also indicate that this region is a large unstructured coil that spans more than 100 residues past the PYD. This lack of structure would make it the ideal region for protease sensitivity. The unstructured nature of this linker also makes it unlikely to be involved in structural recognition of MDP. We therefore hypothesize that primates and specific populations might be exposed to different pathogens and their respective proteases. The differences in NLRP1 responsiveness to these proteases might explain the diversifying evolution of this gene. An advantage to the host is that the pathogen might be restrained in its ability to evade proteolysis of NLRP1 because it needs to retain specificity towards its cognate substrates. We believe this is the case of anthrax LF, as cleavage and inactivation of the MAPKKs is most beneficial to the pathogen. On the side of the host, NLRP1B is a substrate of LF, but the inflammasome response is beneficial to the host for pathogen

clearance (Moayeri et al., 2010; Terra et al., 2010). On the side of the pathogen, LF is constrained to cleave six different MAPKK in multiple species, and LF might not be able to evolve to evade NLRP1B cleavage. Many distinct types of pathogens might deliver proteases into the host cytosol. For example, many viruses encode cytosolic proteases that are essential for their replication life cycle (Tong, 2002), and might be one large type of pathogen to which the NLRP1 family responds to. In this example, a similar constraint might exist on substrate specificity of these viral proteases as seen with LF. Therefore if NLRP1 gains sensitivity to this protease, the virus might not quickly evade recognition, providing a significant increase in fitness to the host.

3.4 Materials and Methods

3.4.1 Plasmids and constructs

The B6-Nlrp1b allele was PCR amplified from a plasmid with a cDNA sequence representing BC141354 from Thermo Fisher Scientific Biosciences using PCR primers 1+2 (Table 3.1), and subcloned into CMSCV-IRES-hCD4 using XhoI and NotI sites. For the N-terminal GFP fusion, B6-NLRP1B was amplified using primers 3+2, and subcloned into MSCV-GFP-MCS into the NotI site. A TEV site was added on the B6 allele using QuickChange Mutagenesis as described in (Chavarria-Smith and Vance, 2013) with primers 4-5. The 129 allele LF cleavage site was mutated with primer 6-7, 8-9, 12-13 separately to generate 129/B6-A, 129/B6-B and K38A/K44A respectively. Then 129/B6-A was sequentially mutated with primers 10-11 to generate 129/B6-C.

An Nlrp1a cDNA template was obtained from Source BioScience (BC156396.1). This sequence was amplified and cloned with primers 18-19 into pcDNA3.1-Myc-HisA into the BamHI and NotI sites. This original sequence contains three splicing differences when compared to the reference sequence NM_001004142. Two of these differences are inclusions of two extra exons not found in the reference sequence. These exons were sequentially deleted using primer pair 22-23 first, followed by primer pair 24-25. The third difference was a missing 3' exon. To correct this difference, we used SOE PCR (Vallejo, 2002) to insert the missing exon. PCR Fragment 1 was amplified with primers 29+26, and PCR fragment 2 was amplified with primers 27+19. PCR Fragment 2 was extended at its 5' end with primers 28+19 to form fragment 3. Fragment 1 and fragment 3 were mixed, allowed to anneal to each other, and extended and amplified with primer 29+19 to form fragment 4. Fragment 4 was digested with EcoRI and NotI, and was used to replace the EcoRI and NotI fragment released from the original Nlrp1a-pCDNA that had been already corrected for the first two exons.

The final Nlrp1a resembling the reference sequence was amplified with primer 20-21. The 5'end of this fragment was extended with primer 17+21, and then subcloned into MSCV-GFP-MCS into the NotI site. For TEV-site insertions primers 30-31 were used.

Human NLRP1 cDNA template was obtained from ATCC (I.M.A.G.E. Clone ID: 5756099), which contains a sequence resembling transcriptional variant 5 (NM_001033053.2). This cDNA is missing the last two 3' exons that are found in transcript variant 1 (NM_033004.3) and are predicted to encode the CARD, and necessary for a signaling competent form of the NLR. We modified the sequence of transcript variant 5 to add these last two exons to match variant 1. The last exon was amplified by PCR with primers 40+33 and gDNA from THP-1 cells to form fragment1. The N-terminal fragment 2 was amplified with primers 39+32. Fragment 1 and 2 were mixed, annealed, extended, and then amplified with primer 32+33. The final PCR product was cloned into pcDNA3.1-Myc-HisA with KpnI and XhoI. The newly modified ORF

was sequenced in the entire length, and a point mutation was identified and modified with primers 34-35 to resemble the reference sequence. To delete the PYD, PCR was done using primer 38+33 and the fragment was cloning back into pcDNA3.1-Myc-HisA. The LRR was deleted, TEV-sites were inserted, and WalkerA mutations were modified via Quickchange methodology using primers 36-37, 41-42,43-44, 45-46, 47-48 respectively.
To make the GFP N-terminal fusions, hNLRP1 was amplified with primers 49,50,51,52 at the 5'end and primer 53 at the 3'end, and these fragments were cloned MSCV-GFP-MCS into the NotI site.

3.4.2 Analysis of positive selection

Publicly available NLRP1 gene sequences were used for all analyses. NLRP1 orthologs from ten primate species (human, chimp, gorilla, orangutan, gibbon, rhesus macaque, baboon, African green monkey, marmoset, and squirrel monkey) were aligned and trimmed. Maximum likelihood analyses were performed on primate NLRP1 genes using FUBAR (DataMonkey.org) to identify codons under positive selection. Specific codons that evolved under recurrent positive selection with a posterior probability of >0.95 were identified.

3.4.3 Cell culture.

HEK293T (ATCC) cells were grown in complete media (DMEM, 10% FBS, 100 U/ml Penicillin, 100 μg/ml Streptomycin, and supplemented with 2mM L-glutamine).

3.4.4 DNA transient transfections

HEK 293T cells were seeded the day prior to transfection at a density of $1.5x10^5$ cells/well in a 24-well plate with complete media. DNA complexes were made with Lipofectamine 2000 (Invitrogen) according to manufacture's instructions and overlaid on cells for 36 hours.

3.4.5 Western Blots

Cells were lysed in RIPA buffer supplemented with 1mM PMSF and 1×X Complete Protease Inhibitor Cocktail (Roche). Lysates were spun down at max speed at 4C for 20min and supernatants were mixed with 6× Laemmli sample buffer. To detect full length NLRP1B, lysates were incubated at room temperature prior to SDS-PAGE. To analyze all other proteins, including the N-terminally cleaved form of NLRP1B, samples were boiled for 10min prior to separation. SDS-PAGE was performed with Novex BisTris gel system according to manufacturer instructions (Invitrogen). Separated proteins were transferred on to Immobilon-FL PVDF membranes. Membranes were blocked with Odyssey® blocking buffer (Licor). The following antibodies were used for the following antigens: HA mAB 3F10 (Roche), MEK-2 SC-13115 (Santa Cruz), MYC mAb 9E10 (Clonetech), IL-1B AF-401-NA (R&D systems). Secondary antibodies anti-rat, mouse and goat were all conjugated to Alexa Flour-680 (Invitrogen)

3.5 Acknowledgements

We would like to give a special thanks to Alvin Ho for his help cloning human NLPR1 into a mammalian expression vector. We also thank Matt Daugherty for his comments and help in performing the positive selection analysis of primate NLRP1.

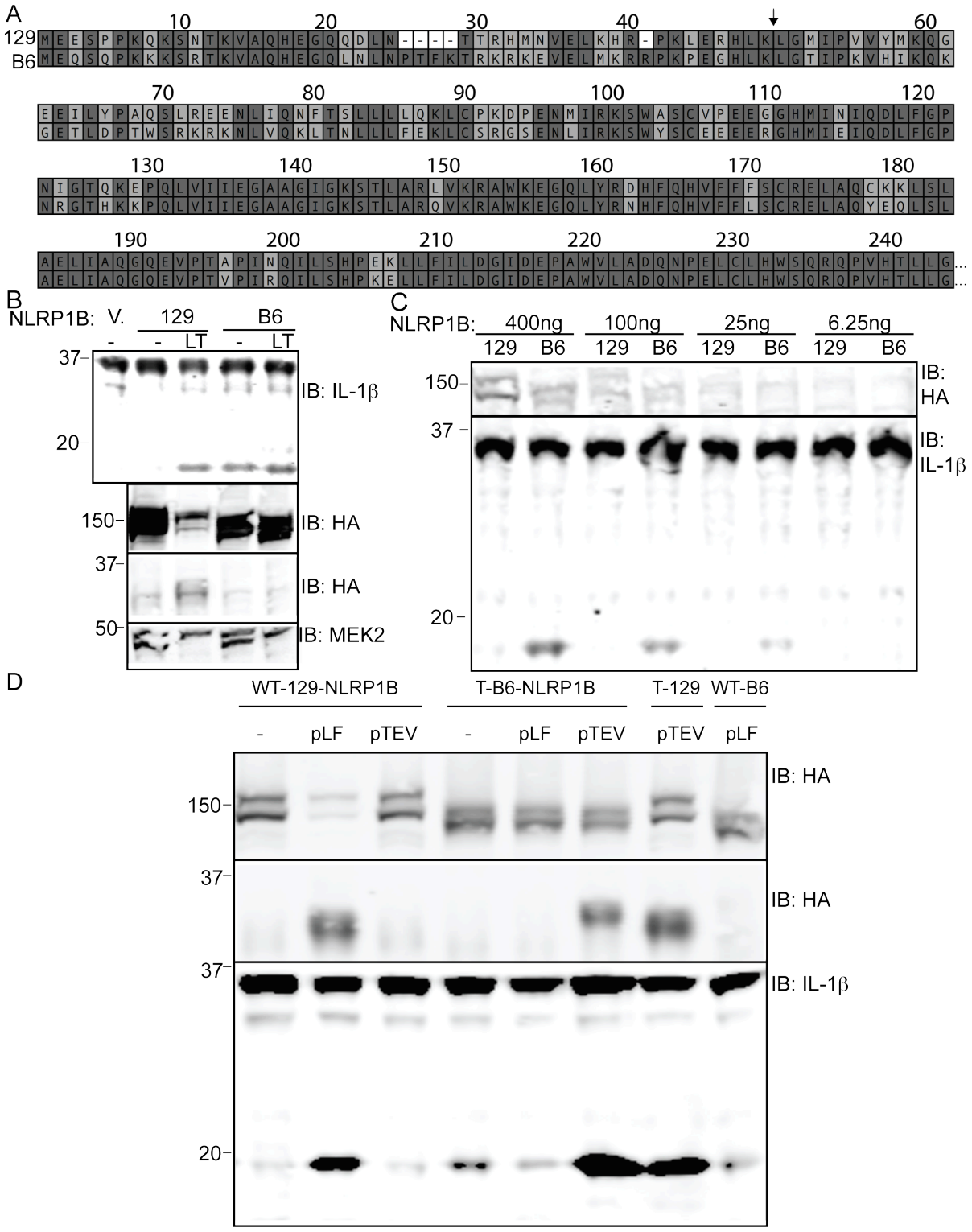

Figure 3.1 The B6 allele of NLRP1B is not cleaved by LF but can form an inflammasome in response to proteolysis.

A) The protein sequence alignment of the first 244 residues of B6 NLRP1B is aligned to allele-1 of NLRP1B found in 129 mice. The arrow above the alignment indicates the

predicted LF-cleavage site in NLRP1B of 129 mice. Dark gray indicates perfect identity and the lighter shades of gray represent non-identities. B) HEK 293T cells were transfected with plasmids encoding GFP-HA-NLRP1B of each allele, along with Casp1 and Il1b expression vectors. Cells were treated overnight with LeTx (1ug/ml) 24h post-transfection, and then lysates were analyzed by immuno-blotting (IB) with the indicated antibodies. For analysis of HA (NLRP1B) the lysates were not boiled prior to loading to prevent aggregation and smearing in the immunoblot. C) 239T cells were transfected similarly to B, but the amount of GFP-HA-NLRP1B plasmid was serially diluted as indicated above the IB, but buffered with empty expression vector. Cells were not treated with LeTx. D) 293T cells were transfected with WT and TEV-protease site (T) 129-NLRP1B, and WT and TEV-protease site (T) B6-NLRP1B along with empty vector (Vec.), TEV-protease (pTEV), or a LF expression plasmid (pLF). In all conditions cells were also cotransfected with Casp1 and Il1b expression vectors.

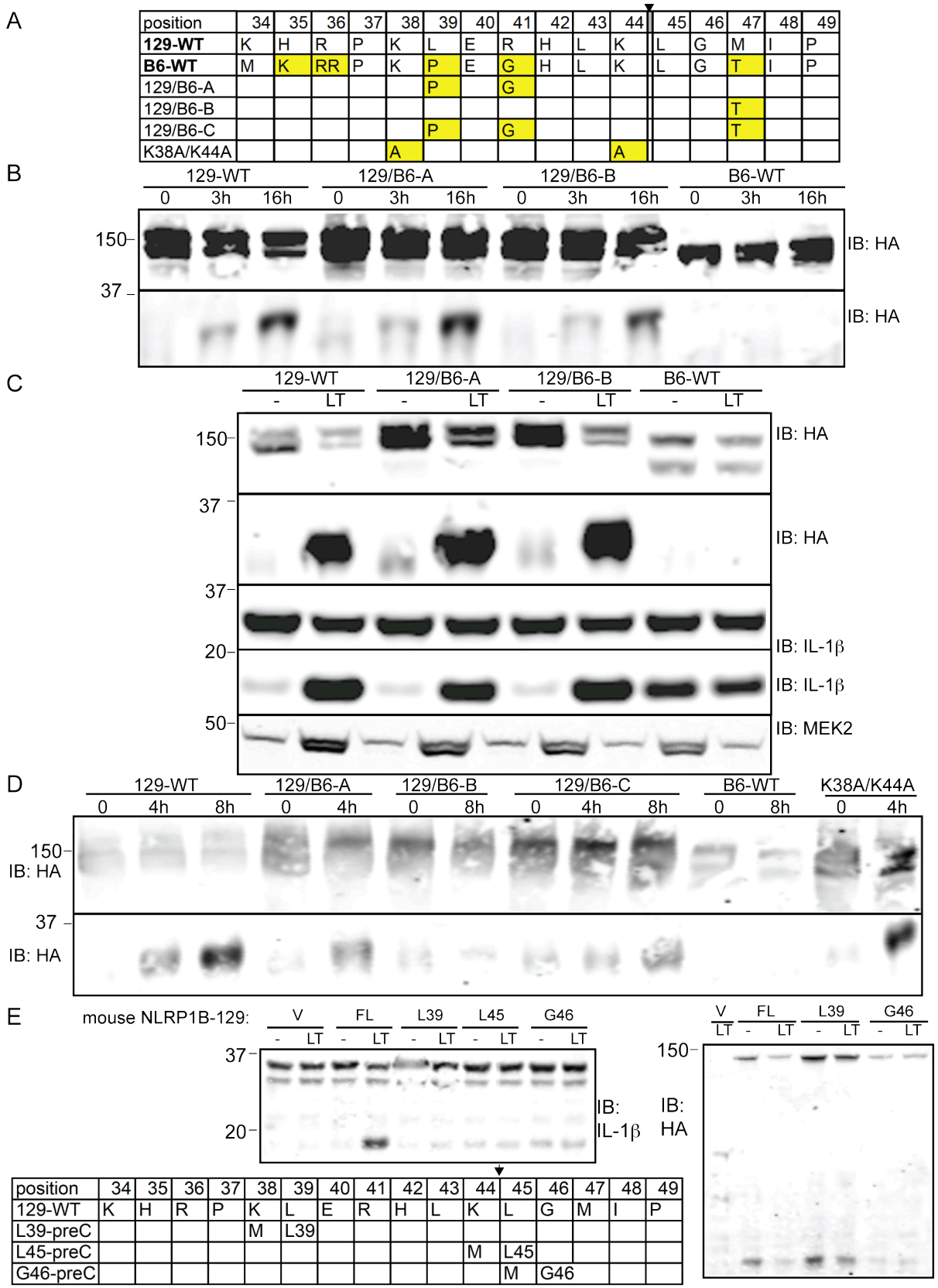
A
position 34 35 36 37 38 39 40 41 42 43 44 45 46 47 48 49
129-WT K H R P K L E R H L K L G M I P
B6-WT M K RR P K P E G H L K L G T I P
129/B6-A P G
129/B6-B T
129/B6-C P G T
K38A/K44A A A
B
129-WT 129/B6-A 129/B6-B B6-WT
0 3h 16h 0 3h 16h 0 3h 16h 0 3h 16h
150
37
IB: HA
IB: HA
C
129-WT 129/B6-A 129/B6-B B6-WT
- LT - LT - LT - LT
150
37
37
20
50
IB: HA
IB: HA
IB: IL-1β
IB: IL-1β
IB: MEK2
D
129-WT 129/B6-A 129/B6-B 129/B6-C B6-WT K38A/K44A
0 4h 8h 0 4h 0 8h 0 4h 8h 0 8h 0 4h
150
IB: HA
37
IB: HA
E
mouse NLRP1B-129: V FL L39 L45 G46
- LT - LT - LT - LT - LT
37
20
IB: IL-1β
V FL L39 G46
LT - LT - LT - LT
150
IB: HA
position 34 35 36 37 38 39 40 41 42 43 44 45 46 47 48 49
129-WT K H R P K L E R H L K L G M I P
L39-preC M L39
L45-preC M L45
G46-preC M G46

Figure 3.2 129 NLRP1B LF sensitivity is explained by the primary sequence surrounding the LF site and additional regions beyond the cleavage site.
A) Diagram depicting the differences in primary sequence between the 129 and B6 allele of NLRP1B. The numbering is based on the 129 allele's N-terminus. The LF-cleavage site predicts cleavage to occur between K44 and L45 in the129 allele as indicated by the arrow head. Yellow highlighted residues indicate non-identities in the B6 allele compared to the 129 allele. 129/B constructs indicate that the 129 allele LF cleavage site was mutated to residues found in the B6 allele. B) 293T cells were transfected with GFP-HA-NLRP1B constructs for 24h, and then treated with LeTx (1ug/ml) for the indicated time. The top IB used lysates that were not boiled prior to loading and running SDS-PAGE. The bottom IB was performed using boiled lysates. C) 293T cells were transfected and treated as done in B, but Casp1 and Il1b expression plasmids were added to assay inflammasome activity. Cells were treated with LeTx for 16h. Non-boiled lysates were used for both HA probed IBs. D) 293T cells were transfected with GFP-HA-NLRP1 as done in panel A, but in the absence of other plasmids, and only non-boiled lysates were analyzed by IB. E) NLRP1B-HA from 129 mice N-terminal truncations were made as indicated in the chart with an initiator methionine prior to the named numbered (e.g. L39). 293T cells were transfected with these NLRP1B constructs, along with mCasp1, mIl1b and then treated with LeTx for 16h prior to cell lysis. For the HA probed IB, non-boiled lysates were used.

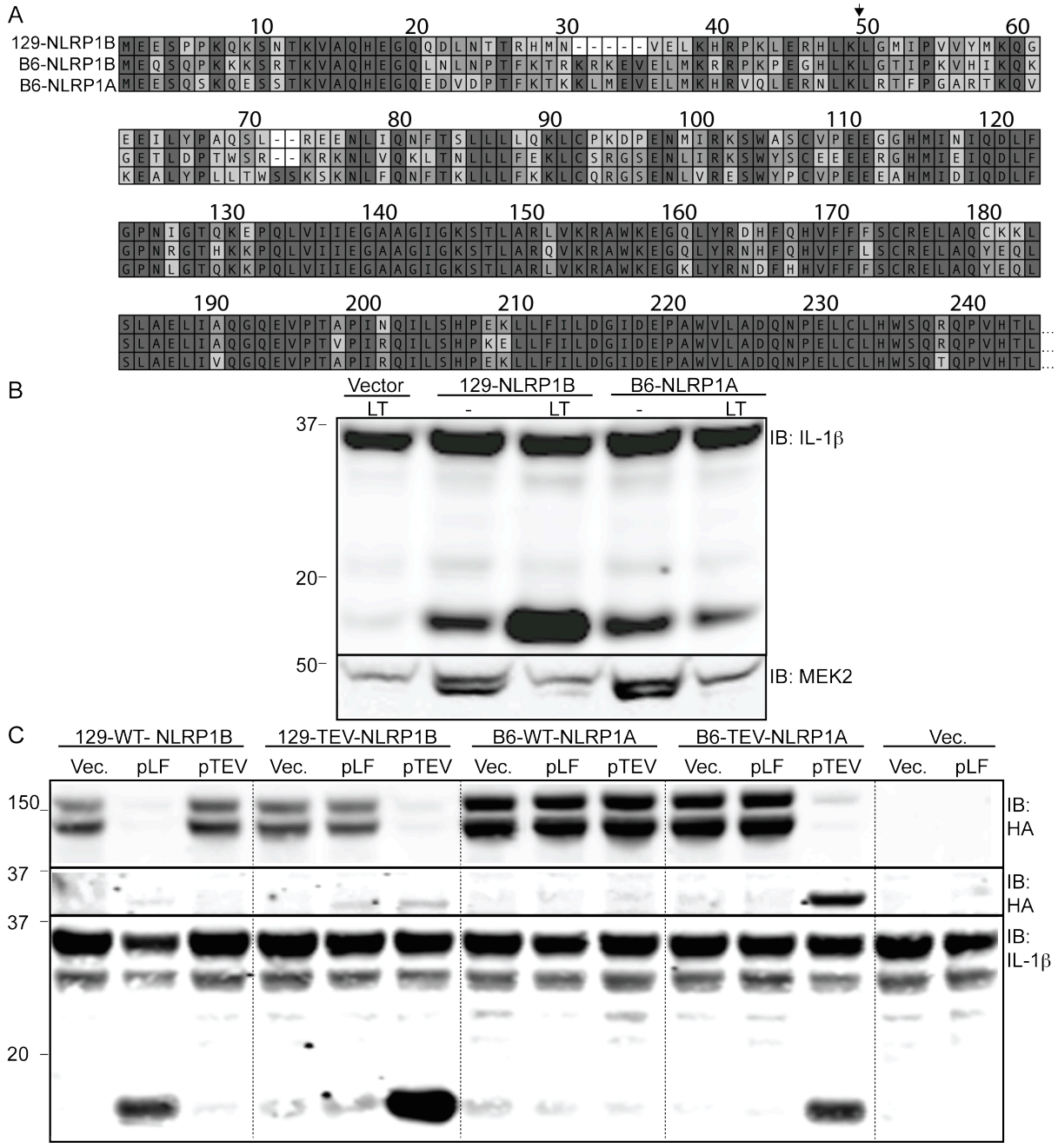

Figure 3.3 NLRP1A can assemble and inflammasome in response to proteolysis by the same mechanism as NLRP1B.

A) Protein sequence of the first 244 residues of B6 NLRP1A was aligned to allele-1 and allele-2 of NLRP1B found in 129 and B6 mice, respectively. The arrow above the alignment indicates the predicted LF-cleavage site in NLRP1B of 129 mice. B) 293T cells were transfected with HA-NLRP1B (129) or NLRP1A-MYC (B6) along with Casp1 and Il1b expression vectors. Cells were treated overnight with LeTx (1ug/ml) 24h post-transfection, and then lysates were analyzed by immuno-blotting (IB) with the indicated antibodies. C) 293T cells were separately transfected with plasmids encoding GFP-HA-NLRP1B (WT-129 and TEV-site 129) or GFP-HA-NLRP1A (WT-B6 and TEV-site-B6) along with empty vector

(Vec.), TEV-protease (pTEV), or a LF expression plasmids (pLF). In all conditions cells were also cotransfected with Casp1 and Il1b expression vectors. Total cell lysates were analyzed by IB with the indicated antibodies.

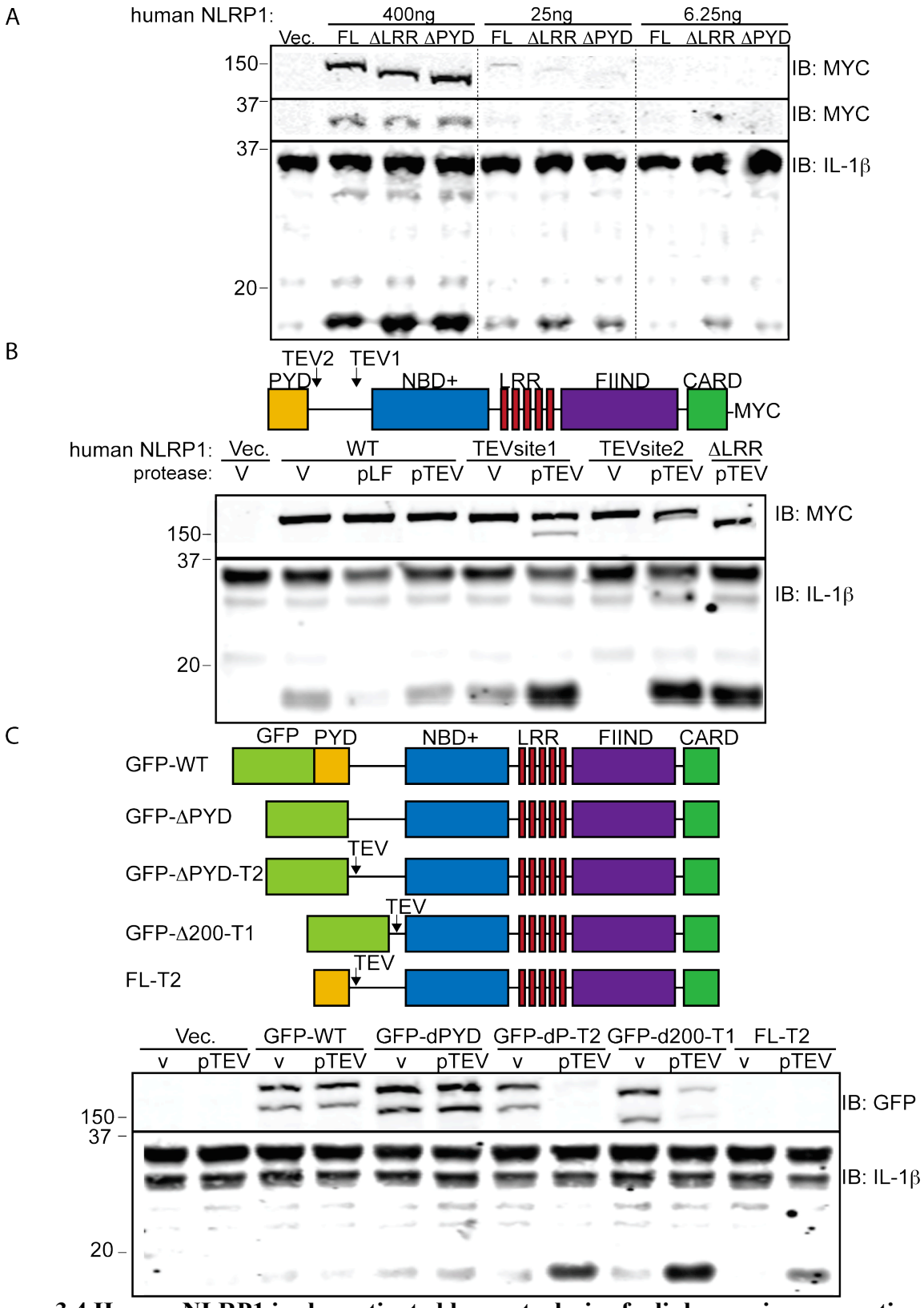

Figure 3.4 Human NLRP1 is also activated by proteolysis of a linker region connecting the PYD and the NBD, and the PYD is necessary for auto-inhibition.

A) 293T cells were cotransfected with a varying amount of plasmid encoding human NLRP1-MYC full-length (FL), NLRP1 with the LRR domain deleted (ΔLRR) or NLRP1 lacking the first 203 N-terminal residues (ΔPYD). The other DNA transfection components had a constant amount of mouse Casp1, human ASC, mouse Il1b encoding plasmids. Cells were allowed to express the component for 36h and then analyzed by IB with anti bodies against MYC and mIL-1B. B) A diagram representing the functional domains found in human NLRP1 also indicates the relative placement of TEV cleavage sites. 293T cells were cotransfected with human NLRP1-MYC representing the wild-type (WT), TEV-site1, TEV-site2 or ΔLRR form; plus vectors encoding LF-protease (pLF), TEV-protease (pTEV), mCasp1, mIl1b, and hASC. A separate set of DNA transfection-complexes were made with a larger amount of hNLRP1 without mCasp1 to detect enough hNLRP1 protein expression and TEV-dependent NLRP1 cleavage. C) A diagram representing the different hNLRP1 construct depicts the relative placement of GFP and the different truncation mutants of NLRP1. 293T cells were transfected with these GFP-NLRP1 along with mCasp1, hASC, mIl1b and TEV-protease (pTEV) expression vectors for 36h. Cell lysates were analyzed by IB with antibodies specific to GFP and IL-1B.

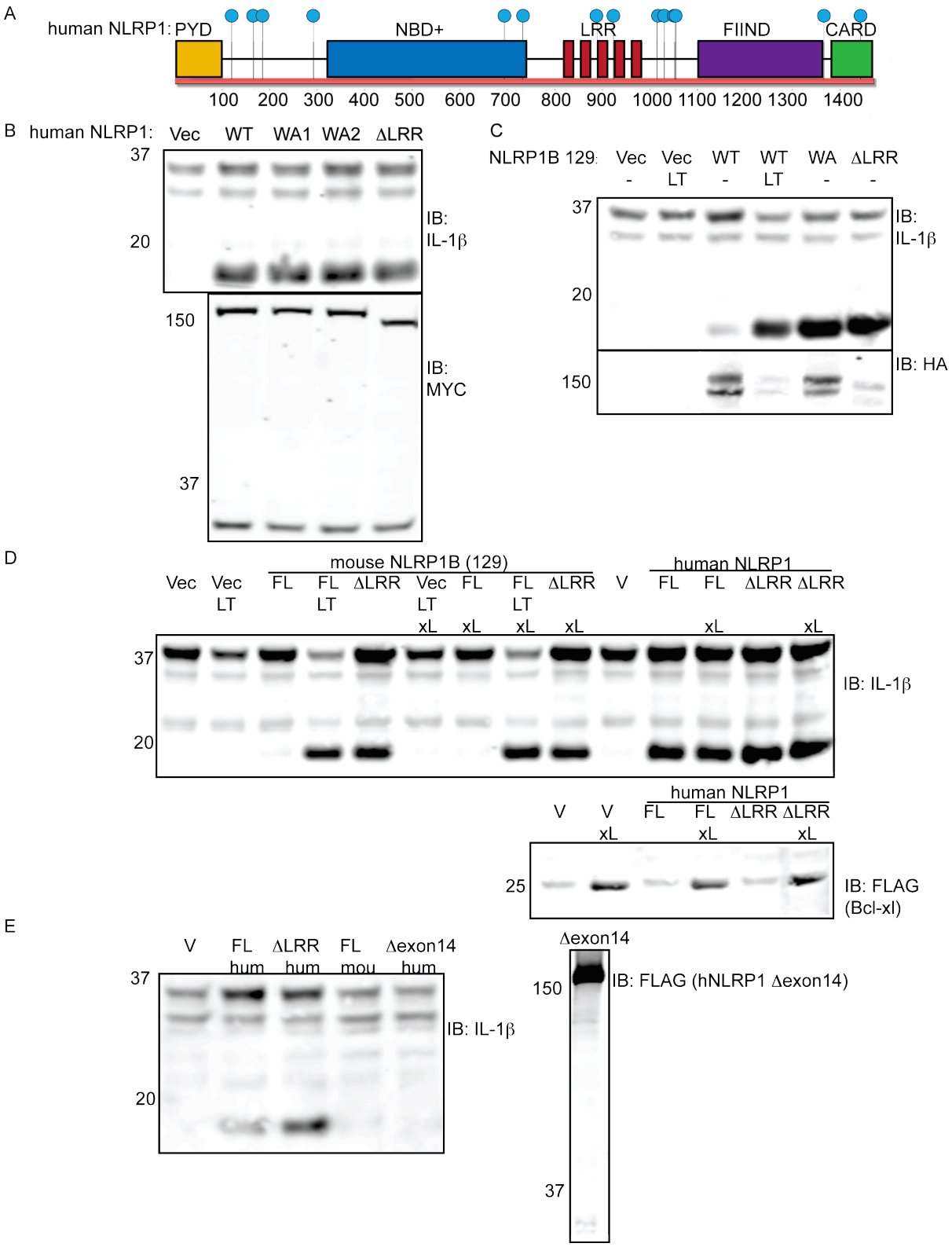

Figure 3.5 Other features of the human NLRP1 inflammasome.
A) Codons with a statistical signature of being under positive selection in primates were

mapped onto the human protein sequence and are identified as blue circles. The predicted functional domains are mapped below these codons/residues. B) 239T cells were transfected with hNLRP1-MYC wild-type (WT), Walker A mutant1 K340A (WA1), Walker A mutant2 K340R (WA2) or ΔLRR expression plasmids. The transfection complexes also contained mCasp1, mIl1b and hASC expression vectors. C) 293T cells were transfected with mouse 129 HA-NLRP1B wild-type (WT) or WalkerA K137R (WA) or ΔLRR expression plasmids. The cells were cotransfected with mCasp1 and Il1b expression vectors. In the HA IB panel, non-boiled lysates were used. D) 293T cells were transfected with either mouse 129 HA-NLRP1B full-length (FL) and ΔLRR, or human NLRP1-MYC that is full-length (FL) and ΔLRR. These cells were also transfected with mCasp1, mIl1b and hASC expression plasmids in all conditions, but mouse Bclxl-FLAG (xL) was added only where indicated. Cells expressing mouse NLRP1B were treated with LeTx (LT) where indicated for 16h prior to lysis. E) 293T cells were transfected with full-length (FL) and ΔLRR human (hum) NLRP1-MYC, mouse FL129 HA-NLRP1B (mou), or human NLRP1-FLAG-Δexon14, along with plasmids encoding mCasp1, mIl1b and hASC.

NLRP1B		
1	tataCTCGAGccacc ATG TACCCATACGACGTCCCAGACTACGCT GAACAATCTCAGCCC	B6 NLRP1-XhoI-HA
2	atatGCGGCCGC TCA GGATCCCAAAGAGACCC	B6 NLRP1-R-stop-NotI
3	atatGCGGCCGCt ATGTACCCATACGACGTCC	GFP-HA--F-Noti
4	GCAGACCCAAG GAGAACCTGTATTTTCAGGGC GGGACAATTCCAAAAGTACACATAAAAC	B6-N1b-TEV3-F
5	CTTTTGGAATTGTCCCgccctgaaaatacaggttctcCTTGGGTCTGCGCTTCATCAGC	B6-N1b-TEV3-R
6	AGAGCTGAAGCACAGACCCAAG ccc GAG ggg CACTTGAAGCTAGGAATGATTCCAGTAG	129-B6-A-F
7	GGAATCATTCCTAGCTTCAAGTGcccCTCgggCTTGGGTCTGTGCTTCAGCTCTACATTC	129-B6-A-R
8	CTAGAGAGACACTTGAAGCTAGGA acc ATTCCAGTAGTATATATGAAGCAGGGAGAAGAG	129-B6-B-F
9	CTCCCTGCTTCATATATACTACTGGAATggtTCCTAGCTTCAAGTGTCTCTCTAGCTTGG	129-B6-B-R
10	CCCGAGGGGCACTTGAAGCTAGGA acc ATTCCAGTAGTATATATGAAGCAGGGAGAAGAG	129-B6-C-F
11	CTCCCTGCTTCATATATACTACTGGAATggtTCCTAGCTTCAAGTGCCCCTCGGGCTTGG	129-B6-C-R
12	GACCCgcGCTAGAGAGACACTTG gcG CTAGGAATGATTCCAGTAGTATATATGAAGCAGG	N1b-K38A-K44A-F
13	TATATACTACTGGAATCATTCCTAGCgcCAAGTGTCTCTCTAGCgcGGGTCTGTGCTTC	N1b-K38A-K44A-R
14	atatCTCGAGgccaccATG CTAGAGAGACACTTGAAGCTAGG	N1b-L39-XhoI-F
15	atatCTCGAGgccaccATG CTA GGAATGATTCCAGTAGTATATATGAAGC	L45-XhoI
16	atatCTCGAGgccaccATG GGAATGATTCCAGTAGTATATATGAAGC	G46-start-xhoI
17	atatGCGGCCGCTCAAGCGTAGTCTGGGACGTCG	HA-stop-NotI-R
NLRP1A		
18	gcatat GGATCC gccacc ATGGAAGAATCTCAGTCCAAGCAGG	NLRP1A-BamHI-F
19	gcatatGCGGCCGCccTTTCACAGAGACCCCACCCAAC	NLRP1A-NotInostop-R
20	atCTCGAGgccaccATG TACCCATACGACGTCCCAGACTACGCT GAAGAATCTCAGTCCAAGCAGG	HA-NLRP1A-XhoI-F
21	ggcatGCGGCCGC TCA GGATTTCACAGAGACCCCACC	NLRP1A-stop-NotI-R
22	GGCTGCCAACTAAAG ACT CTG TGG CTTGTTGAATGCGGCCTCACATCCACATAC	NLRP1A-exonAdel-F
23	ATGTGAGGCCGCATTCAACAAGCCACAGAGTCTTTAGTTGGCAGCCACGC	NLRP1A-exonAdel-R
24	TGAAGCAGCAGAGACAGCAGTCA GGAGACAAACACATGGAACCTCTGGGG	NLRP1A-exonBdel-F
25	GAGGTTCCATGTGTTTGTCTCCTGACTGCTGTCTCTGCTGCTTCAGTAGG	NLRP1A-exonBdel-R
26	GGT GATCTCAGACCTGCACTGC CCAAGATTGCTACAGCCCCC	NLRP1A-SOE
27	GGGGGCTGTAGCAATCTTGGGCAGTGCAGGTCTGAGATCACC	NLRP1A-SOE
28	GCAGTGCAGGTCTGAGATCACCTGGTTTCAGCAAGGCCTCCC	NLRP1A-C' ext3
29	gcagtgacaatagagatcgaattctgtgcc	Nalp1b Seq4
30	TGAAGCACAGAGTgCAG gag AAC CTG TAT TTT CAG ggc AGAACCTTTCCAGGAGCACGTAC	NP1A-TEV3-F2
31	TCCTGGAAAGGTTCTgccCTGAAAATACAGGTTctcCTGcACTCTGTGCTTCATTAGCTCC	NP1A-TEV3-R2
hNLRP1		
32	gctataGGTACC gccacc ATGGCTGGCGGAGCC	hNLRP1-F-KpnI-Kzk
33	gctata CTCGAG GCTGCTGAGTGGCAGGAG	hNLRP1-R-noStop-XhoI
34	GCTGCTACTTCTACAAAGACCTCACCCCAGAAGCCAAGATCCCCTGG	hNP1 C1414T-F
35	GGGATCTTGGCTTCTGGGGTGAGGTCTTTGTAGAAGTAGCAGCTGTGTG	hNP1 C1414T-R
36	CCTCAAGGTCACCAGAAACCCTCAGCTGCTCATCTTCAGC	hNP1-dLRR2-F
37	GAAGATGAGCAGCTGAGGGTTTCTGGTGACCTTGAGGACG	hNP1-dLRR2-R
38	gctata GGTACC gccaccATG ACCCAATGGCCTCTGG	hNP1-PC1
39	CGGGCTGGAGGGATCAGAGTAGTTGCAGGCATGAGATCTCCTGGTTTCACCAAGGCCTCC	hNP1-R-Nt-SOE
40	CTACTCTGATCCCTCCAGCCCG CATAG CCGTACCTTCACCTCTGGATGCC	hNPR1-F-Ct-SOE
41	GGGCTGCTGGAATTGGG gcG TCAACACTGGCCAGGCAGGTGAAGGAAG	hNLRP1-WalkerA-K-A-F
42	CTTCACCTGCCTGGCCAGTGTTGACgcCCCAATTCCAGCAGCCCCCTGC	hNLRP1-WalkerA-K-A-R
43	GGGCTGCTGGAATTGGG agG TCAACACTGGCCAGGCAGGTGAAGGAAG	hNLRP1-WalkerA-K-R-F
44	CTTCACCTGCCTGGCCAGTGTTGAcctCCCAATTCCAGCAGCCCCCTGC	hNLRP1-WalkerA-K-R-R
45	GCGCCCAAGCCCAGGAA AACCTGTATTTTCAGGGC TCATTCCCCTACAGCCCAAGTG	hNP1 TEV2-F
46	GGGCTGTAGGGGAATGAGCCCTGAAAATACAGGTTTTCCTGGGCTTGGGCGCACAGTG	hNP1- TEV2 R
47	CCTAGCACCCAGA GAG aac ctg tat ttt cag ggc CAATGGCCTCTGGATGAAACG	hNP1-Tev1-F
48	CCAGAGGCCATTG gcc ctg aaa ata cag gtt CTCTCTGGGTGCTAGGCTGG	hNP1-TEV1-R
49	atatGCGGCCGCt ATGGCTGGCGGAGCCTGGGG	GFP-notI FL-hNP1
50	atatGCGGCCGCt CCCTCATTCCCCTACAGCCC	GFP-notI-dPYD
51	atatGCGGCCGCt GAA AACCTGTATTTTCAGGGC TCATTCC	GFP-notI-dPYD-T2
52	atatGCGGCCGCt GAG aac ctg tat ttt cag ggc CAA	GFP-notI-d198-T1
53	tgcgat GTCGAC TTAATTCAGATCCTCTTCTGAGATGAGT	MYC-stop-SalI-R
54	ATCTTCCCAATTGCTGAGATTGCA GAGGAAAGCTCCCCAGAGGTAGTACC	hNLRP1-del GKSH-F
55	TACCTCTGGGGAGCTTTCCTCTGCAATCTCAGCAATTGGGAAGATCTTGC	hNLRP1-del GKSH-R

Table 3.1 Oligo sequences used for cloning.

Chapter 4: CASP1 BiFC reporter

4.1 Introduction

Inflammasomes are multi-protein complexes that assemble in the cytosol and recruit CASPASE-1 (CASP1) (Martinon et al., 2009). Recruitment of CASP1 induces dimerization and activation. Once activated, CASP1 auto-proteolyzes, cleaves the cytokines IL-1B/18, and induces pyroptosis. The assembly of inflammasomes is initiated and regulated by AIM-2, MEFV (Pyrin) (Xu et al., 2014), or various members of the Nucleotide binding domain Leucine-rich Repeat (NLR) family (von Moltke et al., 2013). Some NLRs, such as NLRC4 and NLRP1, can directly bind and dimerize CASP1 via their own CARD. Other NLRs, which contain a PYD recruitment domain instead of a CARD, require the adaptor ASC (PYCARD) to recruit CASP1. ASC does not only function as an adaptor, but also aids in the formation of a large (>1μm) cellular aggregate, called a speck or focus, within the cytosol of the activated cell. ASC is required for CASP1 auto-proteolysis and efficient cleavage of the cytokines IL-1β, but can be dispensable for induction of pyroptotic cell death (Broz et al., 2010).

Mice and humans encode approximately 20 different NLR genes. Few of these NLRs are known to form an inflammasome or be activated by defined stimuli. NAIPs/NLRC4, NLRP1 and NLRP3 are known to respond during infection to form an inflammasome (von Moltke et al., 2013). NLRP1 has been discussed extensively in the previous chapters, but is likely to have many undiscovered agonists. NLRP3 responds to a wide variety of stimuli, including extracellular ATP, crystalline particles, and pore-forming toxins. To date, the mechanism by which all these stimuli activate NLRP3 is unclear and/or controversial. NLRP6 and NLRP12 have been genetically inferred to form inflammasomes (von Moltke et al., 2013), but some research groups dispute these claims, proposing instead that NLRP6 and NLRP12 are negative regulators of NF-kB signaling pathways (Allen et al., 2012; Anand et al., 2012). These facts highlight the need to identify new stimuli for these NLRs, and understand the signal transduction pathways upstream of CASP1.

Most methods for studying inflammasome responses depend on the proteolytic activity of CASP1. Examples of these methods include CASP1 self-processing and IL-1B/18 cleavage by western blotting, cytokine secretion by ELISA, and pyroptosis measurement by LDH release. One caveat is that most of these assays are not single-cell based and that CASP1 activation cannot be uncoupled from the cell death. Because pyroptosis lyses the activated cells, new candidate agonists or regulators can only be assessed in a low throughput manner. There are other assays that do not depend on CASP1 activity and instead rely on inflammasome or NLR oligomerization. Examples of these assays include gel filtration of cell lysates, native page, or ASC crosslinking, all followed by western blotting. Most of these assays are also low throughput, and rely on bulk population responses.

Few methods work at a single-cell level, or allow selective recovery of the cells containing an activated inflammasome. One example of this type of assay is Fluorescent Labeled Inhibitor of Caspases (FLICA), which is composed of a CASP1 irreversible inhibitor (YVAD-FMK) attached to a fluorescent molecule such as FAM. The premise is that the FLICA probes react and covalently attach to CASP1, and the excess probe is washed away. One problem is that this inhibitor is not very effective at blocking pyroptosis, nor is it very specific for CASP1 (Broz

et al., 2010; Xiao et al., 2013). ASC speck formation can be analysed by microscopy in live cells if ASC is fused to a fluorescent protein, but these specks cannot be selected by FACS because only the distribution of the fluorescence changes within the cell, and not the MFI of the cells. None of these described methods would allow for a high throughput screen that positively selects novel agonists or factors that positively regulates inflammasome formation. On the other side, loss of function screens have the difficulty of finding negative regulators of inflammasomes because the loss of these factors should enhance pyroptosis and they become depleted from the bulk population.

Most apical or initiator caspases (CASP1/2/8/9) are monomeric zymogens or pro-enzymes, and contain a recruitment CARD or DED at their respective N-termini. These pro-caspases are recruited to a complex termed an inflammasome, PIDDosome, DISC, or apoptosome, respectively (Boatright et al., 2003; Bouchier-Hayes et al., 2009; Martinon et al., 2009). A hallmark of initiator caspases is that they are activated via dimerization (Boatright et al., 2003). The caspase auto-proteolysis that ensues is believed to enhance the stability of the dimmer, but is not strictly necessary for the catalytic activity. Because CASP1 dimerization is the molecular mechanism of activation, we developed an assay that responds to the dimerization step, and not the catalytic activity.

Here we describe a new method of detecting CASP1 dimerization that does not induce pyroptotic cell death of the responding cell. The primary advantage of our method is that since the responding cells do not die, they can be recovered. This might have significant utility in expression cloning strategies to identify upstream inflammasome activators. Our overall strategy was to use bimolecular fluorescence complementation (BiFC) of the yellow fluorescent protein Venus to detect CASP1 dimerization. CASP2 dimerization, which is induced the by the PIDDosome, has already been assayed with this same method (Bouchier-Hayes et al., 2009). The Green group made several constructs that use the CARD of CASP2 and full-length CASP2 and fuse them to the split Venus halves (VN173 and VC155). This group transiently transfected these constructs and could monitor CASP2 activation in live cells stimulated by a heat shock. The response had a high signal to noise readout and had temporal resolution consistent with the endogenous CASP2. We attempted to make CASP1 constructs that were analogous to the CASP2 reporters (Fig. 4.1A-D).

A technical challenge when using BiFC is the propensity of self-assembly or spontaneous signal achieved by high expression of the components. Furthermore, the off-rate of the assembled fluorescent molecules prevents studying the dissociation of the signaling components. The Hu Lab has optimized versions of Venus halves to decreased self-assembly activity (Kodama and Hu, 2010). One example of an optimized component is VN155 (I152L), which has a 4-fold increase in the signal-to-noise ratio compared to wild-type (Kodama, 2010). Here we use two different Venus N-terminal halves, VN155 (I152L) and VN173, and both are complemented with VC155. The CARD of mouse CASP1 is predicted to extend from residue 1-87, but the catalytic domain is connected to the CARD via a large linker that extends up to D103. This extended linker likely provides flexibility for the dimerization of the catalytic domain and might aid also in Venus assembly. We fused the shorter CARD (1-87), termed CARD-S, and the longer CARD (1-103), termed CARD-L, to both versions of VN and VC (Fig. 4.1C). We also fused the full-length catalytically dead mutant of CASP1 (C284A) to the VN and VC pair.

In brief, we developed a 293T cell line that stably expresses the CASP1 reporter components, mouse ASC, and mouse NLRP1B. This reporter line rapidly responds to LeTx, the agonist of NLRP1B, and we could recover the activated cells by FACS. This cell line is an ideal

tool to screen for novel agonists of NLRP1B in a high throughput pooled manner. We also believe that similar cell lines can be developed with different NLRs or inflammasomes.

4.2 Results

4.2.1 CASP1 BiFC cell line analysis by flow cytometry

We first tested the CASP1 reporter by transient expression in 293T cells. We chose these cells because they are highly transfectable and lack endogenous inflammasome components, but a functional inflammasome can be reconstituted by ectopic expression (Kofoed and Vance, 2011). High levels of expression of the CASP1 reporter component (data not shown) resulted in spontaneous Venus assembly, which was independent of ASC or an NLR. We then reduced the amount of plasmid encoding the reporter component and significantly decreased the frequency of cells with spontaneous Venus fluorescence (Fig. 4.2A). High ASC ectopic expression, which is sufficient to induce an ASC speck (Lu et al., 2014), could further enhance the Venus signal for the CASP-S and CASP1-L reporters, but not the CASP1-FL reporter. This suggested that expression of the components must be uniformly low to achieve inflammasome-like dependent activation.

We also made a version of the reporter in which ASC was fused to VN and VC components. The advantage of this system is that cells would only need to express the NLR and the ASC-reporter components to respond. Preliminary experiments suggested this version of the reporter had excessive spontaneous assembly of Venus (data not shown). The Venus signal could be enhanced by further expression of non-reporter ASC. This indicates that creation of an ASC reporter line might be possible, but the ideal range of expression might be smaller and more difficult to achieve than for the CASP1 reporter. This is likely due to the fact that ASC expression promotes speck formation in a concentration-dependent manner, which does not occur with CASP1-CARD expression.

To achieve stable expression of CASP1 within an ideal range in which it remained inducible but not spontaneously active, we retrovirally transduced the reporter components to generate stable cell lines. We then enriched transduced cells by FACS based on the expression of surface markers hCD4 and Thy1.1 for the VN and VC components respectively. The sorted cells were then single-cell cloned into new lines for all the reporter combinations, with the exception of CASP1-FL.

We tested several of these clonal lines for inflammasome activation. Most lines had low percentages (<1%) of spontaneous Venus positive cells (Fig. 4.2B). We chose clonal lines that could be stimulated by high ASC expression. We also tested their responsiveness to NLRP1 inflammasome stimulation with LF expression accompanied by low ASC expression. Here, in Fig. 4.2B, we show the example of 3 different lines with different reporter configurations. We chose these lines because they had the best LF-dependent responsiveness.

We chose clone 28 from the CASP1-S-VN173/VC155 pair for further development into a mature reporter cell line. The clone was selected because it had a low spontaneous Venus signal, but had the largest percentage of Venus positive cells and highest MFI when stimulated with LF and NLRP1B expression (Fig. 4.2B). To further develop this cell line, we transduced the cells with a retroviral vector encoding NLRP1B-IRES-hCD2. We selected NLRP1B^{+} cells by FACS based on surface expression of the hCD2 marker. Even though NLRP1B does not need ASC for CASP1 activity, ASC speck formation is likely required for amplification of the reporter assembly. We therefore further transduced mASC into this line. The integration marker of the

ASC construct is Thy.1. This is also the marker of integration for the CASP1-S-VC155 component. Since the cells were already positive for Thy1.1 it prevented positive enrichment of the ASC expressing cells. We verified that the retroviral-containing supernatant had a high viral titre by transducing naïve 293T cells. This parallel transduction achieved near 90% transduction rate (data not shown) and is expected to be similar in the reporter line. We performed FACS to select Venus negative cells, to deplete the high ASC expressing cells that would not be useful in the final line. We tested the bulk responsiveness of this new line by stimulating the cell with LeTx for 20h. We observed that under 10% of the cells became Venus positive when stimulated (Fig. 4.3A), and this response was completely dependent on ASC. For the line to be an efficient tool, we believed that ASC and NLRP1B would also require uniform expression. Therefore we made new clonally-derived cell lines.

These new and finalized reporter clones were tested for LeTx responsiveness. Here we show the example of clone 43 (Fig. 4.3B), which has a low frequency of spontaneous Venus+ cells, but upon LeTx stimulation close to 70% of the cells become Venus positive. The MFI of the Venus+ cells is significantly larger than the negative cells, and thus FACS sorting of positive cells would be feasible. The kinetics analysis of the response by flow cytometry detects Venus assembly by two hours. The brightness (MFI) of the Venus+ cells continues to increase continuously and is stable up to 20h. Interestingly, the response by 20h is bimodal, for unknown reasons. This is somewhat surprising given that the frequency of Venus+ cells is highest at 6h post treatment. This would suggest that some of the positive cells are lost due to reporter disassembly, but not cell death. Furthermore, titration of the LeTx stimulant affected the final percentage of Venus positive cells, but not the MFI of the positive cells (Fig. 4.3C). This suggests that the strength or the amount of stimulus affects the probability of the reporter, or inflammasomes in general, to form an ASC speck. In other words, the concentration of LeTx affects how many cells respond, but not the strength of the responses of individual cells.

NLRP1B activation is known to be specifically blocked by the proteasome inhibitor MG-132, and a high concentration of extracellular potassium ions (Fink et al., 2008; Wickliffe et al., 2008a). The mechanisms of how these inhibitors block NLRP1B are not known. The effect is expected to be upstream of the activity of CASP1 since they are specific to NLRP1 and not NLRC4 stimuli (Fink et al., 2008). We tested the effect of both MG-132 and 140mM extracellular KCl on the BiFC reporter, and both treatments blocked Venus assembly responses to LeTx, as expected (Fig. 4.3D). This indicates that this reporter recapitulates features of the NLRP1B inflammasome responses observed in macrophages, without inducing or depending on pyroptosis.

We wanted to understand if determinants of the bimodal response were stable and heritable in the population. For example, if NLRPB1 or ASC integration was not truly clonal and uniform in the population, it might explain this response. Alternatively, the bimodal output might reflect some stochastic nature to the response, where a threshold of activation is dependent on probabilistic factors. We also wanted to know the stability of the Venus specks post stimulation. To understand these questions, we treated clone 43 with LeTx overnight, and collected Venus positive (V+) by FACS (Fig. 4.4A), and then cultured the Venus+ cells. One day post sorting, the Venus positive population decreased from 90.5% to 53%, and by three days this decreased even further to 15%. Eight days after being in culture, the percentage of Venus positives was under 4%, which is similar to the original line (Fig. 4.4B). Upon LeTx re-stimulation the Venus positive cells responded comparably to the unsorted naïve population. Since the recall response

of the V+ sorted cells was similar to the response of the naïve reporter cell line, it does not appear that a lack of uniform expression of all the components explains the bimodal response.

4.2.2 CASP1 BiFC cell line analysis by fluorescence microscopy

We further characterized the reporter responses by live cell imaging under time-lapse microscopy. Fig. 4.5A shows the response of clone #15, another final clone, to LeTx over 5 hours when imaged every 15 minutes. At time zero, only one cell in the field of view is Venus positive, but within one hour many Venus specks can be observed in numerous cells. The number of cells and the brightness of the Venus specks continuously increase up to the 5h time point. After the 5h time point several clones were further imaged at a higher magnification to characterize the distribution of the Venus signal. In Fig. 5B, clone #18 shows that most of the Venus signal comes from a single and discrete focus within each cell. This speck size and frequency per cell is consistent with native ASC specks observe in macrophages (Broz et al., 2010).

4.2.3 CASP1 BiFC reporter in macrophages

We also tested the response of the reporter in cells that endogenously express NLRs and ASC, such as a macrophage-like cell line. We chose to transduce immortalized Casp1/11-/- macrophages for several reasons. Since the two reporter halves are encoded by two separate retroviruses, we needed a cell type that would achieve high transduction efficiency. This feature would ensure enough cells to become positive for both components, and is unlikely to be reached with primary cells. We chose the *Casp1*-deficient cell-line to eliminate the pyroptosis that would occur with similar kinetics as the reporter assembly. These cells also contain a functional NAIP5 and NLRC4 inflammasome that can be activated by expression of *Legionella pneumophila's* flagellin (flaA) (Lightfield et al., 2008). We sequentially transduced these cells with CASP1-L-VN173 or CASP1-L-VL155, followed by CASP1-L-VC155. We cultured the cells, and then transduced them with a third retrovirus encoding mCherry-FlaA, and allowed 48h for integration and expression of all the components. We then analyzed reporter activation by flow cytometry. We observed 25-35% spontaneous Venus assembly, but with flaA expression the number of Venus positive cells exceeded 60% (Fig. 4.6). This strongly suggests that the reporter works with other NLRs, and when these components are expressed endogenously. We did not co-stain the cells for the integration markers hCD4 and Thy1.1 due to significant spectral overlap of the fluorescent dyes with Venus and mCherry. Due to this technical challenge, it is unclear what percentage of cells that expressed all the components did not respond to FlaA, but we infer it to be a majority of the cells.

4.3 Discussion

We have generated a new tool to study inflammasome activation regulation with several distinct advantages from previous assays. This method is amenable to single-cell based assays such as flow cytometry and microscopy. Since the reporter does not depend on the catalytic activity of CASP1, the positively activated cells survive and can be enriched by FACS. This provides the opportunity perform complex screens of agonist or regulators of different inflammasomes in a pooled manner. As an example with NLRP1B, LF is the only protease or true agonist that has been identified. Genetic evidence suggests that *T. gondii* can activate NLRP1 in mice and rats, but the factor that activates NLRP1 has not been identified. It is suspected that *T. gondii* might encode a protease that also activates NLRP1. With this system, a *T. gondii* cDNA library could be ectopically expressed in this cell line with high coverage

representation. Venus positive cells could be recovered by FACS, and the cDNAs could be identified by sequencing, and then retested individually for agonism.

Since NLRP1B can be inhibited by MG-132, it has been hypothesized that a negative regulator of NLRP1B must be degraded by the proteasome to achieve full activation post NLRP1B cleavage (see Chapter 1). This cell line could be used in a pooled genetic loss of function screen to identify this potential negative regulator. The loss of this negative regulator would increase the propensity of cells to respond to LeTx, and would be enriched in the Venus positive cell population. This screen would not be possible with current methods unless done in an arrayed method and would still be difficult to detect.

This reporter system should allow the creation of cell lines that are activated by other inflammasomes. In next generations of the system, the CASP1S-VN173/155 clone 28 could be first transduced with mASC-IRES-HygroR, and then by other NLRs such as the NAIP1/2/5 plus NLRC4, NLRP3, or NLRP6. These lines could be useful in testing other stimulants or host factors that participate in the inflammasome assembly. Several NLRP and NLRC proteins have unknown functions or are known to be sufficient to form an inflammasome. This new CASP1 with ASC-HygroR cell line could be responsive to these NLRs of unknown function. Truncations or mutations in the candidate NLR that result in spontaneous oligomerization could be selected with this reporter. This reporter would also allow for saturation mutagenesis to be performed on NLRs of known function based on gain of function mutations, as opposed to loss of function.

Since the CASP1 BiFC reporter works well in assessing inflammasome formation in living cells, it might provide a useful tool to study inflammasome activation *in vivo*. Similar challenges to study inflammasome activation *in vivo* exist as *in vitro*. In particular, most assays depend on the catalytic activity of CASP1, which has not been clearly decoupled from pyroptosis. This is a particular problem *in vivo* because when cells undergo pyroptosis it is expected that the cell remnants get phagocytosed by other cells. The clearance of the activated cells makes it challenging to find the inflammasome-activated cells *in vivo* under homeostatic and infection conditions. We propose that the CASP1S-VN173 and CASP1-VC155 could be both knocked in to endogenous *Casp1* locus. We expect that targeting of the endogenous *Casp1* locus would be ideal, since it would recapitulate cell-type expression patterns of wild-type *Casp1*. This would also circumvent the need to keep the reporter line in a *Casp1*-/- background. Additionally, we expect the *Casp1* locus to induce low expression of the reporter components, and it should not induce spontaneous self-assembly of Venus. The knock-in approach could be done in two different ways. One method could create two separate alleles for each CASP1-S-Venus half. Alternatively, the reporter could be inserted as a single polypeptide with a P2A self-cleaving linker in between each half. Once the mouse line is made, it could be validated by testing *ASC* genetic dependency, and assessing activation in bone-marrow derived macrophages with and without stimulation. This mouse line would help us to understand several interesting questions. For example, it is unclear how much inflammasome activation occurs in response to the normal SPF microbiota, and during infection with a true pathogen. It is also unclear if all cell types that activate the inflammasome undergo pyroptosis. This is difficult to assess in cell types where a few percent of cells are responding. In this case, it might be possible to detect cytokine secretion, but difficult to detect the pyroptosis. This reporter would help determine the percentage of cells that actually get activated, and explain why the pyroptosis cannot be detected.

In summary, our new inflammasome reporter provides an additional tool to evaluate inflammasome activation and allow researchers to ask questions that could not be easily answered with previous methods.

4.4 Methods

4.4.1 Plasmids and constructs

CASP1-L, CASP1-S, and CASP1-FL were amplified by PCR using primers 1+2, 1+3, and 1+4 (Table 4.1) off mouse Casp1-C284A-MSCV2.2 plasmid as a template. All three amplicons were cloned into CMSCV-IRES-hCD4-KC2 and CMSCV-IRES-Thy1.1-KC3 by using BglII and NotI sites. VN155 (152L) was amplified with primers 8+9 from pBiFC-VN155 (I152L) (Addgene plasmid # 27097), and cloned in-frame into CASP-L/S/FL- CMSCV-IRES-hCD4-KC2 via the NotI site. VN173 was amplified with primers 11+12 off pBiFC-VN173 (Addgene plasmid # 22010) and was also cloned in-frame into CASP-L/S/FL-CMSCV-IRES-hCD4-KC2 via the NotI site. VC155 was amplified with primers 10+9 off pBiFC-VC155 (Addgene plasmid # 22011) and cloned in frame into CASP-L/S/FL-CMSCV-IRES- Thy1.1-KC3 via the NotI site. Mouse ASC ORF was amplified from a proB cells cDNA library with primers 5+6 and cloned into CMSCV-IRES-Thy1.1-KC3 into the BglII site and pQXIH into the BamHI site. To make ASC-VN/VC, a similar strategy was done as with CASP1-L/S/FL. ASC was amplified with primers 5+7 and cloned into CMSCV-IRES-hCD4-KC2 and CMSCV-IRES-Thy1.1-KC3 by using BglII/BamHI and NotI sites. The Venus halves were subsequently cloned in the same way as for the CASP1 reporter steps.

4.4.2 Cell culture

HEK293T (ATCC) and GP2-293T (Clontech) cells were grown in complete media (DMEM, 10% FBS, 100 U/ml Penicillin, 100 µg/ml Streptomycin, and supplemented with 2mM L-glutamine). Immortalized Casp1/11$^{-/-}$ macrophages (C57BL6 background) were grown in complete media (RPMI 1640, 10% FBS, 100 U/ml Penicillin, 100 µg/ml Streptomycin). For single cell cloning, cells were plated at 0.3c/well (3c/ml) in four 96-well plates, allowed to grow for 2 weeks, and assessed for the presence of a colony. Cells were then moved to 24well plates to test responsiveness.

4.4.3 DNA transient transfections and retroviral production

HEK 293T cells were seeded the day prior to transfection at a density of 1.5x10^5 cells/well in a 24-well plate with complete media. DNA complexes were made with Lipofectamine 2000 (Invitrogen) according to manufacture's instructions and overlaid on cells for 36 hours. For retroviral production, 5.0x10^5 GP2 cells were seeded in a 6-well plate overnight. The next day 3.5ug of CMSCV vector was combined with VSV-G encoding plasmid and transfected with Lipofectamine 2000 according to manufactures instructions. The next day the media was replaced to 1ml of fresh DMEM, and cells were incubated at 32C for 24 hours. The viral containing supernatant was passed through a 0.45uM syringe-filter and incubated with target cells overnight at 32C. Retroviral integration and expression was assayed 48h post infection. For expression of the integration markers the following antibodies hCD4-PEcy5 (RPA-T4), Thy1.1-PEcy7 (HIS51) and hCD2-PE (RPA-2.10) were used at a dilution of 1:100. Cells were stained for 30 minutes, and then washed prior to flow cytometry or FACS.

4.5 Acknowledgements

We would like to thank Dough Green's lab for providing their CASP2 BiFC reporters (Bouchier-Hayes et al., 2009) as controls in the development of our CASP1 BiFC reporter. We would like to thank Chang-Deng Hu's lab for providing DNA encoding improved split Venus proteins (Kodama and Hu, 2010) which were deposited in Addgene (plasmid # 27097, 22010, and 22011).

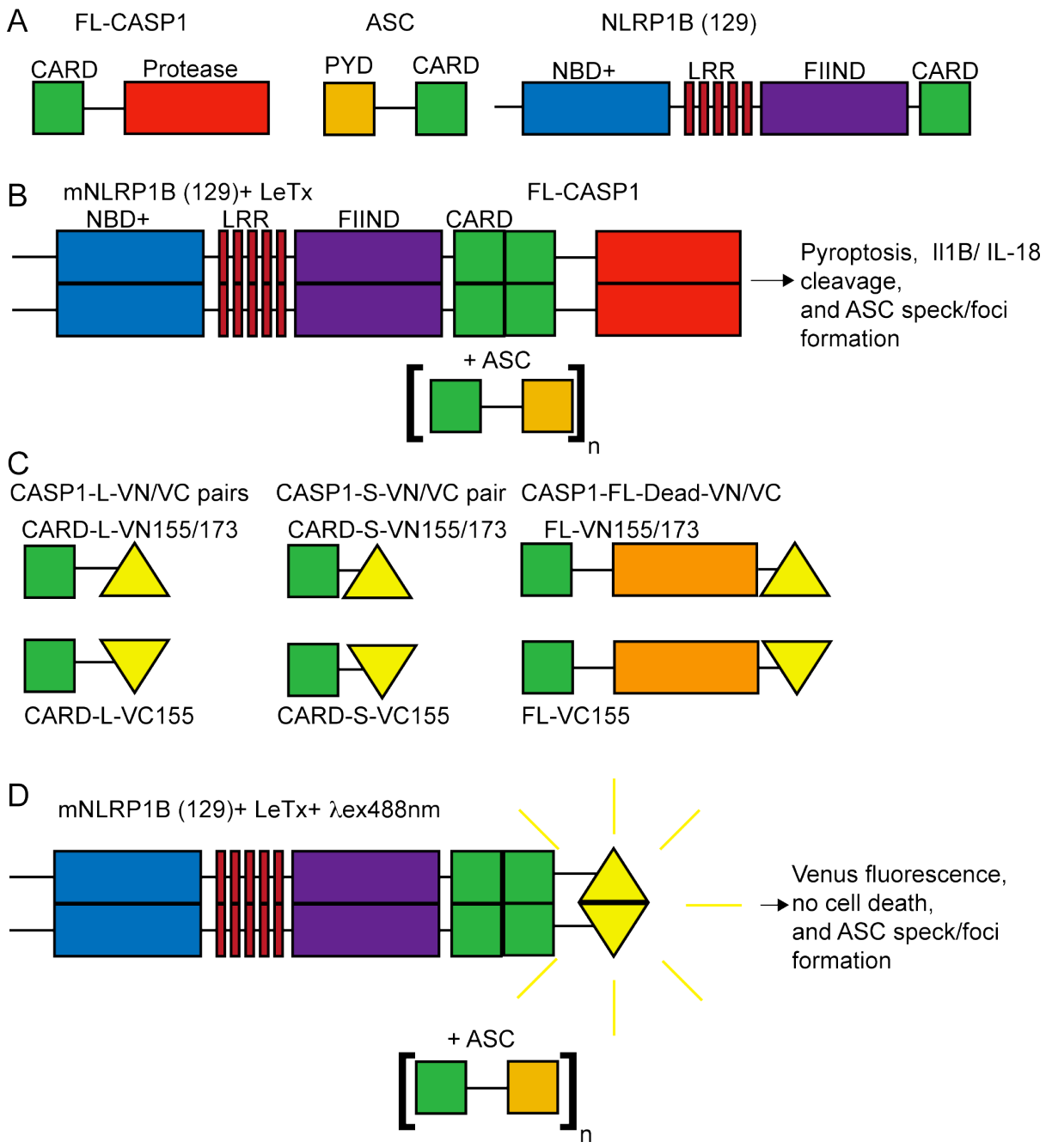

Figure 4.1 CASP1 BiFC reporter system components.
A) Domain architecture of wild-type CASP1, ASC and NLRP1B. B) Model structure of the NLRP1B inflammasome and CASP1 activation outputs. C) Three versions of the CASP1 BiFC reporter are depicted with VN155 or VN173 plus VC155. D) Model of the expected CASP1 BiFC reporter Venus assembly in respose to LeTx and NLRP1B activation.

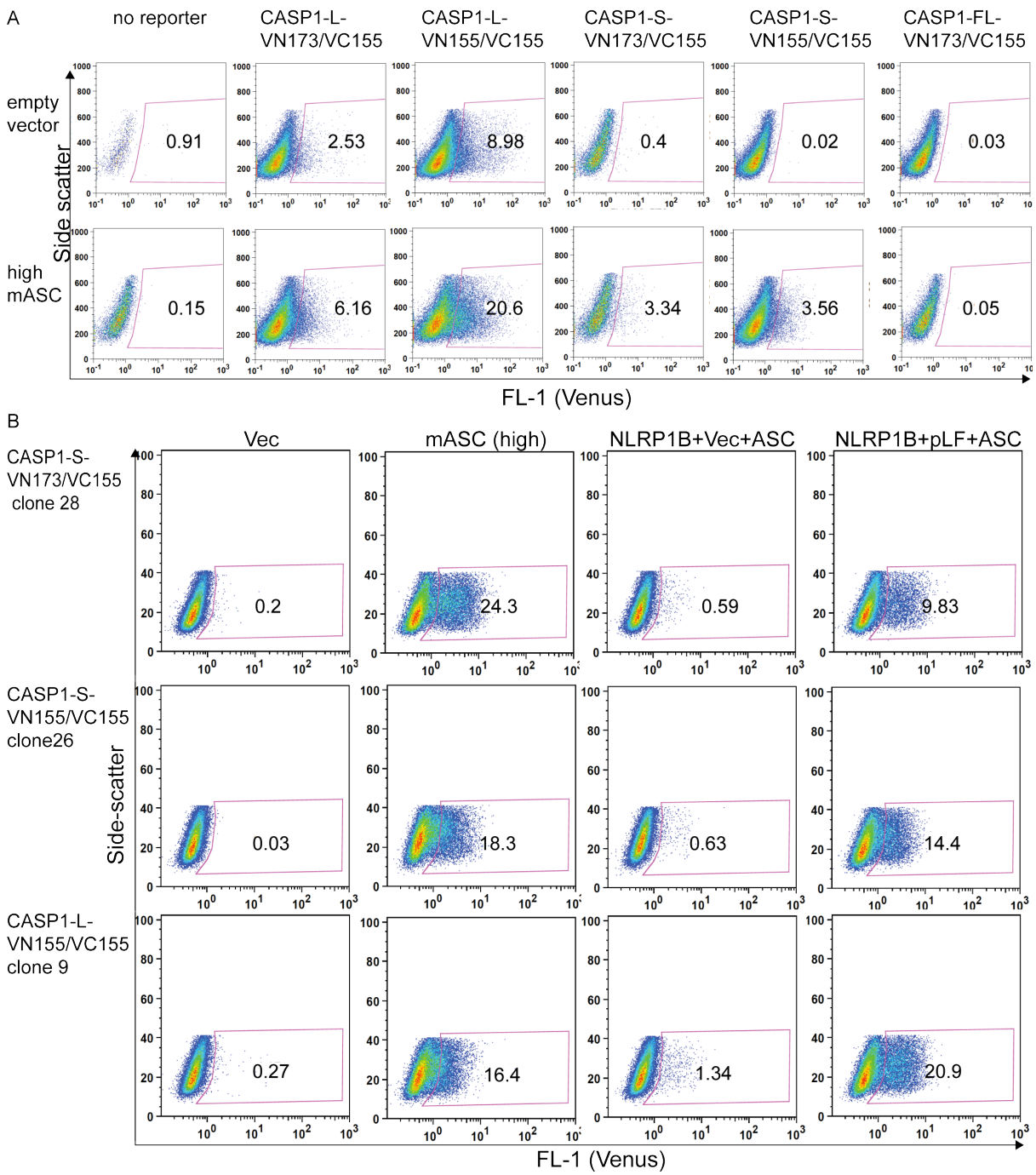

Figure 4.2 CASP1 BiFC reporter performance in 293T cells by flow cytometry.
A) 293T cells were transiently transfected with low amounts of the indicated CASP1 BiFC reporter components with or without high amounts of mASC encoding plasmid. B) Three examples of 293T cell clones which stably express the CASP1 BiFC reporter are shown. The clones' performances were tested by transient expression of high amounts of ASC, or low amounts of ASC, NLRP1B and LF co-expression.

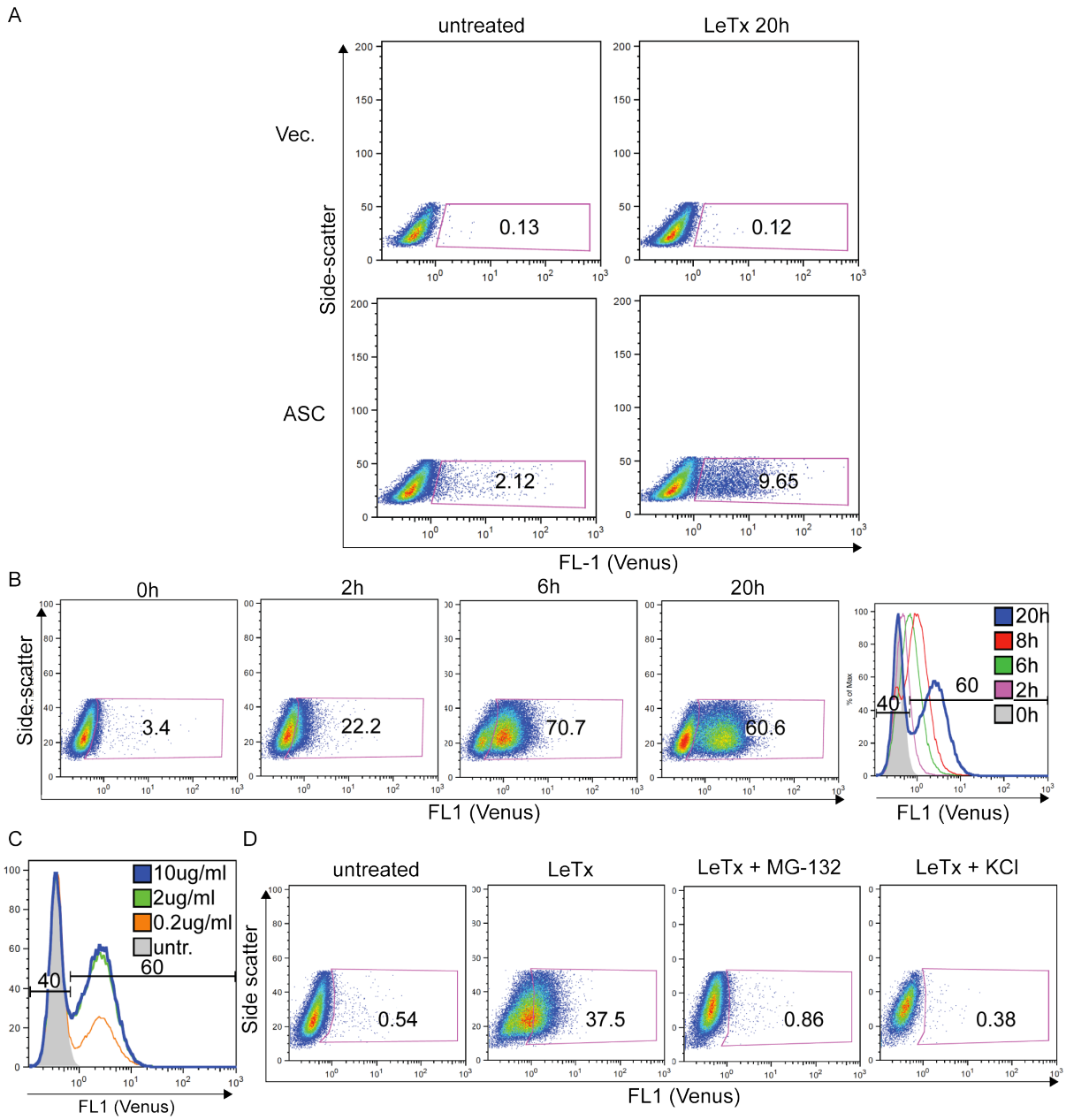

Figure 4.3 CASP1 reporter final cell line analysis by flow cytometry.
A) CASP1-S-VN173/VC155 clone 28 transduced with NLRP1B and mASC was tested with LeTx (1ug/ml) stimulation for 20h. B) LeTx treatment time course of a final reporter line (clone 43) for CASP1-S-VN173/VC155, which stably expresses mASC and mNLRP1B. C) Clone 43 was tested with varying concentrations of LeTx for 20h. D) Clone 43 was tested with LeTx stimulation, MG-132 (10uM) and 140mM KCl in the media for 6h.

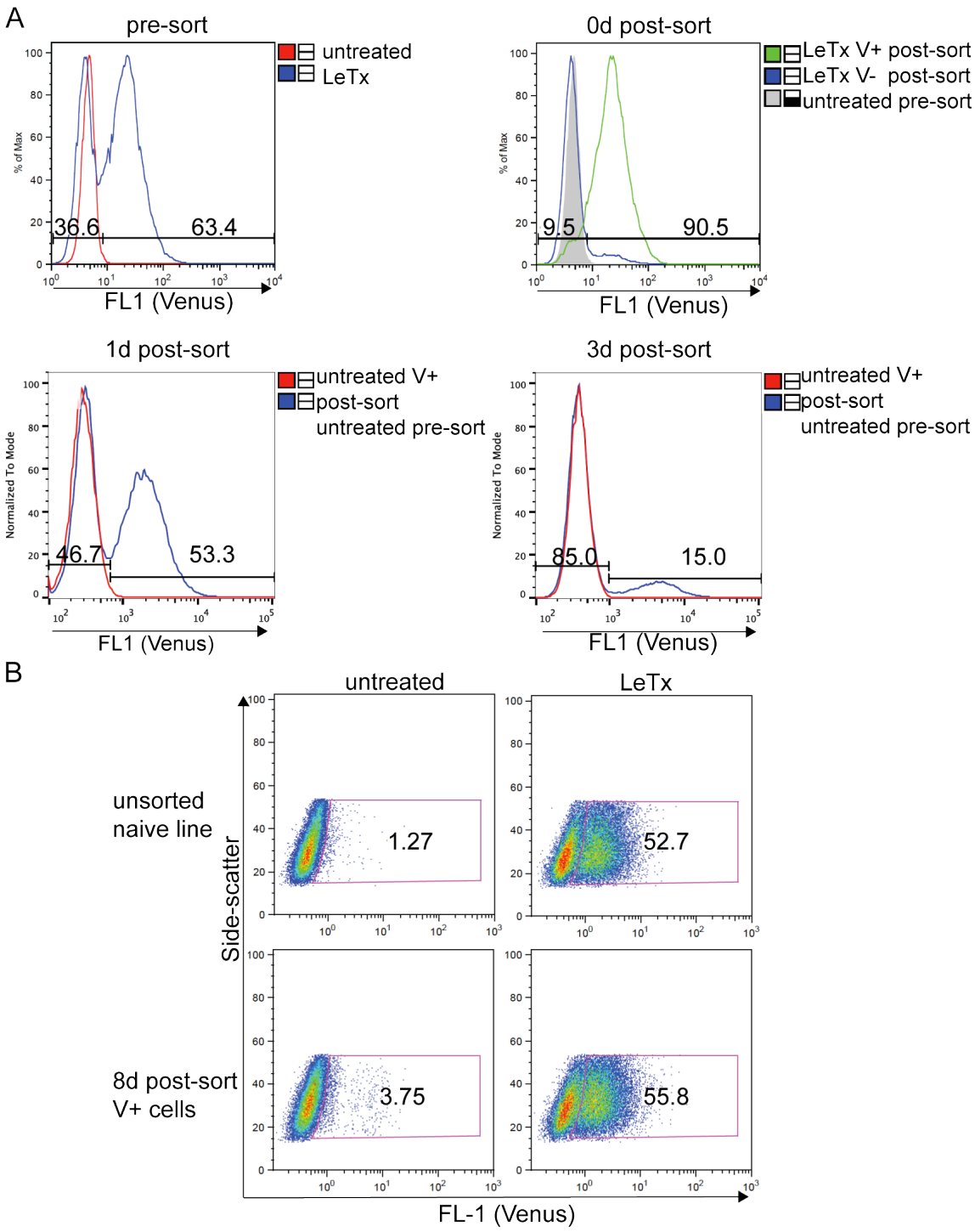

Figure 4.4 CASP1 BiFC reporter FACS and re-stimulation challenge.
A) Clone 43 was treated with LeTx (1ug/ml) for 13 hours and Venus+ (V+) and Venus- (V-) cells were collected by FACS. The V+ cells were cultured and analyzed by flow cytometry 1 and 3 days post the initial sort without stimulation. B) The V+ cells after being in culture for 8 days post the initial sort were re-challenged with LeTx (1ug/ml) for 14h and compared to naïve and clone 43 responses

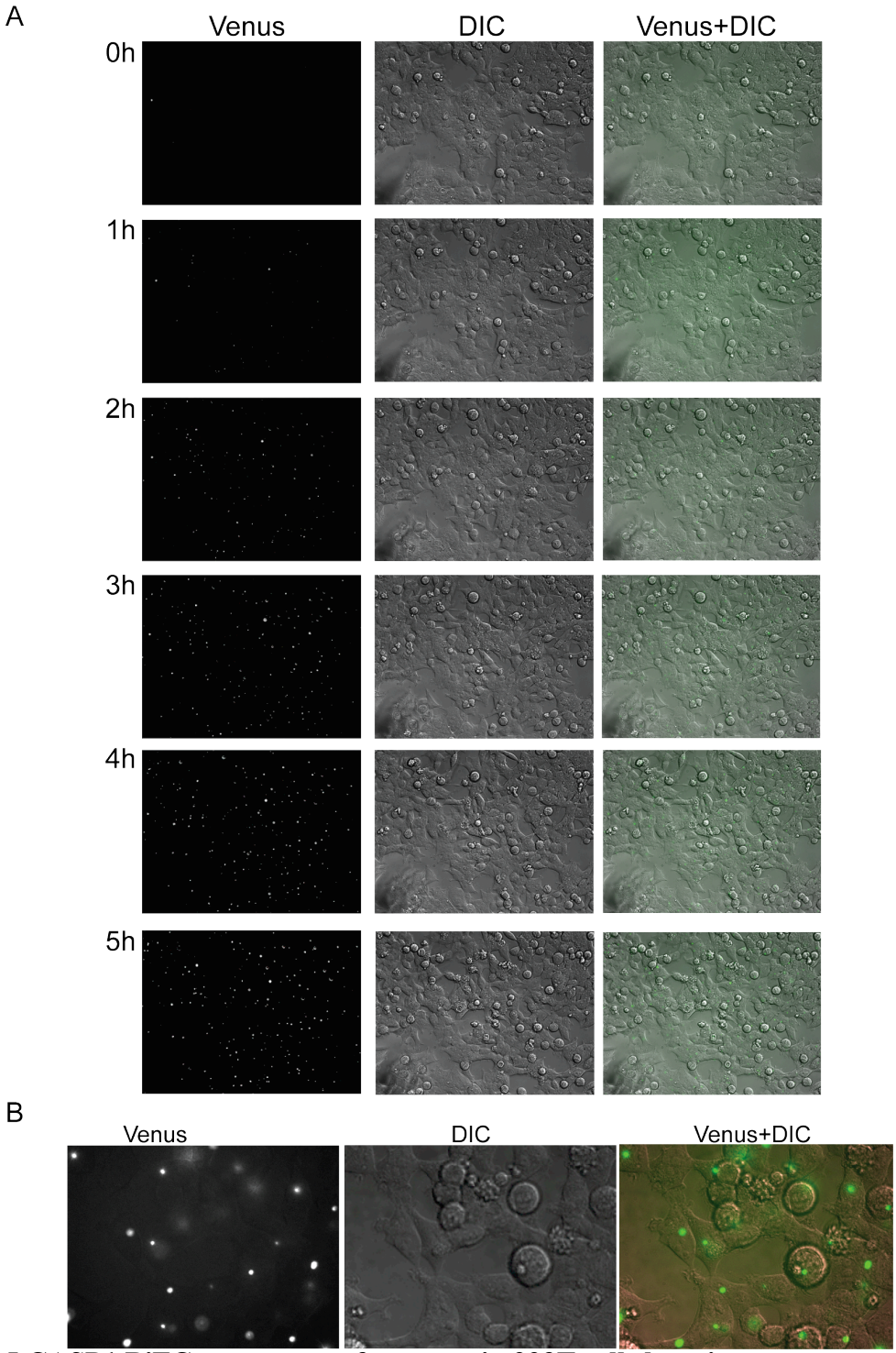

Figure 4.5 CASP1 BiFC reporter performance in 293T cells by microscopy.
A) The final reporter line (clone 15) CASP1-S-VN173/VC155 with stable expression of mASC and mNLRP1B was tested by microscopy. Live cells were treated with 10ug/ml LeTx and then imaged at 37C and 5% CO2 every 15mins with a FITC filter set with the 20X objective for 5 hours. B) A different clone (clone 18) that is similar to clone 15 was imaged with the 60X objective after 5h of LeTx stimulation.

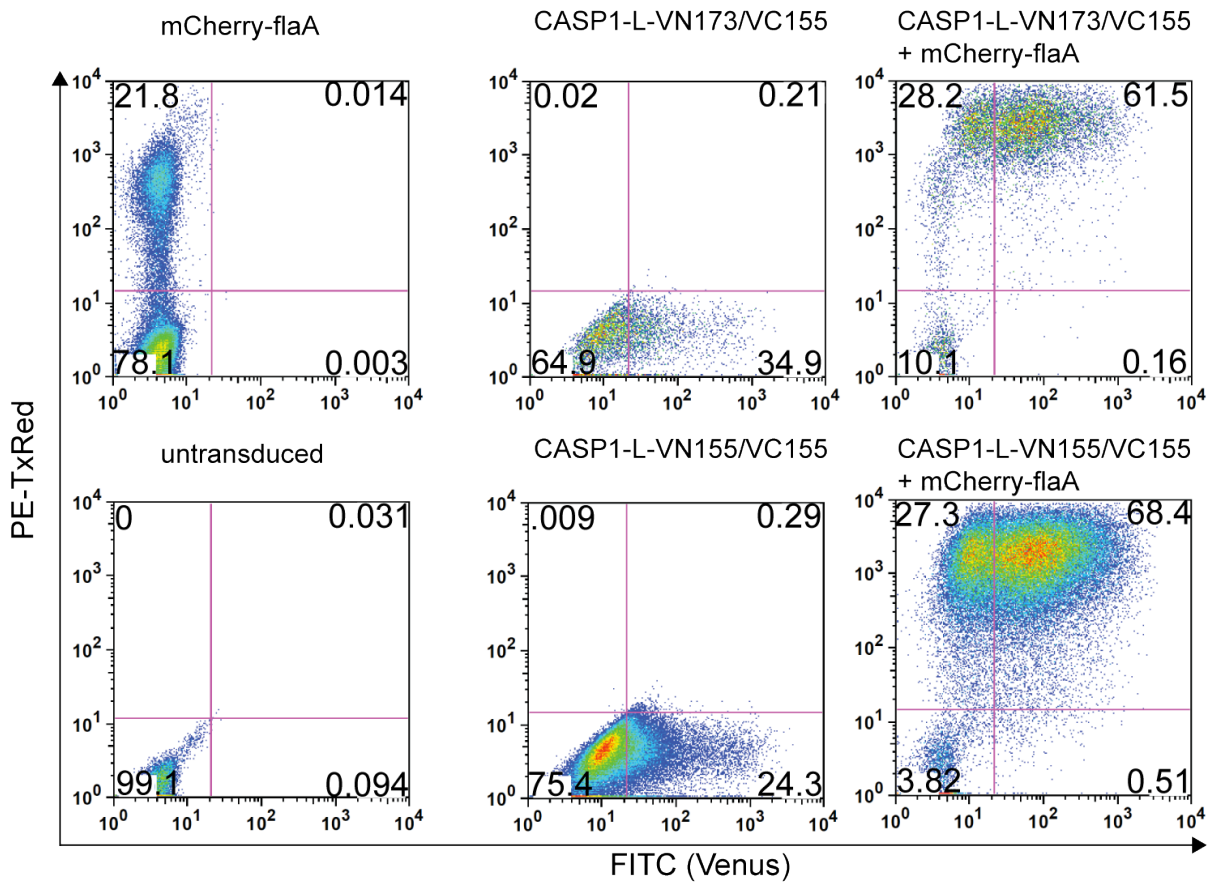

Figure 4.6 CASP1 BiFC reporter performance in a macrophage-like cell line. Immortalized Casp1/11-/- cells transduced with CASP1-L-VN173/VN155+CASP1-L-VC155 were tested for Venus assembly in response to mCherry-flaA co-expression.

primer number	primer sequence	primer name
1	atatAGATCTgccaccATGGCTGACAAGATCCTGAGG	Casp1-BglII-F
2	atatGCGGCCGCtATCTTCTGTAGCAACAAATGTTTCAGC	Casp1-D103-NotI-R
3	atatGCGGCCGCtCAGAATTCCTGCCAGGTAGCAGTC	Casp1-L87-NotI-R
4	atatGCGGCCGCtATGTCCCGGGAAGAGGTAGAAACG	Casp1-FL-NotI-R
5	atatGGATCCgccaccATGGGGCGGGCACGAGATGC	mASC-BamHI-F
6	atatGGATCCGCGGCCGCTCAGCTCTGCTCCAGGTCC	mASC-NotI-BamHI-R
7	atatGCGGCCGCtGCTCTGCTCCAGGTCCATCACC	ASC-NotI-VN/VC-R
8	atatGCGGCCGC GGTACCGGAGGTGGCGGGAGCG	5' VN155-NotI-F
9	TCATGTCTGGATCCCCGCGGCCGC	3' VN155/VC155 NotI-R
10	atatGCGGCCGC GGTACCCGTCCGGCGTGCAAAATCC	5' VC155-NotI-F
11	atatGCGGCCGC TCTAGAAGATCCATCGCCACC	5' VN173 NotI-F
12	atatGCGGCCGCCTACTCGATGTTGTGGCGG	3' VN173 NotI-R

Table 4.1 Primer sequences used for cloning

References:

Ali, S.R., Timmer, A.M., Bilgrami, S., Park, E.J., Eckmann, L., Nizet, V., and Karin, M. (2011). Anthrax toxin induces macrophage death by p38 MAPK inhibition but leads to inflammasome activation via ATP leakage. Immunity *35*, 34-44.

Allen, I.C., Wilson, J.E., Schneider, M., Lich, J.D., Roberts, R.A., Arthur, J.C., Woodford, R.M., Davis, B.K., Uronis, J.M., Herfarth, H.H.*, et al.* (2012). NLRP12 suppresses colon inflammation and tumorigenesis through the negative regulation of noncanonical NF-kappaB signaling. Immunity *36*, 742-754.

Anand, P.K., Malireddi, R.K., Lukens, J.R., Vogel, P., Bertin, J., Lamkanfi, M., and Kanneganti, T.D. (2012). NLRP6 negatively regulates innate immunity and host defence against bacterial pathogens. Nature *488*, 389-393.

Anderson, J., Schiffer, C., Lee, S.K., and Swanstrom, R. (2009). Viral protease inhibitors. Handbook of experimental pharmacology, 85-110.

Axtell, M.J., and Staskawicz, B.J. (2003). Initiation of RPS2-specified disease resistance in Arabidopsis is coupled to the AvrRpt2-directed elimination of RIN4. Cell *112*, 369-377.

Bardwell, A.J., Abdollahi, M., and Bardwell, L. (2004). Anthrax lethal factor-cleavage products of MAPK (mitogen-activated protein kinase) kinases exhibit reduced binding to their cognate MAPKs. The Biochemical journal *378*, 569-577.

Bergsbaken, T., Fink, S.L., and Cookson, B.T. (2009). Pyroptosis: host cell death and inflammation. Nature reviews Microbiology *7*, 99-109.

Boatright, K.M., Renatus, M., Scott, F.L., Sperandio, S., Shin, H., Pedersen, I.M., Ricci, J.E., Edris, W.A., Sutherlin, D.P., Green, D.R.*, et al.* (2003). A unified model for apical caspase activation. Molecular cell *11*, 529-541.

Bouchier-Hayes, L., Oberst, A., McStay, G.P., Connell, S., Tait, S.W., Dillon, C.P., Flanagan, J.M., Beere, H.M., and Green, D.R. (2009). Characterization of cytoplasmic caspase-2 activation by induced proximity. Molecular cell *35*, 830-840.

Boyden, E.D., and Dietrich, W.F. (2006). Nalp1b controls mouse macrophage susceptibility to anthrax lethal toxin. Nature genetics *38*, 240-244.

Boyer, L., Magoc, L., Dejardin, S., Cappillino, M., Paquette, N., Hinault, C., Charriere, G.M., Ip, W.K., Fracchia, S., Hennessy, E.*, et al.* (2011). Pathogen-derived effectors trigger protective immunity via activation of the Rac2 enzyme and the IMD or Rip kinase signaling pathway. Immunity *35*, 536-549.

Broz, P., von Moltke, J., Jones, J.W., Vance, R.E., and Monack, D.M. (2010). Differential requirement for Caspase-1 autoproteolysis in pathogen-induced cell death and cytokine processing. Cell host & microbe *8*, 471-483.

Bruey, J.M., Bruey-Sedano, N., Luciano, F., Zhai, D., Balpai, R., Xu, C., Kress, C.L., Bailly-Maitre, B., Li, X., Osterman, A.*, et al.* (2007). Bcl-2 and Bcl-XL regulate proinflammatory caspase-1 activation by interaction with NALP1. Cell *129*, 45-56.

Burckstummer, T., Baumann, C., Bluml, S., Dixit, E., Durnberger, G., Jahn, H., Planyavsky, M., Bilban, M., Colinge, J., Bennett, K.L.*, et al.* (2009). An orthogonal proteomic-genomic screen identifies AIM2 as a cytoplasmic DNA sensor for the inflammasome. Nature immunology *10*, 266-272.

Cavailles, P., Flori, P., Papapietro, O., Bisanz, C., Lagrange, D., Pilloux, L., Massera, C., Cristinelli, S., Jublot, D., Bastien, O.*, et al.* (2014). A highly conserved Toxo1 haplotype directs

resistance to toxoplasmosis and its associated caspase-1 dependent killing of parasite and host macrophage. PLoS pathogens *10*, e1004005.
Cavailles, P., Sergent, V., Bisanz, C., Papapietro, O., Colacios, C., Mas, M., Subra, J.F., Lagrange, D., Calise, M., Appolinaire, S.*, et al.* (2006). The rat Toxo1 locus directs toxoplasmosis outcome and controls parasite proliferation and spreading by macrophage-dependent mechanisms. Proceedings of the National Academy of Sciences of the United States of America *103*, 744-749.
Chavarria-Smith, J., and Vance, R.E. (2013). Direct proteolytic cleavage of NLRP1B is necessary and sufficient for inflammasome activation by anthrax lethal factor. PLoS pathogens *9*, e1003452.
Chavarría-Smith, J., and Vance, R.E. (2015). The NLRP1 inflammasomes. Immunological reviews *265*, 22-34.
Chisholm, S.T., Coaker, G., Day, B., and Staskawicz, B.J. (2006). Host-microbe interactions: shaping the evolution of the plant immune response. Cell *124*, 803-814.
Chopra, A.P., Boone, S.A., Liang, X., and Duesbery, N.S. (2003). Anthrax lethal factor proteolysis and inactivation of MAPK kinase. The Journal of biological chemistry *278*, 9402-9406.
Cirelli, K.M., Gorfu, G., Hassan, M.A., Printz, M., Crown, D., Leppla, S.H., Grigg, M.E., Saeij, J.P., and Moayeri, M. (2014). Inflammasome sensor NLRP1 controls rat macrophage susceptibility to Toxoplasma gondii. PLoS pathogens *10*, e1003927.
Cordoba-Rodriguez, R., Fang, H., Lankford, C.S., and Frucht, D.M. (2004). Anthrax lethal toxin rapidly activates caspase-1/ICE and induces extracellular release of interleukin (IL)-1beta and IL-18. The Journal of biological chemistry *279*, 20563-20566.
D'Osualdo, A., Weichenberger, C.X., Wagner, R.N., Godzik, A., Wooley, J., and Reed, J.C. (2011). CARD8 and NLRP1 undergo autoproteolytic processing through a ZU5-like domain. PloS one *6*, e27396.
Daugherty, M.D., and Malik, H.S. (2012). Rules of engagement: molecular insights from host-virus arms races. Annual review of genetics *46*, 677-700.
Duesbery, N.S., Webb, C.P., Leppla, S.H., Gordon, V.M., Klimpel, K.R., Copeland, T.D., Ahn, N.G., Oskarsson, M.K., Fukasawa, K., Paull, K.D.*, et al.* (1998). Proteolytic inactivation of MAP-kinase-kinase by anthrax lethal factor. Science *280*, 734-737.
Ewald, S.E., Chavarria-Smith, J., and Boothroyd, J.C. (2014). NLRP1 is an inflammasome sensor for Toxoplasma gondii. Infection and immunity *82*, 460-468.
Faustin, B., Lartigue, L., Bruey, J.M., Luciano, F., Sergienko, E., Bailly-Maitre, B., Volkmann, N., Hanein, D., Rouiller, I., and Reed, J.C. (2007). Reconstituted NALP1 inflammasome reveals two-step mechanism of caspase-1 activation. Molecular cell *25*, 713-724.
Fernandes-Alnemri, T., Yu, J.W., Datta, P., Wu, J., and Alnemri, E.S. (2009). AIM2 activates the inflammasome and cell death in response to cytoplasmic DNA. Nature *458*, 509-513.
Finger, J.N., Lich, J.D., Dare, L.C., Cook, M.N., Brown, K.K., Duraiswami, C., Bertin, J., and Gough, P.J. (2012). Autolytic proteolysis within the function to find domain (FIIND) is required for NLRP1 inflammasome activity. The Journal of biological chemistry *287*, 25030-25037.
Fink, S.L., Bergsbaken, T., and Cookson, B.T. (2008). Anthrax lethal toxin and Salmonella elicit the common cell death pathway of caspase-1-dependent pyroptosis via distinct mechanisms. Proceedings of the National Academy of Sciences of the United States of America *105*, 4312-4317.

Fontana, M.F., Banga, S., Barry, K.C., Shen, X., Tan, Y., Luo, Z.Q., and Vance, R.E. (2011). Secreted bacterial effectors that inhibit host protein synthesis are critical for induction of the innate immune response to virulent Legionella pneumophila. PLoS pathogens *7*, e1001289.
Franchi, L., Munoz-Planillo, R., and Nunez, G. (2012). Sensing and reacting to microbes through the inflammasomes. Nature immunology *13*, 325-332.
Frew, B.C., Joag, V.R., and Mogridge, J. (2012). Proteolytic processing of Nlrp1b is required for inflammasome activity. PLoS pathogens *8*, e1002659.
Friedlander, A.M. (1986). Macrophages are sensitive to anthrax lethal toxin through an acid-dependent process. The Journal of biological chemistry *261*, 7123-7126.
Friedlander, A.M., Bhatnagar, R., Leppla, S.H., Johnson, L., and Singh, Y. (1993). Characterization of macrophage sensitivity and resistance to anthrax lethal toxin. Infection and immunity *61*, 245-252.
George, R.D., McVicker, G., Diederich, R., Ng, S.B., MacKenzie, A.P., Swanson, W.J., Shendure, J., and Thomas, J.H. (2011). Trans genomic capture and sequencing of primate exomes reveals new targets of positive selection. Genome research *21*, 1686-1694.
Gerlic, M., Faustin, B., Postigo, A., Yu, E.C., Proell, M., Gombosuren, N., Krajewska, M., Flynn, R., Croft, M., Way, M.*, et al.* (2013). Vaccinia virus F1L protein promotes virulence by inhibiting inflammasome activation. Proceedings of the National Academy of Sciences of the United States of America *110*, 7808-7813.
Girardin, S.E., Boneca, I.G., Viala, J., Chamaillard, M., Labigne, A., Thomas, G., Philpott, D.J., and Sansonetti, P.J. (2003). Nod2 is a general sensor of peptidoglycan through muramyl dipeptide (MDP) detection. The Journal of biological chemistry *278*, 8869-8872.
Gorfu, G., Cirelli, K.M., Melo, M.B., Mayer-Barber, K., Crown, D., Koller, B.H., Masters, S., Sher, A., Leppla, S.H., Moayeri, M.*, et al.* (2014). Dual role for inflammasome sensors NLRP1 and NLRP3 in murine resistance to Toxoplasma gondii. mBio *5*.
Gregory, S.M., Davis, B.K., West, J.A., Taxman, D.J., Matsuzawa, S., Reed, J.C., Ting, J.P., and Damania, B. (2011). Discovery of a viral NLR homolog that inhibits the inflammasome. Science *331*, 330-334.
Hellmich, K.A., Levinsohn, J.L., Fattah, R., Newman, Z.L., Maier, N., Sastalla, I., Liu, S., Leppla, S.H., and Moayeri, M. (2012). Anthrax lethal factor cleaves mouse nlrp1b in both toxin-sensitive and toxin-resistant macrophages. PloS one *7*, e49741.
Hornung, V., Ablasser, A., Charrel-Dennis, M., Bauernfeind, F., Horvath, G., Caffrey, D.R., Latz, E., and Fitzgerald, K.A. (2009). AIM2 recognizes cytosolic dsDNA and forms a caspase-1-activating inflammasome with ASC. Nature *458*, 514-518.
Hsu, L.C., Ali, S.R., McGillivray, S., Tseng, P.H., Mariathasan, S., Humke, E.W., Eckmann, L., Powell, J.J., Nizet, V., Dixit, V.M.*, et al.* (2008). A NOD2-NALP1 complex mediates caspase-1-dependent IL-1beta secretion in response to Bacillus anthracis infection and muramyl dipeptide. Proceedings of the National Academy of Sciences of the United States of America *105*, 7803-7808.
Hu, Z., Yan, C., Liu, P., Huang, Z., Ma, R., Zhang, C., Wang, R., Zhang, Y., Martinon, F., Miao, D.*, et al.* (2013). Crystal structure of NLRC4 reveals its autoinhibition mechanism. Science *341*, 172-175.
Ichinohe, T., Pang, I.K., and Iwasaki, A. (2010). Influenza virus activates inflammasomes via its intracellular M2 ion channel. Nature immunology *11*, 404-410.
Inohara, N., Ogura, Y., Fontalba, A., Gutierrez, O., Pons, F., Crespo, J., Fukase, K., Inamura, S., Kusumoto, S., Hashimoto, M.*, et al.* (2003). Host recognition of bacterial muramyl dipeptide

mediated through NOD2. Implications for Crohn's disease. The Journal of biological chemistry *278*, 5509-5512.
Janeway, C.A., Jr. (1989). Approaching the asymptote? Evolution and revolution in immunology. Cold Spring Harbor symposia on quantitative biology *54 Pt 1*, 1-13.
Jin, Y., Mailloux, C.M., Gowan, K., Riccardi, S.L., LaBerge, G., Bennett, D.C., Fain, P.R., and Spritz, R.A. (2007). NALP1 in vitiligo-associated multiple autoimmune disease. The New England journal of medicine *356*, 1216-1225.
Jones, J.D., and Dangl, J.L. (2006). The plant immune system. Nature *444*, 323-329.
Kayagaki, N., Warming, S., Lamkanfi, M., Vande Walle, L., Louie, S., Dong, J., Newton, K., Qu, Y., Liu, J., Heldens, S.*, et al.* (2011). Non-canonical inflammasome activation targets caspase-11. Nature *479*, 117-121.
Klimpel, K.R., Arora, N., and Leppla, S.H. (1994). Anthrax toxin lethal factor contains a zinc metalloprotease consensus sequence which is required for lethal toxin activity. Molecular microbiology *13*, 1093-1100.
Kodama, Y., and Hu, C.D. (2010). An improved bimolecular fluorescence complementation assay with a high signal-to-noise ratio. BioTechniques *49*, 793-805.
Kofoed, E.M., and Vance, R.E. (2011). Innate immune recognition of bacterial ligands by NAIPs determines inflammasome specificity. Nature *477*, 592-595.
Kovarova, M., Hesker, P.R., Jania, L., Nguyen, M., Snouwaert, J.N., Xiang, Z., Lommatzsch, S.E., Huang, M.T., Ting, J.P., and Koller, B.H. (2012). NLRP1-dependent pyroptosis leads to acute lung injury and morbidity in mice. J Immunol *189*, 2006-2016.
Lamkanfi, M., and Dixit, V.M. (2009). Inflammasomes: guardians of cytosolic sanctity. Immunological reviews *227*, 95-105.
Levandowski, C.B., Mailloux, C.M., Ferrara, T.M., Gowan, K., Ben, S., Jin, Y., McFann, K.K., Holland, P.J., Fain, P.R., Dinarello, C.A.*, et al.* (2013). NLRP1 haplotypes associated with vitiligo and autoimmunity increase interleukin-1beta processing via the NLRP1 inflammasome. Proceedings of the National Academy of Sciences of the United States of America *110*, 2952-2956.
Levinsohn, J.L., Newman, Z.L., Hellmich, K.A., Fattah, R., Getz, M.A., Liu, S., Sastalla, I., Leppla, S.H., and Moayeri, M. (2012). Anthrax lethal factor cleavage of Nlrp1 is required for activation of the inflammasome. PLoS pathogens *8*, e1002638.
Li, H., Child, M.A., and Bogyo, M. (2012). Proteases as regulators of pathogenesis: examples from the Apicomplexa. Biochimica et biophysica acta *1824*, 177-185.
Liao, K.C., and Mogridge, J. (2009). Expression of Nlrp1b inflammasome components in human fibroblasts confers susceptibility to anthrax lethal toxin. Infection and immunity *77*, 4455-4462.
Liao, K.C., and Mogridge, J. (2012). Activation of the Nlrp1b Inflammasome by Reduction of Cytosolic ATP. Infection and immunity.
Liao, K.C., and Mogridge, J. (2013). Activation of the Nlrp1b inflammasome by reduction of cytosolic ATP. Infection and immunity *81*, 570-579.
Lightfield, K.L., Persson, J., Brubaker, S.W., Witte, C.E., von Moltke, J., Dunipace, E.A., Henry, T., Sun, Y.H., Cado, D., Dietrich, W.F.*, et al.* (2008). Critical function for Naip5 in inflammasome activation by a conserved carboxy-terminal domain of flagellin. Nature immunology *9*, 1171-1178.
Liu, S., Zhang, Y., Moayeri, M., Liu, J., Crown, D., Fattah, R.J., Wein, A.N., Yu, Z.X., Finkel, T., and Leppla, S.H. (2013). Key tissue targets responsible for anthrax-toxin-induced lethality. Nature *501*, 63-68.

Lu, A., Magupalli, V.G., Ruan, J., Yin, Q., Atianand, M.K., Vos, M.R., Schroder, G.F., Fitzgerald, K.A., Wu, H., and Egelman, E.H. (2014). Unified polymerization mechanism for the assembly of ASC-dependent inflammasomes. Cell *156*, 1193-1206.
Lupfer, C.R., and Kanneganti, T.D. (2012). The role of inflammasome modulation in virulence. Virulence *3*, 262-270.
Mackey, D., Belkhadir, Y., Alonso, J.M., Ecker, J.R., and Dangl, J.L. (2003). Arabidopsis RIN4 is a target of the type III virulence effector AvrRpt2 and modulates RPS2-mediated resistance. Cell *112*, 379-389.
Mariathasan, S., Weiss, D.S., Newton, K., McBride, J., O'Rourke, K., Roose-Girma, M., Lee, W.P., Weinrauch, Y., Monack, D.M., and Dixit, V.M. (2006). Cryopyrin activates the inflammasome in response to toxins and ATP. Nature *440*, 228-232.
Martinon, F., Agostini, L., Meylan, E., and Tschopp, J. (2004). Identification of bacterial muramyl dipeptide as activator of the NALP3/cryopyrin inflammasome. Current biology : CB *14*, 1929-1934.
Martinon, F., Burns, K., and Tschopp, J. (2002). The inflammasome: a molecular platform triggering activation of inflammatory caspases and processing of proIL-beta. Molecular cell *10*, 417-426.
Martinon, F., Mayor, A., and Tschopp, J. (2009). The inflammasomes: guardians of the body. Annual review of immunology *27*, 229-265.
Masters, S.L., Gerlic, M., Metcalf, D., Preston, S., Pellegrini, M., O'Donnell, J.A., McArthur, K., Baldwin, T.M., Chevrier, S., Nowell, C.J.*, et al.* (2012). NLRP1 inflammasome activation induces pyroptosis of hematopoietic progenitor cells. Immunity *37*, 1009-1023.
Moayeri, M., Crown, D., Newman, Z.L., Okugawa, S., Eckhaus, M., Cataisson, C., Liu, S., Sastalla, I., and Leppla, S.H. (2010). Inflammasome sensor Nlrp1b-dependent resistance to anthrax is mediated by caspase-1, IL-1 signaling and neutrophil recruitment. PLoS pathogens *6*, e1001222.
Moayeri, M., Martinez, N.W., Wiggins, J., Young, H.A., and Leppla, S.H. (2004). Mouse susceptibility to anthrax lethal toxin is influenced by genetic factors in addition to those controlling macrophage sensitivity. Infection and immunity *72*, 4439-4447.
Moayeri, M., Sastalla, I., and Leppla, S.H. (2012). Anthrax and the inflammasome. Microbes and infection / Institut Pasteur *14*, 392-400.
Neiman-Zenevich, J., Liao, K.C., and Mogridge, J. (2014). Distinct regions of NLRP1B are required to respond to anthrax lethal toxin and metabolic inhibition. Infection and immunity *82*, 3697-3703.
Newman, Z.L., Printz, M.P., Liu, S., Crown, D., Breen, L., Miller-Randolph, S., Flodman, P., Leppla, S.H., and Moayeri, M. (2010). Susceptibility to anthrax lethal toxin-induced rat death is controlled by a single chromosome 10 locus that includes rNlrp1. PLoS pathogens *6*, e1000906.
Nour, A.M., Yeung, Y.G., Santambrogio, L., Boyden, E.D., Stanley, E.R., and Brojatsch, J. (2009). Anthrax lethal toxin triggers the formation of a membrane-associated inflammasome complex in murine macrophages. Infection and immunity *77*, 1262-1271.
Park, J.M., Greten, F.R., Li, Z.W., and Karin, M. (2002). Macrophage apoptosis by anthrax lethal factor through p38 MAP kinase inhibition. Science *297*, 2048-2051.
Potempa, J., and Pike, R.N. (2009). Corruption of innate immunity by bacterial proteases. Journal of innate immunity *1*, 70-87.

Rathinam, V.A., Jiang, Z., Waggoner, S.N., Sharma, S., Cole, L.E., Waggoner, L., Vanaja, S.K., Monks, B.G., Ganesan, S., Latz, E.*, et al.* (2010). The AIM2 inflammasome is essential for host defense against cytosolic bacteria and DNA viruses. Nature immunology *11*, 395-402.
Rayamajhi, M., Zak, D.E., Chavarria-Smith, J., Vance, R.E., and Miao, E.A. (2013). Cutting edge: Mouse NAIP1 detects the type III secretion system needle protein. J Immunol *191*, 3986-3989.
Reubold, T.F., Hahne, G., Wohlgemuth, S., and Eschenburg, S. (2014). Crystal structure of the leucine-rich repeat domain of the NOD-like receptor NLRP1: implications for binding of muramyl dipeptide. FEBS letters *588*, 3327-3332.
Roberts, T.L., Idris, A., Dunn, J.A., Kelly, G.M., Burnton, C.M., Hodgson, S., Hardy, L.L., Garceau, V., Sweet, M.J., Ross, I.L.*, et al.* (2009). HIN-200 proteins regulate caspase activation in response to foreign cytoplasmic DNA. Science *323*, 1057-1060.
Sastalla, I., Crown, D., Masters, S.L., McKenzie, A., Leppla, S.H., and Moayeri, M. (2013). Transcriptional analysis of the three Nlrp1 paralogs in mice. BMC genomics *14*, 188.
Shi, J., Zhao, Y., Wang, Y., Gao, W., Ding, J., Li, P., Hu, L., and Shao, F. (2014). Inflammatory caspases are innate immune receptors for intracellular LPS. Nature *514*, 187-192.
Shin, S., Case, C.L., Archer, K.A., Nogueira, C.V., Kobayashi, K.S., Flavell, R.A., Roy, C.R., and Zamboni, D.S. (2008). Type IV secretion-dependent activation of host MAP kinases induces an increased proinflammatory cytokine response to Legionella pneumophila. PLoS pathogens *4*, e1000220.
Solle, M., Labasi, J., Perregaux, D.G., Stam, E., Petrushova, N., Koller, B.H., Griffiths, R.J., and Gabel, C.A. (2001). Altered cytokine production in mice lacking P2X(7) receptors. The Journal of biological chemistry *276*, 125-132.
Squires, R.C., Muehlbauer, S.M., and Brojatsch, J. (2007). Proteasomes control caspase-1 activation in anthrax lethal toxin-mediated cell killing. The Journal of biological chemistry *282*, 34260-34267.
Takeuchi, O., and Akira, S. (2010). Pattern recognition receptors and inflammation. Cell *140*, 805-820.
Tanabe, T., Chamaillard, M., Ogura, Y., Zhu, L., Qiu, S., Masumoto, J., Ghosh, P., Moran, A., Predergast, M.M., Tromp, G.*, et al.* (2004). Regulatory regions and critical residues of NOD2 involved in muramyl dipeptide recognition. The EMBO journal *23*, 1587-1597.
Tenthorey, J.L., Kofoed, E.M., Daugherty, M.D., Malik, H.S., and Vance, R.E. (2014). Molecular basis for specific recognition of bacterial ligands by NAIP/NLRC4 inflammasomes. Molecular cell *54*, 17-29.
Terra, J.K., Cote, C.K., France, B., Jenkins, A.L., Bozue, J.A., Welkos, S.L., LeVine, S.M., and Bradley, K.A. (2010). Cutting edge: resistance to Bacillus anthracis infection mediated by a lethal toxin sensitive allele of Nalp1b/Nlrp1b. J Immunol *184*, 17-20.
Terra, J.K., France, B., Cote, C.K., Jenkins, A., Bozue, J.A., Welkos, S.L., Bhargava, R., Ho, C.L., Mehrabian, M., Pan, C.*, et al.* (2011). Allelic variation on murine chromosome 11 modifies host inflammatory responses and resistance to Bacillus anthracis. PLoS pathogens *7*, e1002469.
Ting, J.P., Lovering, R.C., Alnemri, E.S., Bertin, J., Boss, J.M., Davis, B.K., Flavell, R.A., Girardin, S.E., Godzik, A., Harton, J.A.*, et al.* (2008). The NLR gene family: a standard nomenclature. Immunity *28*, 285-287.
Toh, E.C., Huq, N.L., Dashper, S.G., and Reynolds, E.C. (2010). Cysteine protease inhibitors: from evolutionary relationships to modern chemotherapeutic design for the treatment of infectious diseases. Current protein & peptide science *11*, 725-743.

Tong, L. (2002). Viral proteases. Chemical reviews *102*, 4609-4626.
Tschopp, J., Martinon, F., and Burns, K. (2003). NALPs: a novel protein family involved in inflammation. Nature reviews Molecular cell biology *4*, 95-104.
Turk, B.E. (2007). Manipulation of host signalling pathways by anthrax toxins. The Biochemical journal *402*, 405-417.
Turk, B.E., Wong, T.Y., Schwarzenbacher, R., Jarrell, E.T., Leppla, S.H., Collier, R.J., Liddington, R.C., and Cantley, L.C. (2004). The structural basis for substrate and inhibitor selectivity of the anthrax lethal factor. Nature structural & molecular biology *11*, 60-66.
van der Hoorn, R.A., and Kamoun, S. (2008). From Guard to Decoy: a new model for perception of plant pathogen effectors. The Plant cell *20*, 2009-2017.
Vance, R.E., Isberg, R.R., and Portnoy, D.A. (2009). Patterns of pathogenesis: discrimination of pathogenic and nonpathogenic microbes by the innate immune system. Cell host & microbe *6*, 10-21.
Vitale, G., Pellizzari, R., Recchi, C., Napolitani, G., Mock, M., and Montecucco, C. (1998). Anthrax lethal factor cleaves the N-terminus of MAPKKs and induces tyrosine/threonine phosphorylation of MAPKs in cultured macrophages. Biochemical and biophysical research communications *248*, 706-711.
von Moltke, J., Ayres, J.S., Kofoed, E.M., Chavarria-Smith, J., and Vance, R.E. (2012a). Recognition of Bacteria by Inflammasomes. Annual review of immunology.
von Moltke, J., Ayres, J.S., Kofoed, E.M., Chavarria-Smith, J., and Vance, R.E. (2013). Recognition of bacteria by inflammasomes. Annual review of immunology *31*, 73-106.
von Moltke, J., Trinidad, N.J., Moayeri, M., Kintzer, A.F., Wang, S.B., van Rooijen, N., Brown, C.R., Krantz, B.A., Leppla, S.H., Gronert, K.*, et al.* (2012b). Rapid induction of inflammatory lipid mediators by the inflammasome in vivo. Nature *490*, 107-111.
Welkos, S.L., Keener, T.J., and Gibbs, P.H. (1986). Differences in susceptibility of inbred mice to Bacillus anthracis. Infection and immunity *51*, 795-800.
Wickliffe, K.E., Leppla, S.H., and Moayeri, M. (2008a). Anthrax lethal toxin-induced inflammasome formation and caspase-1 activation are late events dependent on ion fluxes and the proteasome. Cellular microbiology *10*, 332-343.
Wickliffe, K.E., Leppla, S.H., and Moayeri, M. (2008b). Killing of macrophages by anthrax lethal toxin: involvement of the N-end rule pathway. Cellular microbiology *10*, 1352-1362.
Witola, W.H., Mui, E., Hargrave, A., Liu, S., Hypolite, M., Montpetit, A., Cavailles, P., Bisanz, C., Cesbron-Delauw, M.F., Fournie, G.J.*, et al.* (2011). NALP1 influences susceptibility to human congenital toxoplasmosis, proinflammatory cytokine response, and fate of Toxoplasma gondii-infected monocytic cells. Infection and immunity *79*, 756-766.
Xiao, J., Broz, P., Puri, A.W., Deu, E., Morell, M., Monack, D.M., and Bogyo, M. (2013). A coupled protein and probe engineering approach for selective inhibition and activity-based probe labeling of the caspases. Journal of the American Chemical Society *135*, 9130-9138.
Xu, H., Yang, J., Gao, W., Li, L., Li, P., Zhang, L., Gong, Y.N., Peng, X., Xi, J.J., Chen, S.*, et al.* (2014). Innate immune sensing of bacterial modifications of Rho GTPases by the Pyrin inflammasome. Nature *513*, 237-241.
Yazdi, A.S., Guarda, G., Riteau, N., Drexler, S.K., Tardivel, A., Couillin, I., and Tschopp, J. (2010). Nanoparticles activate the NLR pyrin domain containing 3 (Nlrp3) inflammasome and cause pulmonary inflammation through release of IL-1alpha and IL-1beta. Proceedings of the National Academy of Sciences of the United States of America *107*, 19449-19454.

Zakharova, M.Y., Kuznetsov, N.A., Dubiley, S.A., Kozyr, A.V., Fedorova, O.S., Chudakov, D.M., Knorre, D.G., Shemyakin, I.G., Gabibov, A.G., and Kolesnikov, A.V. (2009). Substrate recognition of anthrax lethal factor examined by combinatorial and pre-steady-state kinetic approaches. The Journal of biological chemistry *284*, 17902-17913.
Zhao, Y., Yang, J., Shi, J., Gong, Y.N., Lu, Q., Xu, H., Liu, L., and Shao, F. (2011). The NLRC4 inflammasome receptors for bacterial flagellin and type III secretion apparatus. Nature *477*, 596-600.